Development and Validation of a Constitutive Model for Dental Composites during the Curing Process

A THESIS
SUBMITTED TO THE FACULTY OF
UNIVERSITY OF MINNESOTA BY

Lauren Wickham Kolstad

IN PARTIAL FULFILLMENT OF THE REQUIREMENTS
FOR THE DEGREE OF
MASTER OF SCIENCE IN MECHANICAL ENGINEERING

Dr. Susan Mantell, Dr. Alex Fok

May 2017

Acknowledgements

First, I would like to thank my advisors Sue Mantell and Alex Fok for their engagement and financial support during the research process. Sue, thank you for the encouragement, patience, and motivation needed to make it through the thesis. I would also like to thank Jim Van de Ven for taking time out of his busy schedule to be on my committee. Thank you to all my committee members for your insightful comments on my thesis.

I would like to thank my lab mates from the MDRCBB and Polymer Mechanics labs. I am grateful to Hanxiao Ge, Yung-Chung Chen, and Wondwosen Aregawi who mentored me in my Abaqus work. Evan Cosgriff and Alex Hargus, thank you for the insightful discussions during long hours that lead to breakthroughs in different parts of my research. Thank you for supporting and attending the polymer mechanics lab adventures during the summer, which lead to great friendships.

I would like to thank my friends Sydney Bergeron, Kenya Mejia, Emily Vance, and Bonnie vanHeel for their guidance, support, and laughs. Without you, grad school would not have been as fun!

Finally, thank you to my boyfriend, parents, and sister for your countless hours of support and all that they have done for me.

Abstract

Debonding is a critical failure of a dental composites used for dental restorations. Debonding of dental composites can be determined by comparing the shrinkage stress of to the debonding strength of the adhesive that bonds it to the tooth surface. It is difficult to measure shrinkage stress experimentally. In this study, finite element analysis is used to predict the stress in the composite during cure. A new constitutive law is presented that will allow composite developers to evaluate composite shrinkage stress at early stages in the material development.

Shrinkage stress and shrinkage strain experimental data were gathered for three dental resins, Z250, Z350, and P90. Experimental data were used to develop a constitutive model for the Young's modulus as a function of time of the dental composite during cure. A Maxwell model, spring and dashpot in series, was used to simulate the composite. The compliance of the shrinkage stress device was also taken into account by including a spring in series with the Maxwell model. A coefficient of thermal expansion was also determined for internal loading of the composite by dividing shrinkage strain by time.

Three FEA models are presented. A spring-disk model validates that the constitutive law is self-consistent. A quarter cuspal deflection model uses separate experimental data to verify that the constitutive law is valid. Finally, an axisymmetric tooth model is used to predict interfacial stresses in the composite. These stresses are compared to the

debonding strength to check if the composite debonds. The new constitutive model accurately predicted cuspal deflection data. Predictions for interfacial bond stress in the tooth model compare favorably with debonding characteristics observed in practice for dental resins.

Table of Contents

List of Tables

List of Figures

Nomenclature

a	coefficient, MPa^{-1}
A	cross-sectional area, mm^2
b	coefficient
c	coefficient, MPa^{-1}
D	diameter, mm
$d\varepsilon$	total strain increment
$d\varepsilon_c$	creep strain
$d\varepsilon_e$	elastic strain
$d\varepsilon_s$	shrinkage strain
$d\sigma$	shrinkage stress, MPa
E	Young's modulus, MPa
k	machine stiffness, N/mm
ℓ	thickness, mm
t_i	time for step i, s
U1, U2, U3	displacement in the 1-, 2-, and 3- directions, mm

Greek Symbols:

δ	deflection, mm
ε_{axial}	axial shrinkage strain
ε_s	shrinkage strain
η	viscosity, Pa s
σ	shrinkage stress, MPa
Δ	change
α_i	coefficient of thermal expansion for step i, s^{-1}
ν	Poisson's ratio

1 Introduction and Literature Review

1.1 Introduction

Dental composites are commonly used as fillings in teeth because of their esthetics. However, shrinkage stress is one of the biggest downfalls [1–3]. Composites are cured with visible light for a short period of time (20-40 seconds), over which the elastic modulus increases exponentially from 0 to 10 GPa [4–6]. Shrinkage occurs when monomers become polymers: the composite can shrink up to 4% volumetrically [7]. As dental composites cure, photoinitiators set off a polymerization process where polymers cross-link to become polymer chains. When the polymer crosslinks, the stiffness develops. The relative development of the stiffness compared with the shrinkage is critical. If the stiffness develops faster than the shrinkage, high stress occurs in the composite. If the shrinkage develops faster than the stiffness, then the stress in the composite is low.

The stress in the composite must be compared to the bond strength of the adhesive to determine if debonding occurs. If there is a cured adhesive layer in place before the composite filling is applied, shrinkage stress at the interface between the composite and tooth on the order of 35 MPa [8] can cause debonding and microleakage (Figure 1.1). When the adhesive and composite are cured at the same time, the rate of cure bond strength and stress development must be monitored to determine when debonding occurs

[9]. In cases where the composite remains bonded through the adhesive to the tooth surface, shrinkage stress can cause fracture of teeth [10].

The shrinkage stress that develops in dental composites during cure depends on geometry, material properties, and size of the restoration [3,11], which makes it difficult to measure shrinkage stress of composites experimentally. No one has developed a method to measure the developing stress as the composite restoration is cured [12].

Experiments involving stress and strain of dental composites are generally measurements of shrinkage stress and free shrinkage strain, where none of the surfaces of the composite are bonded [7,12]. A common method of measuring shrinkage stress involves a cantilever tensometer. A composite is placed between two glass rods and the deflection of a cantilever beam is measured as the composite is cured. Stress is calculated from the deflection of the beam [7]. Digital image correlation (DIC) is a method to measure shrinkage strain. A surface is sprayed with spray paint, which leaves a pattern of small irregular dots. There is a large contrast between the dark spray painted dots and the white surface of the composite. The dots are tracked by a camera, and the resulting strain is calculated. DIC assumes a flat surface, unless multiple cameras are used. It is difficult to achieve a flat surface with composites [12]. It is ideal to develop a numerical approach for calculating material properties of a composite based on experimentally measured shrinkage stress and strain values. This numerical approach allows for accurate

predictions of shrinkage stress in composites at early stages in development. It saves time and money in developing new composites.

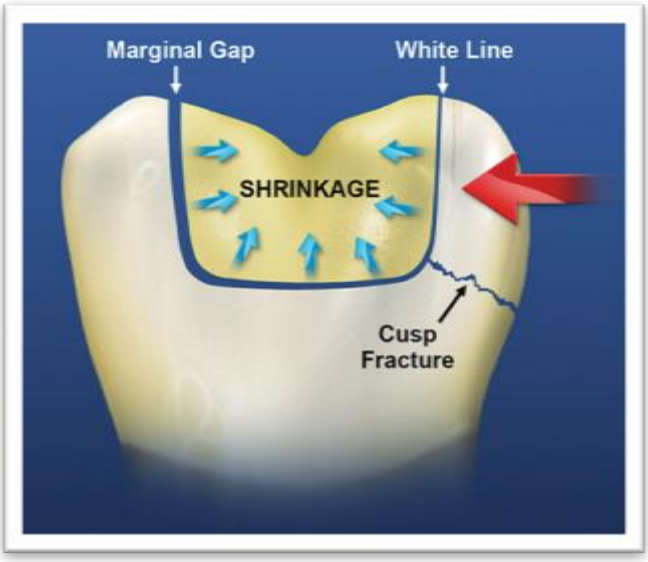

Figure 1.1 Shrinkage stress in a tooth can cause marginal gaps and cusp fractures

Stress in a restoration occurs because of shrinkage. To predict the shrinkage stress with a numerical approach, we need to find the Young's modulus and the shrinkage strain of the restoration as a function of time. This paper focuses on the derivation and validation of a constitutive law, which relates shrinkage stress and shrinkage strain data to the Young's modulus of a material as a function of time.

1.2 Literature Review

Because interfacial stress is impossible to measure, most predictions of shrinkage stress are based on FEA models. For an accurate FEA model of the shrinking process, one must take into account the geometry, boundary conditions, loading, and material properties. The geometry and boundary conditions of models cited in literature are accurate, but accurate material properties are still to be found.

Most FEA models do not take into account their time dependence when developing material properties. For example, a linear-elastic model was used in the FEA model of Versluis et. al [11]. Material properties depended on light intensity and curing time.

Elasto-visco-plastic properties were used in Hübsch et al. [2]. Time dependence was used, associated with the viscosity, and higher stresses were seen at the base of the restoration interface than on the edges. However, the interfacial stress is much lower than expected, 6 MPa, which depends on the Young's modulus that was used in the model. This means more work must be completed to develop an accurate model of Young's modulus.

A visco-elastic model was used by Li et al. [3] to find shrinkage stress in a Class I cavity, but results were high compared to experimental data. Li et al. split the model into multiple steps and summed stress incrementally. They estimated Young's modulus as the

final value in each of the steps, leading to higher shrinkage stress values at the end of cure than shown experimentally.

Visco-elastic models, including the Maxwell model, have been proven to have good agreement with experimental results [10]. Material properties defined by the Maxwell model are Young's modulus and viscosity [10,12]. The models for [10,12] also use the final value of Young's modulus in each step, within the first 100 seconds of cure, when the slope of Young's modulus vs. time is highest.

It is important to understand how Young's modulus behaves during the curing process. As the Young's modulus increases more quickly as a function of time, composite resins develop more stress at the tooth interface. However, the Young's modulus is difficult to measure as a function of time during cure. Because the composite resin changes from a liquid state to a solid during the polymerization process, the composite must develop enough stiffness before the modulus can be experimentally measured. Common methods for measuring the elastic modulus of dental composites include: loading in three-point bending [13], microindentation [14], and impulse excitation [15]. However, these methods only provide measurements of Young's modulus after the composite is cured. The importance of Young's modulus measurement with time is shown experimentally by [10,12]. Dauvillier et al. [10] explains that Young's modulus is low at early points in cure and increases until the composite is fully cured. [10] also showed that the cure rate

will significantly change based on shrinkage stress and shrinkage strain data as well as the model used.

The polymer morphology and filler content of dental composites influences their shrinkage and mechanical properties. Four composites were used in this study: 3M Filtek Z250, 3M Filtek Z350, 3M Filtek P90, and 3M Clearfil P10. Z250 and Z350 are "methacrylate-based composites" [4,5]. As methacrylate-composites cure, linear chains of monomers connect to form polymers, which results in volumetric shrinkage [6]. Z250 and Z350 were reported to have a total volumetric shrinkage of 2% [4,5]. P90 is a "silorane-based composite." Silorane monomers are ring-shaped. During the curing process, the rings open and monomers "flatten and extend to connect." P90 was developed to be a low shrinkage composite, and the technical product profile reports total volumetric shrinkage of about 1% [6]. Interfacial shrinkage stress of 3M Clearfill P10 has been predicted for a class I cavity in an anatomically correct axisymmetric model [3]. The highest stress at the tooth-composite interface was nearly 45 MPa, at the corner of the restoration.

FEA programs such as ABAQUS have modeling capabilities to characterize time-dependent behavior. FEA models can be correlated with experimental cuspal deflection measurements. Cuspal deflections can be measured easily in an experimental setup by using an LVDT as the composite is cured [16]. Early finite element models for shrinkage

such as [1] used only a final value of Young's modulus over the curing time to predict cuspal deflections. However, the cuspal deflections were overpredicted when compared with experimental data. Time-dependent material parameters have been shown to give better correlation to experimental results [2,3,11].

Using only the Young's modulus and Poisson's ratio is not enough for the FEA model. When the dental composite is cured, a reaction occurs. Assuming that the composite is bonded to the tooth interface, the shrinkage strain must be input into the model. More recent FEA models have used the coefficient of thermal expansion (alpha) to input shrinkage strain as a function of temperature, which correlates to the cure time [1,2,11,17].

Dental composites have different levels of opacity. When they are light-cured, not all the light will make it to the bottom of the restoration to cure it. Because the light intensity drops off with depth of composite [17], the shrinkage will be different at different depths. This means that the coefficient of thermal expansion should change with depth of the composite.

1.3 Scope of Work

In this paper, a new method for deriving Young's modulus of dental composites during cure will be discussed. This work is based off of Fok's shrinkage stress and strain numerical relationship from [18].

Experimental shrinkage stress and strain data from Min et al. [7] was used to find the time-dependent Young's modulus of three dental composites: 3M Filtek Z250, Z350, and P90 [4–6]. The developed material properties were applied to an FEA model of the cantilever tensometer used to measure shrinkage stress to prove the self-consistency of the numerical method.

The same material properties were next applied to a cuspal deflection model – an aluminum block with a slot. FEA results were compared to experimental data from Park et al. [16]. The model was refined to use a layered coefficient of thermal expansion approach, which reflects the change in intensity of light with depth of the composite.

Finally, the same material properties were used in a case study of an anatomical tooth. Material properties were applied to an axisymmetric FEA tooth model from Li [17]. Material properties were also calculated for 3M Clearfil P10, and interfacial shrinkage stress results were compared to Li et al. [3].

2 Elastic Modulus Development

2.1 Derivation of Constitutive Law

A one-dimensional model of a composite in an experimental apparatus was used to find a relationship between shrinkage stress and shrinkage strain, or constitutive law, during cure. A Maxwell model, spring and dashpot in series is shown in Figure 2.1. The Maxwell model simulates the composite, and the attached spring refers to the machine stiffness of the experimental apparatus, k. The composite is modeled as a Maxwell element with a stiffness, E, and damping, η, to capture creep.

The composite and apparatus are bounded by fixed conditions on either end. During cure, the composite shrinks (as shown by the net displacement δ), which leads to shrinkage stress, σ, and shrinkage strain, ε_s. An equation for Young's modulus, E, as a function of time, t, will be developed.

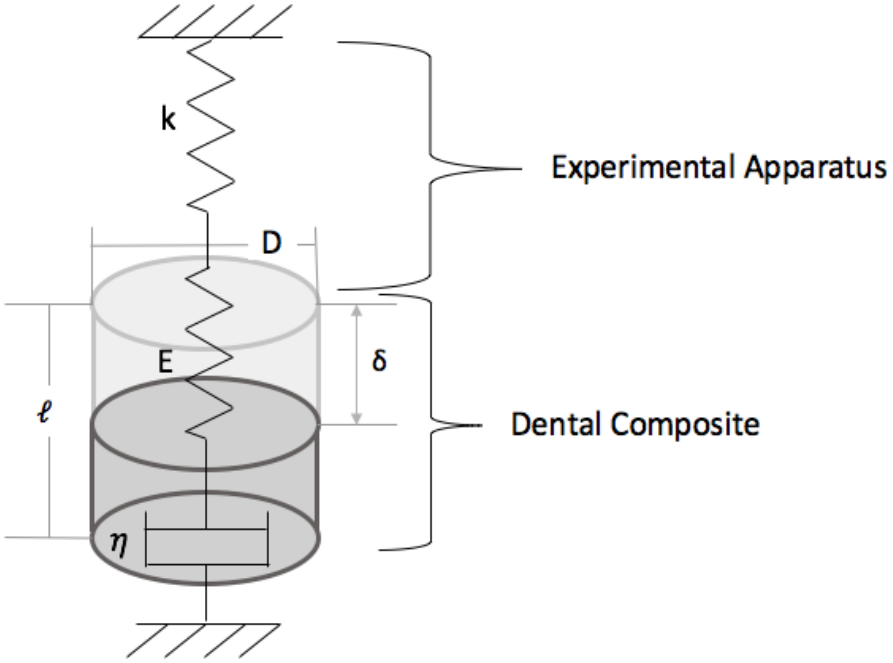

Figure 2.1 Maxwell model used in deriving the constitutive law

The incremental strain of the dental composite can be expressed as

$$d\varepsilon = -\frac{\delta}{l}. \tag{1}$$

where δ is an equilibrium state of the net displacement between the shrinkage of the composite and the machine stiffness and l is the original thickness of the composite.

As derived in Fok's paper [18], the total strain increment ($d\varepsilon$) can be found by summing the elastic ($d\varepsilon_e$), creep ($d\varepsilon_c$), and shrinkage components ($d\varepsilon_s$)

$$d\varepsilon = d\varepsilon_e + d\varepsilon_c - d\varepsilon_s \,. \tag{2}$$

Creep occurs when a material is subjected to stress for long periods of time. The curing time of dental composites is very short (20-40 seconds) and stress development doesn't occur until the composite has been mostly cured. Therefore, creep is very small and can be omitted. So, the total incremental strain is:

$$d\varepsilon = d\varepsilon_e - d\varepsilon_s \,. \tag{3}$$

For the elastic portion, Hooke's law, a relationship between incremental strain, incremental stress ($d\sigma$) and temporal Young's modulus (E) is assumed:

$$d\varepsilon_e = \frac{d\sigma}{E} \,. \tag{4}$$

Substituting (4) into (3) yields

$$d\varepsilon = \frac{d\sigma}{E} - d\varepsilon_s \quad (5)$$

Because the composite and the apparatus are in series:

$$d\sigma = -\frac{k\delta}{A} \quad (6)$$

where k is the machine stiffness and l is the composite thickness. For a cylindrical composite sample, the cross-sectional area is:

$$A = \frac{\pi D^2}{4} . \quad (7)$$

Combining equations (1) and (6)

$$d\varepsilon = -\frac{A}{kl} d\sigma . \quad (8)$$

Substituting (8) into (5)

$$-d\sigma\frac{A}{kl} = \frac{d\sigma}{E} - d\varepsilon_s \quad (9)$$

Then rearranging,

$$d\varepsilon_s = d\sigma\left(\frac{A}{kl} + \frac{1}{E}\right) \quad (10)$$

Finally, the modulus can be determined as a function of shrinkage strain, shrinkage stress, the thickness of the sample, area of the sample, and machine stiffness

$$E = \frac{1}{\frac{d\varepsilon_s}{d\sigma} - \frac{A}{kl}} \quad (11)$$

2.1.1 Reflecting on the Constitutive Law

The derivative of shrinkage strain with respect to shrinkage stress is obtained from experimental data. Although it is hard to measure $\frac{d\varepsilon_s}{d\sigma}$ directly, stress and strain are material characteristics that can be measured experimentally as the composite cures. The strain can be plotted against stress, and the derivative can be found, which is equivalent to $\frac{d\varepsilon_s}{d\sigma}$. For a given experiment, the cross-sectional area and thickness will be defined.

Experimental data must be collected for one-dimensional shrinkage stress as a function of time and one-dimensional shrinkage strain as a function of time. Although time is not shown explicitly in the model, it is implied within the stress and strain values. Temporal strain and stress values are assumed to be known, and the time of cure for stress and strain data are assumed to be the same. Then the derivative of shrinkage strain as a function of shrinkage stress can be found.

When looking at equation (11), the Young's modulus and spring stiffness of the experimental apparatus are unknown. The goal is to determine the Young's modulus as a function of time. So, the spring stiffness must be determined to solve for the Young's modulus.

2.2 Determination of Young's Modulus as a Function of Time

The model described in section 2.1 is applied to determine Young's modulus as a function of time during cure of several dental composites. Published axial shrinkage strain and shrinkage stress data were found for the dental composite resins, 3M Filtek Z250, Filtek Z350, and Filtek P90 [7]. The data were extracted from the paper using WebPlotDigitizer [19]. The same methods can be completed for any one-dimensional stress or strain experimental data.

2.2.1 One-Dimensional Shrinkage Stress

The model requires shrinkage stress to be in a one-dimensional format. In [7], the shrinkage stress was recorded using a cantilever tensometer, which imposes lateral constraints on the composite specimen. The cantilever tensometer records axial shrinkage stress, so the data from the paper is already one-dimensional shrinkage stress. No further calculations need to be completed before using these data in the model. Experimental shrinkage stress data are seen in Figure 2.2.

Note that the shrinkage stress data were taken for 600 seconds of cure. The curing light was turned on after twenty seconds of data collection, so the stress does not begin increasing until this point. The curing light remained on for 40 seconds. After this time, the light was turned off.

The stress increases quickly and shows an exponential trend from zero to a final value of stress as the composites cure. It is questionable whether Z350 has been fully cured, as it does not taper off to a final value of stress at the end data collection at 600 seconds. The final values of shrinkage stress for Z250, Z350, and P90 are 1.59 MPa, 2.74 MPa, and 0.49 MPa, respectively.

The final value of stress is reached at different times for each composite. For Z250, Z350, and P90, the stress reaches the final value at around 420 seconds, 600 seconds, and 300

seconds, respectively. Although P90 reaches its final value before the other composites, it does not initiate until about 60 seconds, much later than the 20 second initiation of the other two composites.

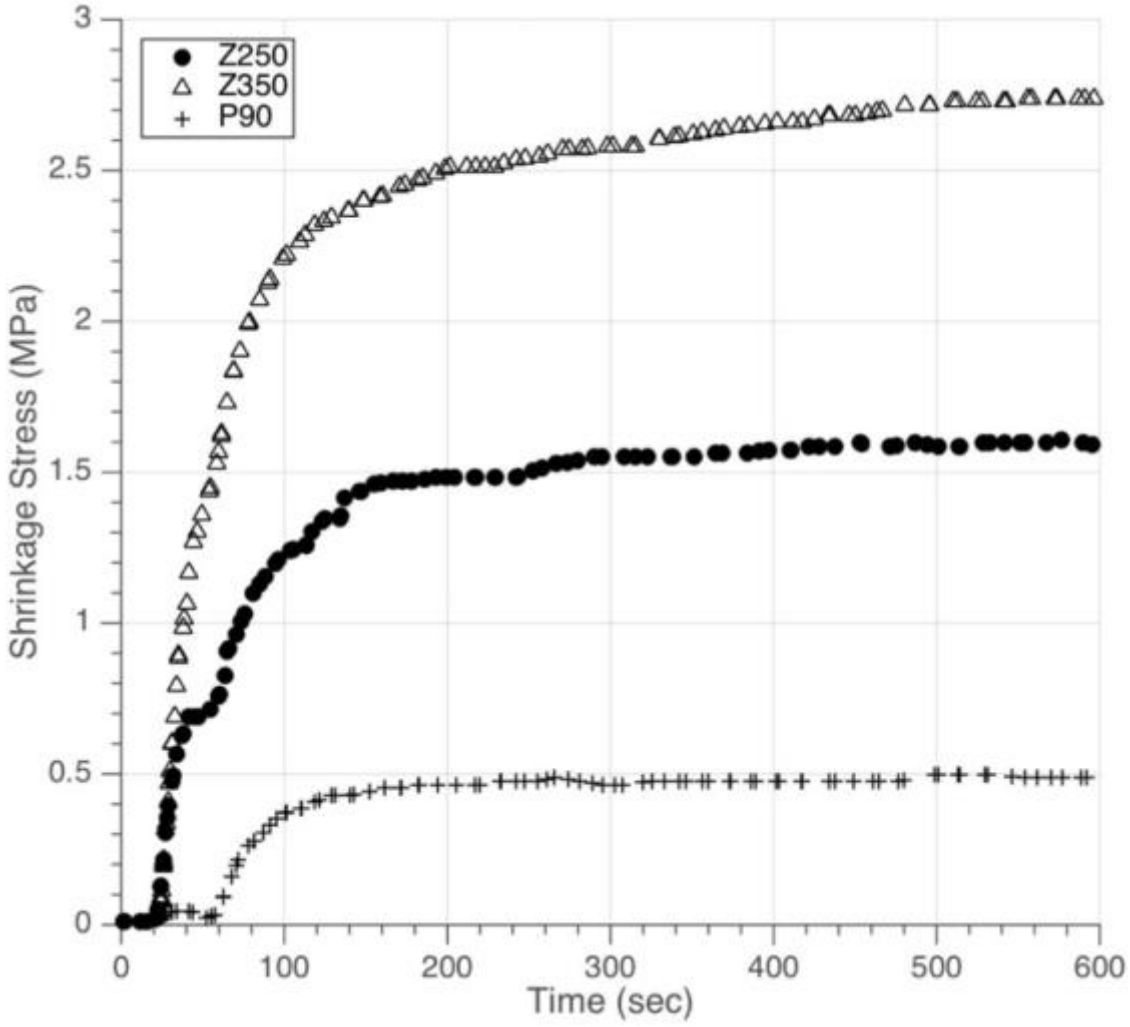

Figure 2.2 Shrinkage stress data for 3 composites from [7]

2.2.2 One-Dimensional Shrinkage Strain

Strain data were gathered separately from the stress data. The strain data from [7] were collected using the bonded-disc method, which imposes lateral constraints on the composite specimen. The lateral constraints cause the strain recorded to be volumetric, or three-dimensional strain. The axial shrinkage strain was extracted from [7] using WebPlotDigitizer [19].

The Maxwell model, equation (11), assumes that stress and strain are given in 1-dimensional values. The stress was given as a 1-dimensional linear shrinkage stress. The strain was given as laterally constrained axial shrinkage strain. Therefore, the strain must be converted to a 1-dimensional linear shrinkage strain.

Hooke's law can be used to relate the linear shrinkage strain (ε_s) to the three-dimensional shrinkage strain (ε_{axial}) reported in the paper and Poisson's ratio (ν):

$$\varepsilon_s = \varepsilon_{axial}\left(\frac{1-\upsilon}{1+\upsilon}\right) \quad (12)$$

Assuming that each composite has low viscosity during cure, the Poisson's ratio was set equal to 0.49. The three-dimensional shrinkage strain was used in equation (12) to find the one-dimensional shrinkage strain.

In the past, one-dimensional shrinkage strain was approximated by dividing the three-dimensional shrinkage strain by three. When the Poisson's ratio is 0.5, assumed to be incompressible, the equation is equivalent to dividing the three-dimensional strain by three.

The experimental data for the one-dimensional shrinkage strain as a function of time can be found in Figure 2.3. Data were collected for 600 seconds, and the curing light was not turned on until the 20 second mark. The strain shows an exponential trend from zero to a final point. Each composite levels out at a final value, which is expected when the composite is fully cured. The final shrinkage strain values for Z250, Z350, and P90 are 0.008, 0.014, and 0.003.

The final strain values for Z250, Z350, and P90 are reached at 300 seconds, 500 seconds, and 200 seconds, respectively. When comparing the final strain values to the final stress values, the stress lags behind the strain by 100 seconds. In the derivation of the model, it was assumed that the strain and stress would cure at the same time. This may cause problems with future finite element results.

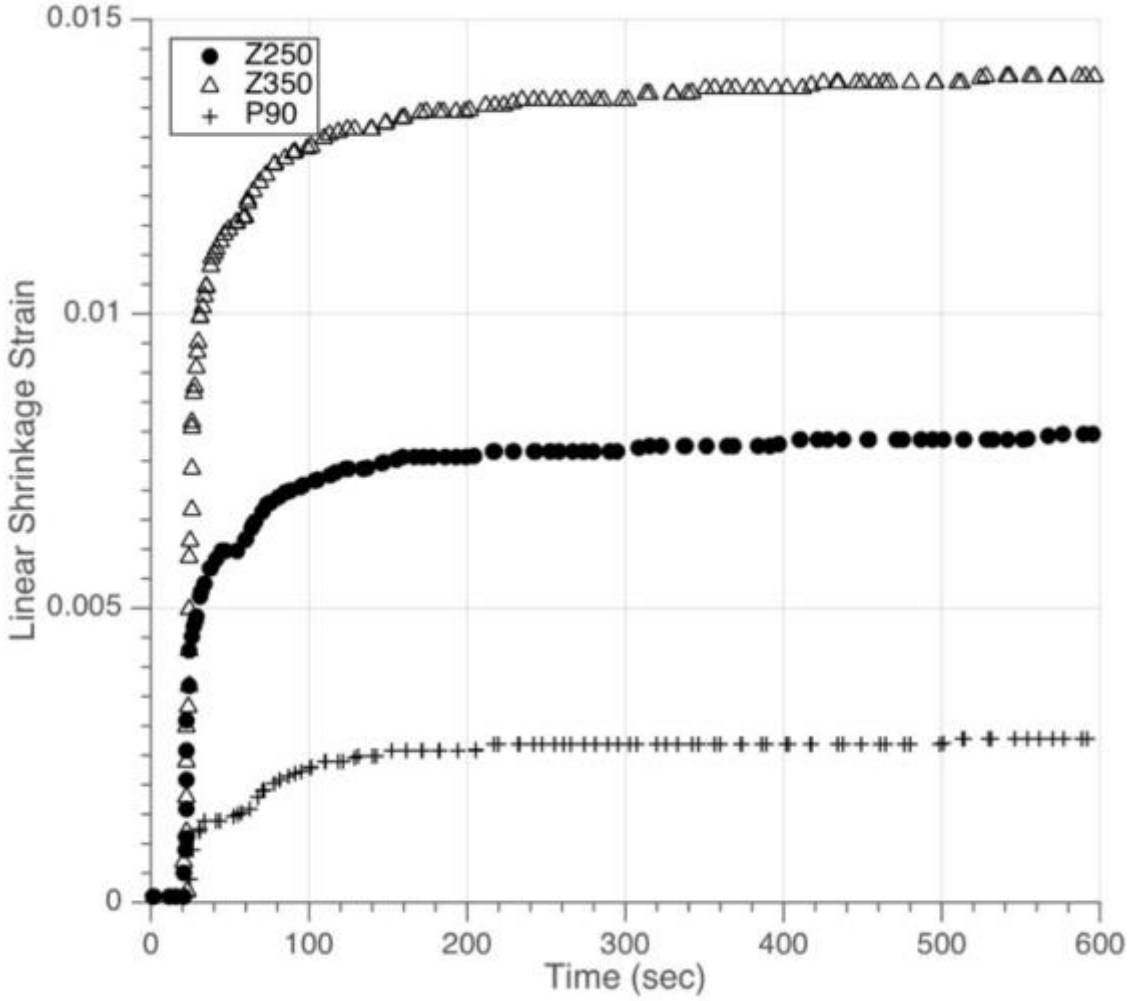

Figure 2.3 Shrinkage strain data for three composites from [7]

2.2.3 Derivative of Shrinkage Strain with Respect to Stress

The derivative of shrinkage strain with respect to stress must be found. So far, the one-dimensional shrinkage stress and strain have been obtained experimentally. Assuming that the curing time was the same for both sets of data, the strain can be plotted against stress, as seen in Figure 2.4.

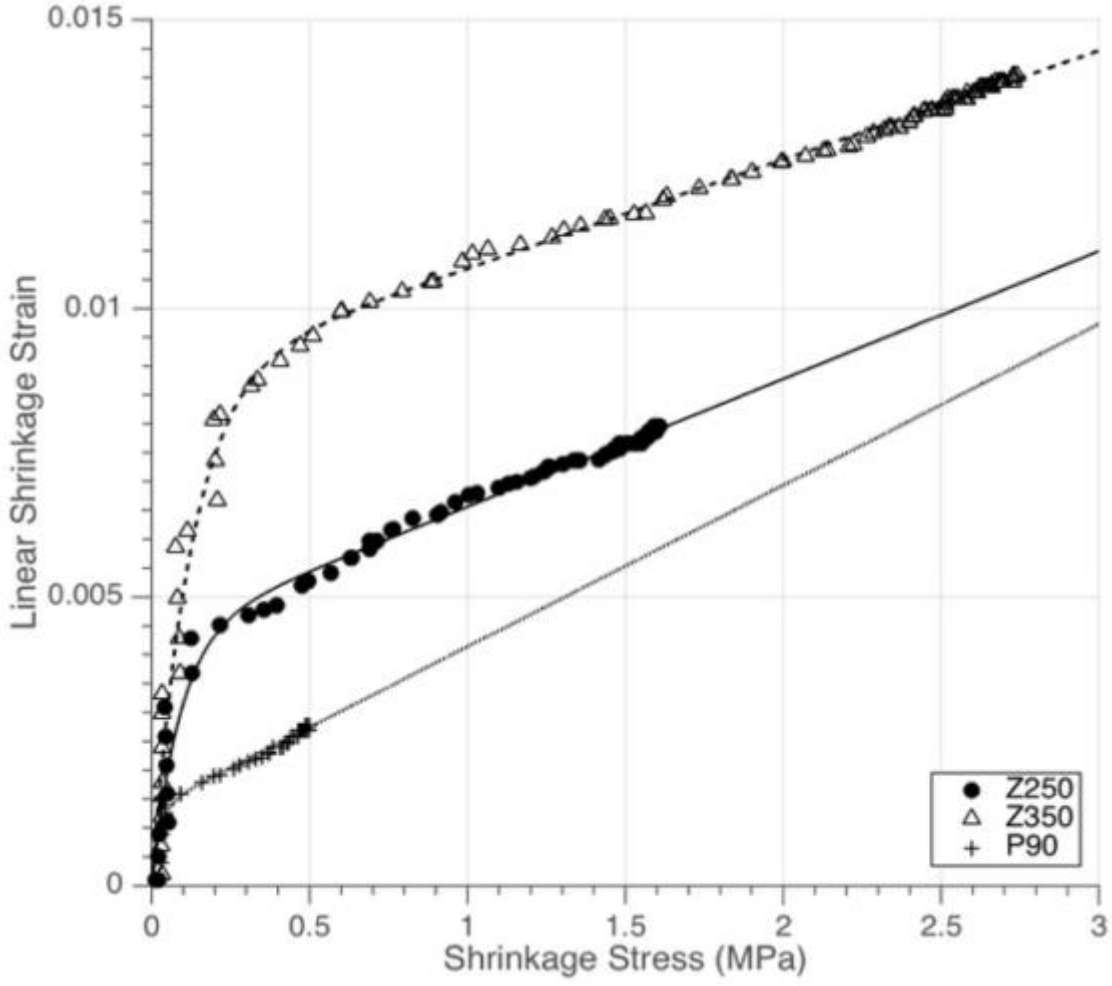

Figure 2.4 Fitting a curve to linear shrinkage strain as a function of shrinkage stress

Each of the data sets shows an exponential trend at the beginning of cure and a linear trend at the end of cure. MATLAB [20] was used to fit shrinkage strain and stress experimental data to an equation of the form:

$$\varepsilon_s = (a\sigma + b)(1 - e^{-c\sigma}) . \quad (13)$$

At the beginning of time, when stress is small, the equation is exponential. When the stress is higher, the exponential part of the equation is negligible, and the linear part is active.

The shrinkage strain vs. shrinkage stress data were fit using nonlinear least squares and optimizing to equation (13). The parameters a, b, and c were determined, and can be seen in Table 2.1 below.

Table 2.1 Coefficients of dental composites for strain-stress fit

	a (MPa^{-1})	b	C (MPa^{-1})
Z250	0.002	0.004	11.838
Z350	0.002	0.009	8.362
P90	0.003	0.001	37.622

The fit lines with the coefficients shown in Table 2.1 are also plotted in Figure 2.4. The R-squared error for each fit line to the experimental data were 0.9869, 0.9885, and 0.9193 for Z250, Z350, and P90, respectively. The end points of each set of data correlate to the final stress and strain data points from the early temporal plots, Figure 2.2 and Figure 2.3.

The derivative of equation (13) is:

$$\frac{d\varepsilon_s}{d\sigma} = a + bc(e^{-c\sigma}) - a(e^{-c\sigma}) + ac\sigma(e^{-c\sigma}) . \quad (14)$$

For each composite, the constants a, b, and c were used with the one-dimensional stress to find $\frac{d\varepsilon_s}{d\sigma}$.

2.2.4 Finding the Spring Stiffness of the Experimental Apparatus

To find the Young's modulus in equation (11), E(t) should be the only unknown. The thickness and cross-sectional area of the experiment are known from examination of the composite sample. The derivative of shrinkage strain as a function of stress is assumed to be known from section 2.2.3. The spring stiffness of the machine apparatus is unknown and must be determined.

The stiffness of an experimental apparatus can be difficult to measure. In a cantilever tensometer, the instrument used to measure shrinkage stress in [7], the stiffness will vary based on the placement of the composite and the stiffness of joints. If the composite was shifted slightly between runs, the machine stiffness would change.

If final values of the variables are used in equation (11), the spring stiffness can be evaluated. Equation (11) is rearranged to obtain the stiffness of the measuring instrument

$$k = - \frac{A}{l\left(\frac{1}{E_{final}} - \frac{d\varepsilon_s}{d\sigma}\Big|_{final}\right)}. \quad (15)$$

The final value of Young's modulus is known from technical product profiles of each dental composite. The derivative of shrinkage strain with respect to stress is known. The cross-sectional area and thickness of the composite sample are known.

The derivative of shrinkage strain with respect to shrinkage stress is taken as the final result from section 2.2.3. After closer analysis, the final result of the derivative is equivalent to the slope of the line in Figure 2.4.

Values for these parameters and the calculated stiffness are listed in Table 2.2.

Table 2.2 : Experimental values and calculated stiffness for Z250, Z350, and P90

	Z250	Z350	P90
E_{final} (GPa)	11	9.2	9.6
$\left.\frac{d\varepsilon}{d\sigma}\right\|_{final}$ (1/MPa)	0.002	0.02	0.003
A (mm^2)	7.07	7.07	7.07
ℓ (mm)	1	1	1
k (N/mm)	3300	3980	2630

The spring stiffness was calculated for Z250, Z350, and P90 as 3300 N/mm, 3980 N/mm, and 2630 N/mm.

Min et al. measured the stiffness of the experimental apparatus used to collect stress data [7]. The machine stiffness was reported to be 2128 N/mm. This value is similar in magnitude to the values that were calculated for Z250, Z350, and P90. However, the values calculated above are all higher than the reported value. The difference may come from the lag in stress data behind strain data.

2.2.5 Young's Modulus as a Function of Time

Now that all other variables in equation (11) are known, the Young's modulus can be calculated. Equation (11) was used with one-dimensional stress and strain data to find the temporal Young's modulus. Plots for each resin are shown in Figure 2.5.

The Young's modulus shows an exponential trend. The final values for Z250, Z350, and P90 are 11 GPa, 9.2 GPa, and 9.6 GPa, which matches the values in technical product profiles. P90 increases more slowly than the other two resins, which is likely due to the slow initiation of stress development that was discussed in Figure 2.2.

Once cure has been initiated, Young's modulus increases quickly. At twenty seconds, the curing light was turned on, and the composites began polymerizing. After cure initiation, Z250, Z350, and P90 reach the final value of Young's modulus within 70 seconds, 40 seconds, and 60 seconds, respectively.

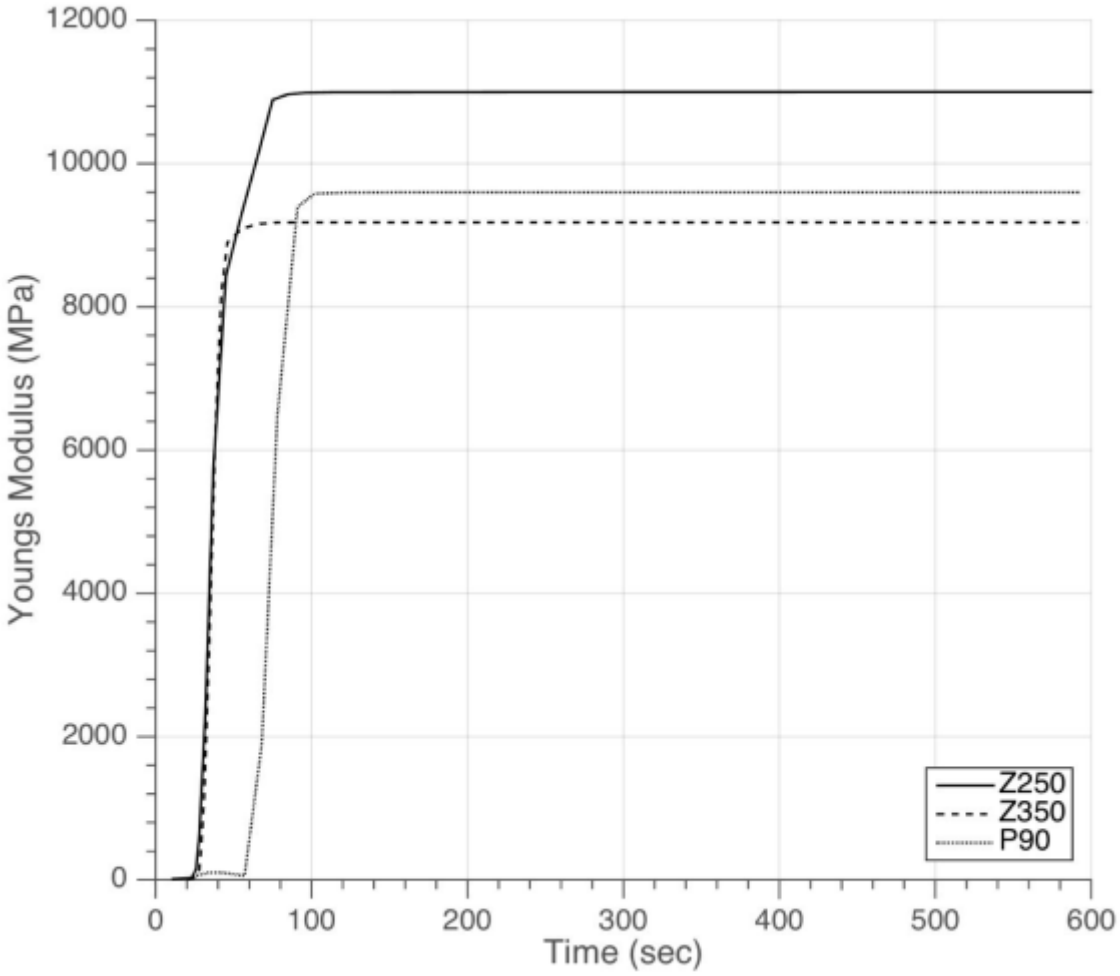

Figure 2.5 Young's Modulus for Z250, Z350, and P90

3 Finite Element Implementation

Shrinkage stress at the interface between a dental composite and the surface of a tooth cavity is difficult, if not impossible, to measure experimentally. Therefore, shrinkage stress at the tooth-composite interface was calculated numerically using finite element models.

First, material properties (time-dependent Young's modulus and Poisson's ratio) derived in the previous chapter were verified for self-consistency by comparing finite element analysis results to experimental results for the shrinkage stress measurement [7], which provided the data for material property derivation. The same material properties and loading conditions (shrinkage strain) were then applied to an aluminum block that modeled a restored tooth, and the "cuspal" deflections and interfacial shrinkage stress were calculated as a function of time. The "cuspal" deflection results for the model tooth were compared to experimental results from [16] to validate the procedure. Finally, an anatomically accurate model was used to analyze the shrinkage stress at the tooth-composite interface of a restored tooth.

3.1 Modeling Approach

3.1.1 Loading Conditions

The loading due to polymerization shrinkage of the composite was modeled as thermal shrinkage by giving the composite a pseudo coefficient of thermal expansion with

negative values that changed with time. The model was subjected to an increase in temperature, which was numerically the same as the time increment (Δt_i) at each step. To implement the changes in material properties with time, the temperature (or time) was defined in Abaqus as a field, and the material properties as field variables. The shrinkage strain increment at every step ($\Delta \varepsilon_s$) was implemented via a coefficient of thermal expansion for the ith time increment (α_i) using the following equation:

$$\alpha_i = -\frac{\Delta \varepsilon_{si}}{\Delta t_i}. \tag{16}$$

The minus sign implies shrinkage of the composite.

Stresses and displacements were calculated for each time increment. The results were cumulatively summed with MATLAB to find the final stress and displacement values. The process can be seen in Figure 3.1, below, together with that for determining the time-dependent material properties. After completing this analysis, it was discovered that NLGEOM can be added to steps in ABAQUS to allow model restart. If this were used, ABAQUS would automatically sum stresses from each step.

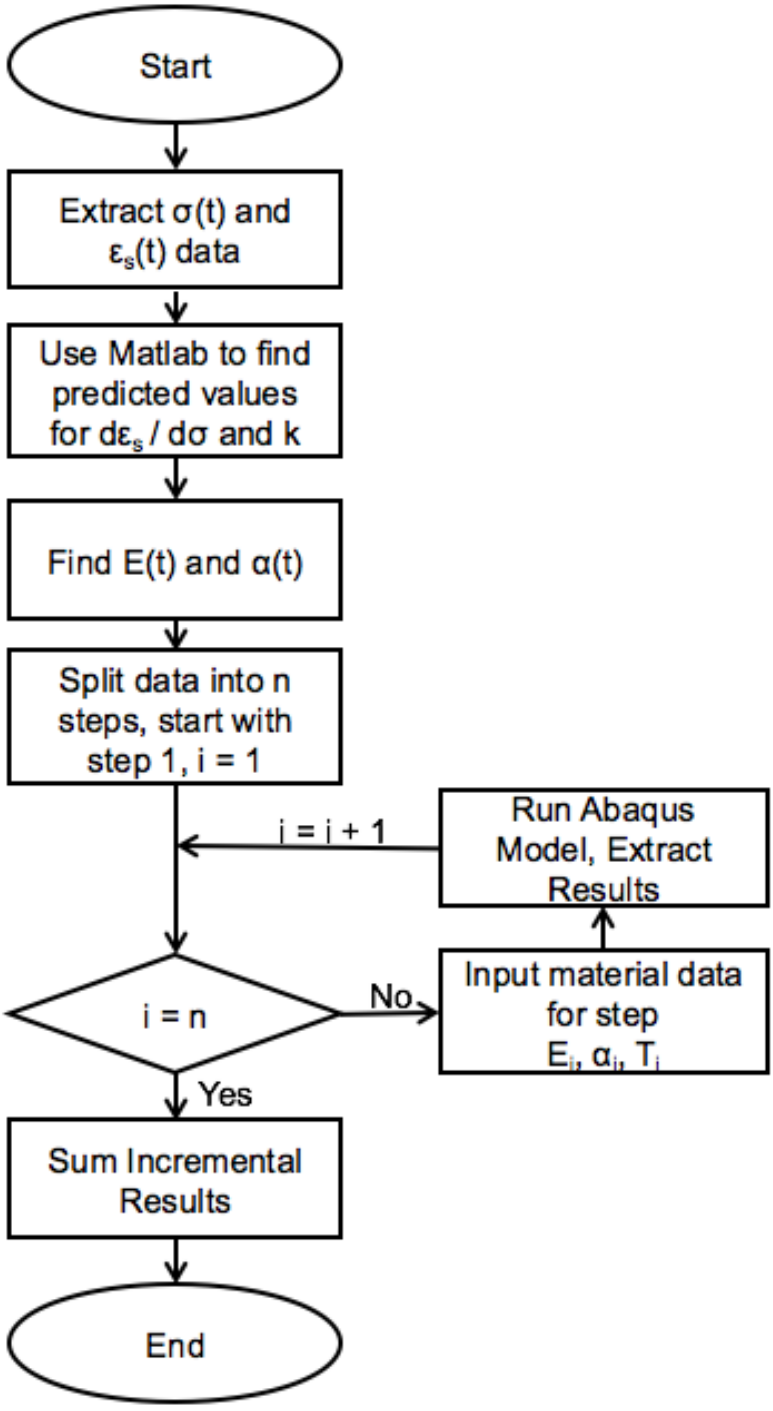

Figure 3.1 Flow chart for shrinkage stress calculation

3.1.2 Material Properties

During cure the Young's modulus of a dental composite shows an exponential relationship with time. Thus, shrinkage stress must be calculated incrementally, using Young's modulus values as a function of time. The increase in Young's modulus was more rapid at the beginning of cure, so more steps with smaller time increments were used at the beginning of time. Fewer steps with larger time increments were used towards the end of cure when the values were nearly constant.

For the finite element analysis, the material was modeled as isotropic with the derived Young's modulus, coefficient of thermal expansion, and Poisson's ratio. Shrinkage stress and shrinkage strain data from Min et al. [7] were used to determine the coefficient of thermal expansion and Young's modulus as a function of time.

The Poisson's ratio was defined as a step function of time based on the shrinkage strain value. The Young's modulus reaches a fully cured state within 40 seconds, so the dependence of Poisson's ratio with time is minimal. When the composite is flowable, it is assumed to be behaving like an incompressible liquid, i.e., the Poisson's ratio is 0.49—a value just below 0.5 is used to avoid numerical problems. When the composite reaches the gel point, the Poisson's ratio is 0.35, a typical value for polymers. The Poisson's ratio changed from 0.49 to 0.35 when the shrinkage strain reached 90% of the final value.

Material properties for the three dental composites for each step of the finite element analysis are found in Table 3.1.

Table 3.1 Material property data for Z250, Z350, and P90

Z250				
Step #	Time (sec)	Young's Modulus (MPa)	Alpha	Poisson's Ratio
1	11	12	-4.96E-05	0.49
2	21	24	-4.00E-05	0.49
3	23	31	-5.40E-04	0.49
4	24	61	-1.57E-03	0.49
5	26	157	-4.18E-04	0.49
6	28	632	-3.06E-04	0.49
7	32	2383	-9.34E-05	0.49
8	37	5735	-6.24E-05	0.49
9	45	8423	-1.74E-05	0.49
10	55	9290	-5.09E-06	0.49
11	66	10152	-4.11E-05	0.49
12	75	10891	-2.86E-05	0.49
13	85	10969	-2.20E-05	0.49
14	96	10990	-1.67E-05	0.49
15	113	10995	-6.32E-06	0.35
16	216	10998	-4.85E-06	0.35
17	315	11000	-1.53E-06	0.35
18	411	11000	-5.40E-07	0.35
19	513	11000	-2.36E-07	0.35
20	595	11000	-1.73E-07	0.35

Z350				
Step #	Time (sec)	Young's Modulus (MPa)	Alpha	Poisson's Ratio
1	21	9	-9.58E-05	0.49
2	23	18	-6.57E-05	0.49
3	24	23	-2.46E-03	0.49
4	26	51	-1.48E-03	0.49
5	28	142	-6.51E-04	0.49
6	29	406	-6.36E-04	0.49
7	31	1088	-1.87E-04	0.49
8	34	3054	-1.36E-04	0.49
9	38	6054	-9.35E-05	0.49
10	42	8154	-8.60E-05	0.49
11	46	8899	-6.54E-05	0.49
12	55	9088	-3.03E-05	0.49
13	65	9156	-5.34E-05	0.49
14	78	9178	-3.78E-05	0.49
15	91	9180	-2.14E-05	0.35
16	124	9180	-1.11E-05	0.35
17	149	9180	-5.08E-06	0.35
18	202	9180	-4.01E-06	0.35
19	301	9180	-1.29E-06	0.35
20	402	9180	-1.48E-06	0.35
21	496	9180	-1.14E-06	0.35
22	597	9180	-4.23E-07	0.35

P90				
Step #	Time (sec)	Young's Modulus (MPa)	Alpha	Poisson's Ratio
1	22	23	-3.68E-05	0.49
2	25	52	-4.71E-05	0.49
3	27	63	-4.26E-05	0.49
4	30	82	-4.72E-05	0.49
5	34	99	-7.08E-06	0.49
6	42	303	0.00E+00	0.49
7	52	75	3.97E-05	0.49
8	57	58	-4.63E-05	0.49
9	68	1885	-6.77E-05	0.49
10	78	6465	-2.89E-05	0.49
11	91	9398	-1.47E-05	0.49
12	102	9581	-1.14E-05	0.49
13	122	9596	-5.72E-06	0.49
14	152	9599	-2.50E-06	0.35
15	172	9600	-1.61E-06	0.35
16	206	9600	-9.30E-07	0.35
17	247	9600	-7.71E-07	0.35
18	303	9600	5.65E-07	0.35
19	346	9600	-7.36E-07	0.35
20	402	9600	0.00E+00	0.35
21	501	9600	-6.39E-07	0.35
22	592	9600	-6.48E-07	0.35

3.1.3 Coefficient of Thermal Expansion: Uniform vs. Layered

For the tooth model case study, the effect of depth in the curing process was considered. The amount of cure in a composite depends on the distance from the light source. Li et al. [17] showed that shrinkage strain decreases with depth from the light curing source (Figure 3.2). Due to oxygen inhibition of polymerization at the surface, the highest strain occurred 1 mm from the surface. The strain decreased from 1 mm to 5 mm away from the surface. The volumetric shrinkage strain vs. depth data were extracted from [7] using

WebPlotDigitizer, and the data were normalized to express as percentages of the peak shrinkage strain with respect to depth. In formulating the finite element model of the restoration, the restoration was divided into several layers. For each layer, the strain data from Min et al. [7], and therefore the coefficient of thermal expansion of the composite, were modified for each step to take the depth of cure into account. The original coefficient of thermal expansion, α_i at each step, i, was multiplied by the relative shrinkage strain in the layer to find the new coefficient of thermal expansion for that layer.

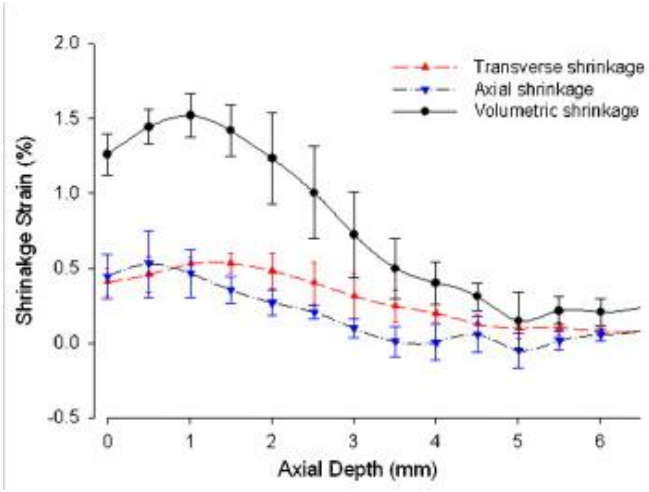

Figure 3.2 Shrinkage strain as a function of distance from the irradiation surface [17]

3.2 Self-Consistency Check

A spring-disc model was created for the shrinkage stress measuring experiment to check the self-consistency of the constitutive model. The predicted stress results were expected to match the experimental values used to find Young's modulus.

The geometry of the axisymmetric model can be seen in Figure 3.3. The bottom of the disc was fixed in the vertical direction. A spring, representing the stiffness of the experimental apparatus, was connected to the top center node of the composite disc. The stiffness of the spring was calculated. The other end of the spring was fixed in space.

The shrinkage strain of the composite as a function of time was applied to the model as described above. The resulting force in the spring was used to calculate the axial stress and compared with the experimental results from [7].

The Young's modulus and shrinkage strain were input incrementally as functions of time in several input files. The input files were run, and the force in the spring was output. Stress was assumed to be axial only, so the force in the spring was divided by the cross-sectional area of the disc. The stress was summed over the increments to find the increase in total stress as a function of time. This was compared to the original stress data from the experiment by Min et al. [7].

Eight-node axisymmetric (CAX8 or CAX8R) elements were used for the disc model. A total of 600 elements made up the composite section. A single node defined the fixed end of the spring in space above the model. Reduced-integration elements (CAX8R) were used when Poisson's ratio was 0.49. When Poisson's ratio switched to 0.35, full-integration elements were used.

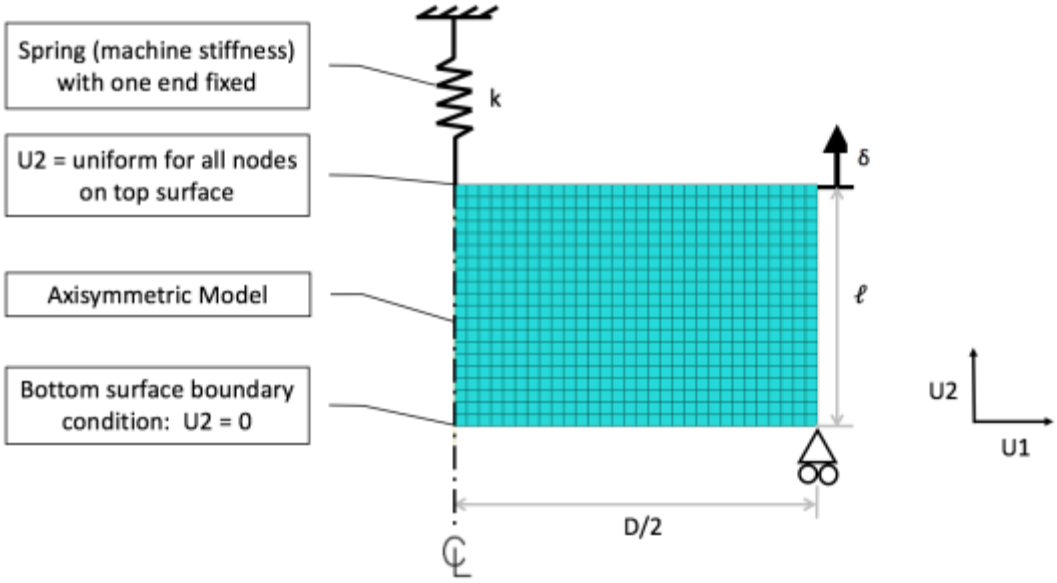

Figure 3.3 Axisymmetric disc model for self-consistency check

3.3 Aluminum Cuspal Model

The aluminum block used by Park et al. [16] to model a restored tooth was simulated. Cuspal deflection results from [16] were used to validate the constitutive model. A 3D model was created in Abaqus [21] of the aluminum block with dimensions 10 mm x 8 mm x 15 mm. A 6 mm x 8 mm x 4 mm slot was machined from the top of the block. A separate composite restoration with dimensions 6 mm x 8 mm x 4 mm was created to fill the cavity in the aluminum model.

An adhesive was used on the bottom and two side faces of the composite and was bonded to the corresponding surfaces of the slot in the aluminum block. The geometry of the model can be seen in Figure 3.4. Loading was applied through the shrinkage strain of the composite as a function of time. The horizontal displacement of the "cusps" was extracted at each time step, and the results were cumulatively summed to determine the increase in displacement with curing time. The deflection results were compared to the experimental data by Park et al. [16]. Interfacial stresses were also evaluated to characterize the relative magnitude between materials and the location of peak stress.

The material properties for the aluminum cuspal model remained the same as those for the self-consistency model. Data for Young's modulus and the shrinkage strain for the first 600 seconds were derived from the results given by Min et al. [7]. The model was compared to experimental results from [16].

Three-dimensional 20-node (3D20) elements were used for the aluminum block and the composite sections. The aluminum section contained 45306 elements, and the dental composite section contained 50880 elements. Reduced-integration elements were used at the beginning of time, when the composite was assumed to be nearly incompressible and have a Poisson's ratio of 0.49. When the Poisson's ratio dropped to 0.35, full-integration elements were used.

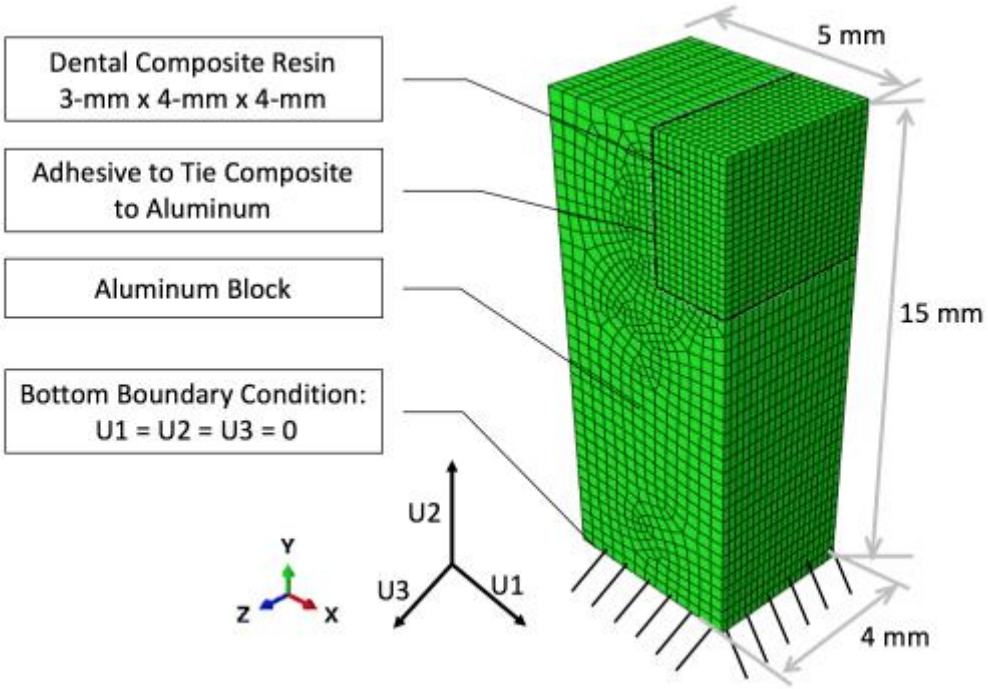

Figure 3.4 Aluminum block used for "cuspal" deflection measurements

3.4 Anatomically Accurate Tooth Model

The interfacial stresses were calculated for a tooth restoration using an anatomically accurate model. The axisymmetric model was adopted from Li et al. [3], who determined the stresses by performing linear elastic calculations only at each time point, albeit with changing Young's modulus and shrinkage strain values. The model contained three different material sections: enamel, dentine, and composite. The enamel and dentine sections were given constant material properties over all the steps. The composite section was given the same time-dependent material properties and loading conditions used in the previous finite element models, and stresses were calculated incrementally.

In [3], the shrinkage stress was measured at the composite-tooth interface for 3M Clearfill P10. Radial shrinkage stress of P10 was calculated at the vertical interface between the tooth and composite surfaces. The average radial stress was also calculated for two sections of nodes at section 1 and section 2, as seen in Figure 3.5. The stress-state of the nodes depended on the depth in the restoration.

Young's modulus and the coefficient of thermal expansion were calculated for P10 using the same methods described in Chapter 2. Interfacial shrinkage stress results for the vertical portion of the interface for 3M Clearfill P10 were compared to results in [3].

Radial shrinkage stress averaged over section 1 and section 2 was also compared to results in [3]. Calculations were also completed for Z250, Z350, and P90.

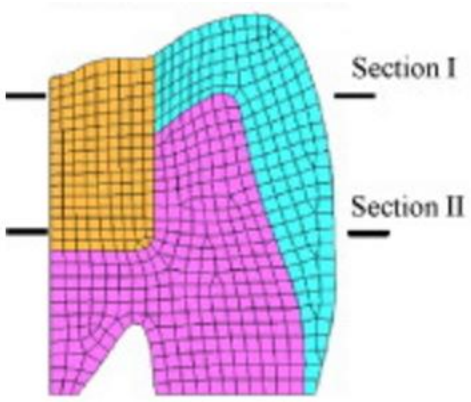

Figure 3.5 Section assignments for axisymmetric tooth [3]

The tooth is 6 mm wide and 8.3 mm high at the highest point. The composite restoration is 2.3 mm wide and 4 mm high. The dentine and enamel are created with CAX4I elements, while the composite section contains CAX3 elements. Dentine, enamel, and composite contain the following number of elements: 275, 160, and 145, respectively.

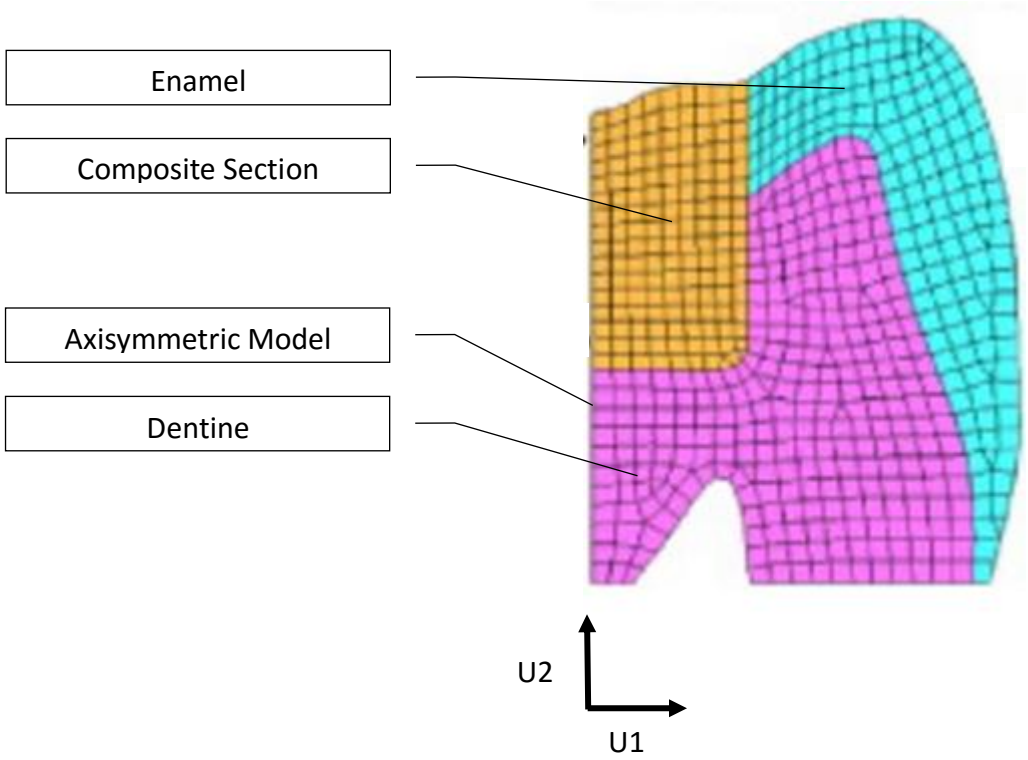

Figure 3.6 Axisymmetric model for a restored tooth

4 Results and Discussion

4.1 Self-Consistency Check

An axisymmetric model of the one-dimensional Maxwell model that is shown in Figure 2.1 was created. The axisymmetric disc model was used to check the self-consistency of the incrementally averaged approach to determine the Young's modulus and coefficient of thermal expansion. The reaction force in the spring was determined for each time step and divided by the cross-sectional area to find the incremental axial stress. The

incremental axial stress was cumulatively summed to find the total stress as a function of time.

Z250

Experimental data from Min et al. [7] were compared to the proposed incremental averaged method incremental averaged method of calculating Young's modulus (see Chapter 2) and the stepwise method of calculating Young's modulus, described in [3]. In the incremental averaged method, Young's modulus was averaged between time steps, which leads to lower Young's modulus values for each time step than the stepwise method. The stepwise method does not include averaging between steps, leading to higher values for each time step.

Figure 4.1 shows stress vs. time predictions for two sets of Young's modulus and coefficient of thermal expansion data, where the incremental averaged method results are based on material properties from Table 2.2, and stepwise method results are based on material properties from Table 1 in Li et al. [3]. These model predictions are compared to experimental data provided by Min et al. [7].

FE results and experimental data for modulus vs. time showed an exponential trend. The final experimental stress for Z250 was 1.59 MPa [7]. The incremental averaged and stepwise methods gave final stress values of 1.68 MPa and 2.06 MPa, respectively. The

incremental averaged method averages the Young's modulus between time steps, which yields smaller values for modulus (compared to the stepwise method), especially at the beginning of time when the modulus increases very quickly.

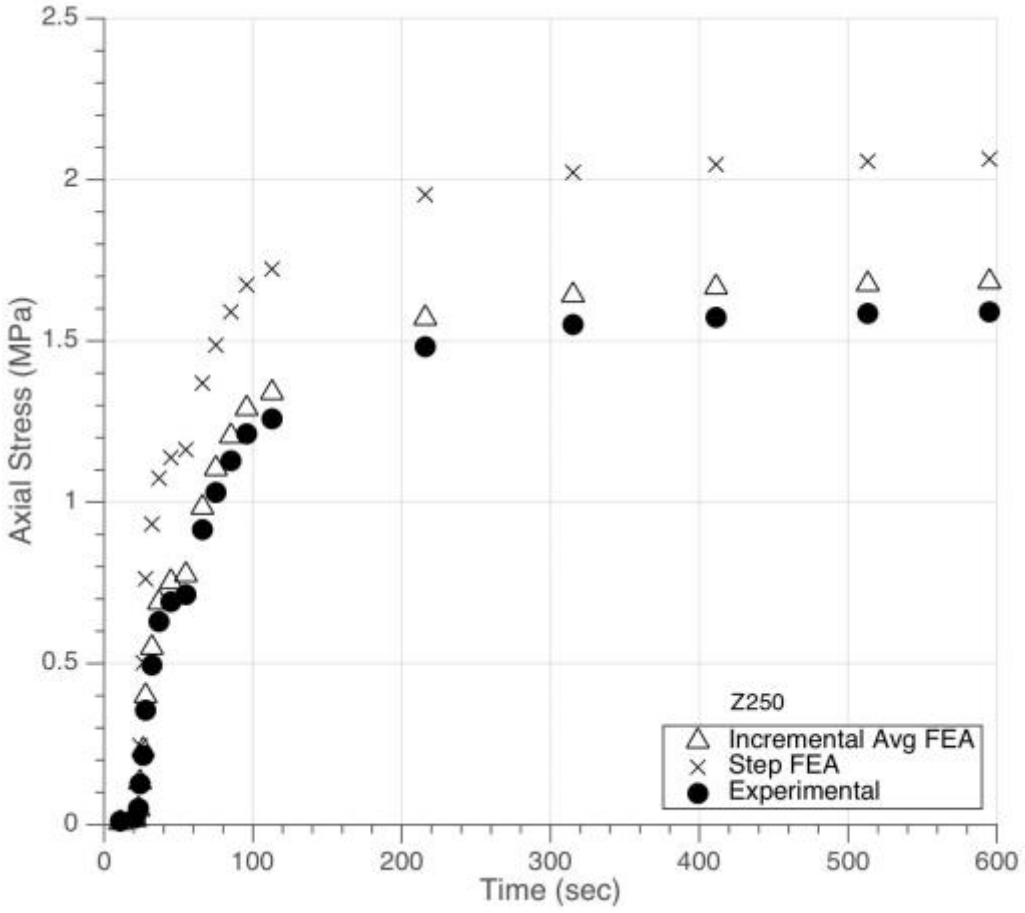

Figure 4.1 Axial stress comparison of spring-disc self-consistency results for Z250 from Min et al. [7]

High resolution experimental data are important to avoid discrepancies between finite element results and experimental results. The Young's modulus critically affects the axial

stress. With a higher Young's modulus, the axial stress increases. When steps in Young's modulus are large at the beginning of cure, there are large jumps in axial stress. With 10 time steps, or data points, FEA results overshoot the experimental data, as seen in Figure 4.2. With 22 time steps, as shown in Figure 4.3, the FEA results more closely match experimental data. Experimental data for material properties were extracted using an online digitizer [19], and the stress-strain data had a low resolution. As many data points were extracted as resolution allowed at the beginning of time, when the slope of Young's modulus is the greatest. Small time increments are required for FEA to obtain an accurate prediction of stress, especially early in cure when the Young's modulus is increasing rapidly. With the incremental averaged method that is presented here, fewer time steps must be used to achieve an accurate calculation of stress. Previous finite element analysis used only the final value of Young's modulus at a step. At least 2 times more data points must be used with the step method to match the incremental averaged method results.

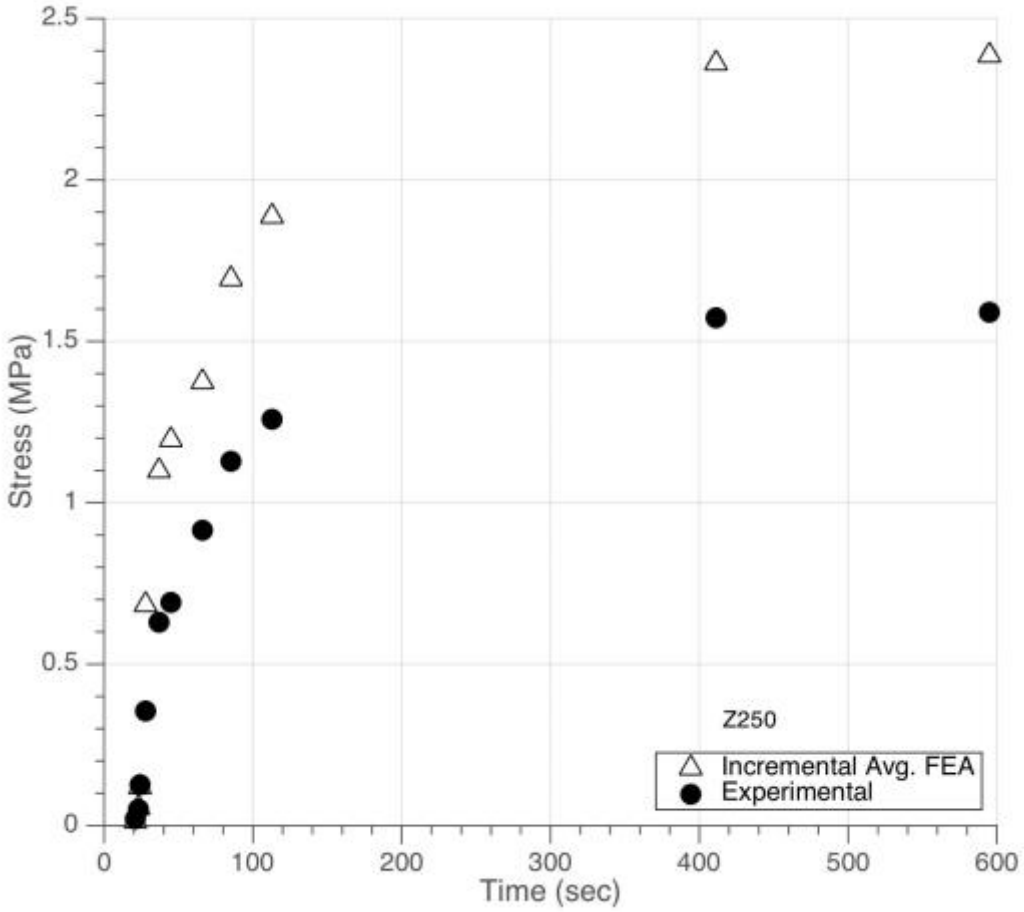

Figure 4.2 Axial Stress comparison of spring-disc self-consistency results for Z250, fewer data points with experimental results from Min et al. [7]

Z350 and P90

FEA results for Z350 and P90, labeled "Incremental Avg. FEA," were compared to experimental data from [7], labeled "Experimental." As with the Z250 resin composite, axial stress in both Z350 and P90 rapidly increases and asymptotically approaches a final value. For Z350 (Figure 4.3), the FEA results show a final stress of 2.48 MPa, compared

to an exponential value of 2.74 MPa. The stress increases quickly in the first 80 seconds of cure.

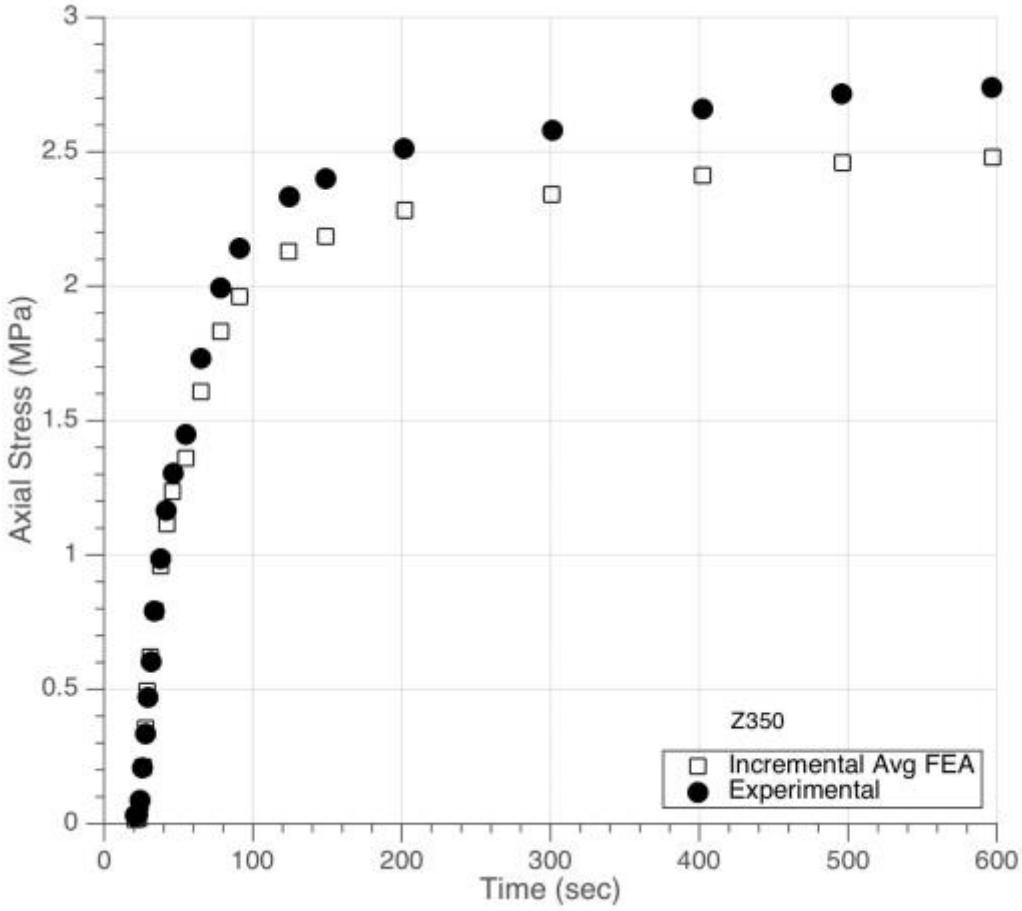

Figure 4.3 Axial stress comparison of spring-disc self-consistency results for Z350 from Min et al. [7]

The "silorane-based" P90 is reported to develop the lowest stress of the three composites that were analyzed. Results for P90 are shown in Figure 4.4. Experimental data for P90 reached a final stress of 0.49 MPa, and the FEA data showed a final stress of 0.56 MPa.

During the first 40 seconds of cure, silorane monomer rings opened and then linked up to form polymers. This resulted in lower stress values between 20 seconds and 60 seconds. At 60 seconds, the "ring-opening" process has been completed. Final cross-linking in the polymer chains occurs along with some volumetric shrinkage, associated with axial stress [7].

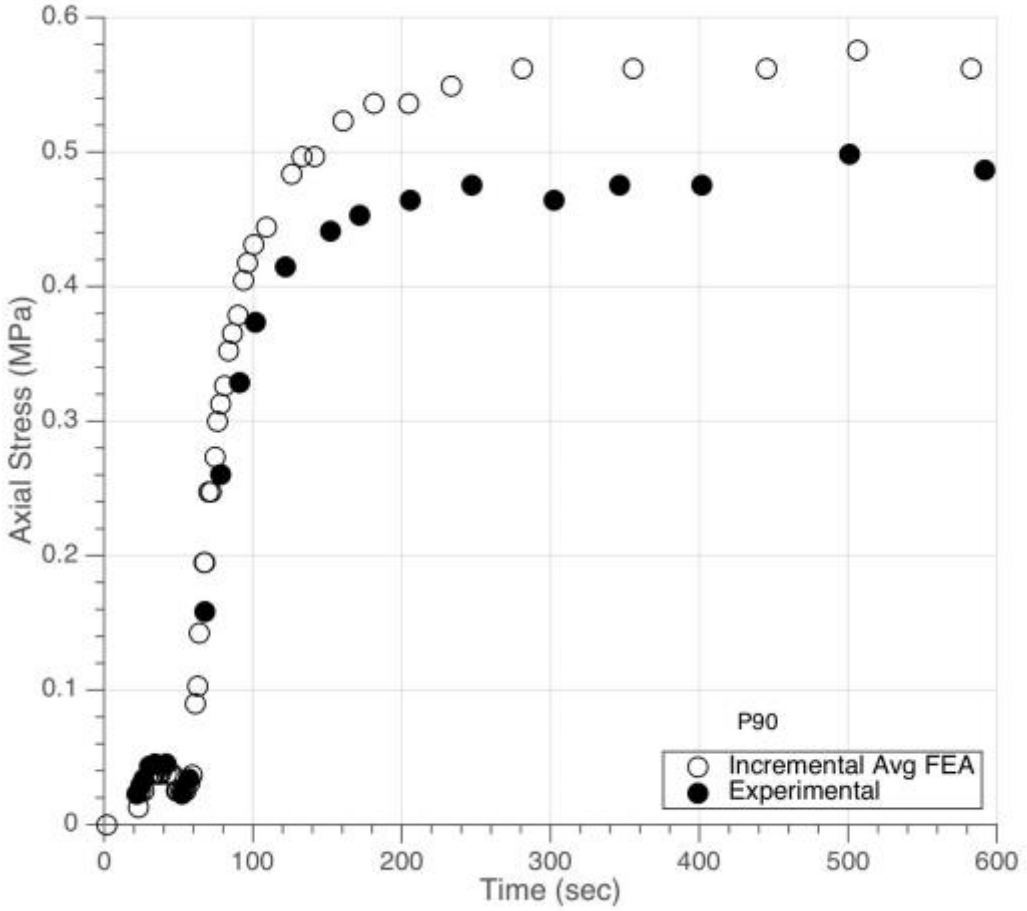

Figure 4.4 Axial stress comparison of spring-disc self-consistency results for P90 from Min et al. [4]

In summary, FEA results showed final axial stresses of 1.68 MPa, 2.48 MPa, and 0.56 MPa of Z250, Z350, and P90, respectively. Z250 and Z350 are methacrylate-based polymers, so higher shrinkage stress is anticipated when compared with P90. These values are compared with the final experimental results of 1.59 MPa, 2.74 MPa, and 0.49 MPa. Overall, the fit is good. The initial cure is critical. The steep rise at the beginning of the stress and strain charts, seen in Figure 2.2 and Figure 2.3 is difficult to capture with WebPlotDigitizer [19] since experimental data used were directly from plots in published papers. The maximum number of data points was extracted for each graph, but the points are almost vertical at the beginning of time. More resolution on graphs, especially at the beginning of cure, is needed for better agreement between experimental and predicted stress values.

4.2 Cuspal Deflection Model

4.2.1 Deflection Data and Model Predictions

Z250

The "cuspal" deflection of the side of the aluminum block FEA model was extracted at 1 mm from the top at the center edge of the aluminum block. The deflections were incrementally summed to find the deflection of the aluminum edge as a function of time.

The Young's modulus and coefficient of thermal expansion are obtained from data for Z250, Z350, and P90. These data are available through 600 seconds from Min et al. [7]. Park et al. [16] published deflection data for Z250, which is available through 3500 seconds.

In Figure 4.5, model predictions for deflection of Z250 composite in aluminum are compared with the Park data for up to 3500 seconds. Note the model prediction for 600 to 3500 seconds is based on an extrapolation of material properties (i.e. Young's modulus and coefficient of thermal expansion). Detailed deflection predictions based on the material properties up to 600 seconds are shown in Figure 4.6.

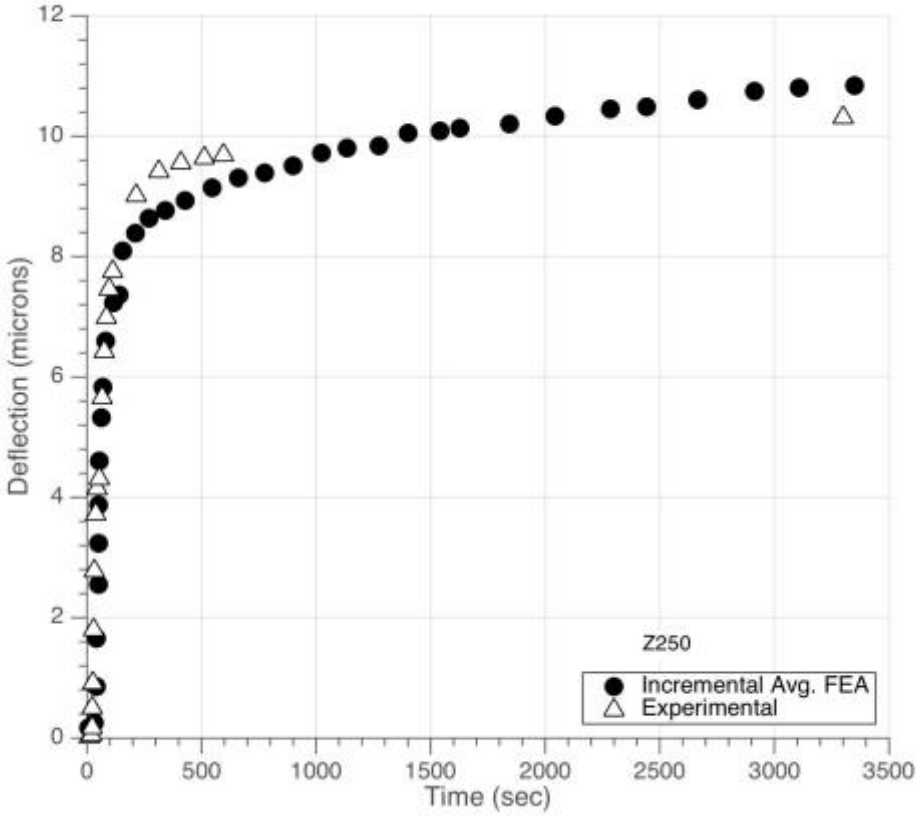

Figure 4.5 Deflection results for Aluminum block model with extrapolated material properties compared with experimental data from Park et al. [16]

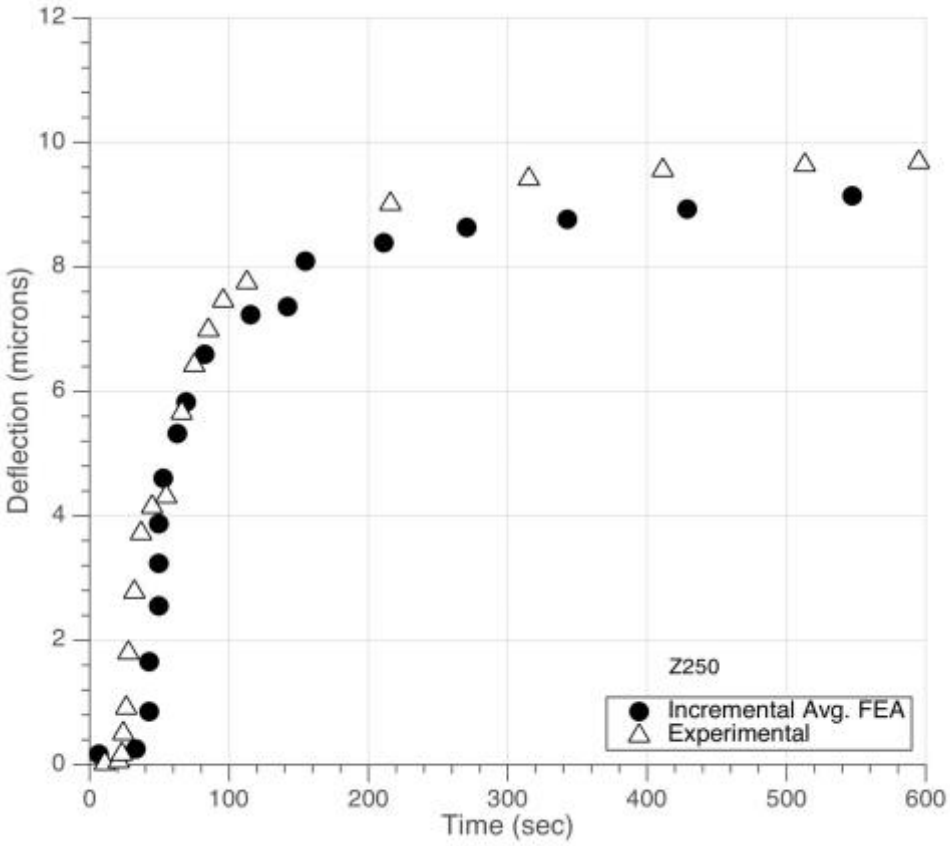

Figure 4.6 Cuspal Deflections for Z250 compared with experimental data from Park et al. [16]

There is good correlation between experimental and finite element data for deflection of the aluminum block filled with Z250, as seen in Figure 4.5 and Figure 4.6. The deflection of the edge of the aluminum block at 600 seconds measured 9.1 microns for both the experimental data and finite element results. FEA results diverge from the experimental data after 600 seconds, where the material properties were extrapolated to 3500 seconds. For better agreement, stress and strain experimental results should be recorded for each composite for at least 3500 seconds.

At the beginning of cure, between 0 and 60 seconds, the finite element prediction of deflection lags experimental data. Recall that the material properties were generated from shrinkage stress and strain data from [7]. Stress and strain were collected using two different experiments. It was assumed that the time of cure, light intensity, and direction were the same for these two experiments. If the experiments were not collected at exactly the same time, there would be a discrepancy in the results that were generated. It is difficult to collect data at exactly the same time for both experiments, and in experimental data from [7], the stress appears to lag behind the strain. This would cause a lag in deflection.

Z350 and P90

The "cuspal" deflection of the aluminum block was also calculated when the cavity is filled with Z350 or P90 (Figure 4.7). The final deflection of the aluminum edge was 16 microns for Z350, much higher than 10 microns seen for Z250. This agrees with axial stress results reported in Figure 4.1and Figure 4.3, where Z350 showed a significantly higher stress Z250. P90 has the lowest shrinkage, and therefore the deflection is expected to be smallest when compared with Z250 and Z350. The final "cuspal" deflection of P90 was 5 microns, very small compared to the 10 microns for Z250 and 16 microns for Z350.

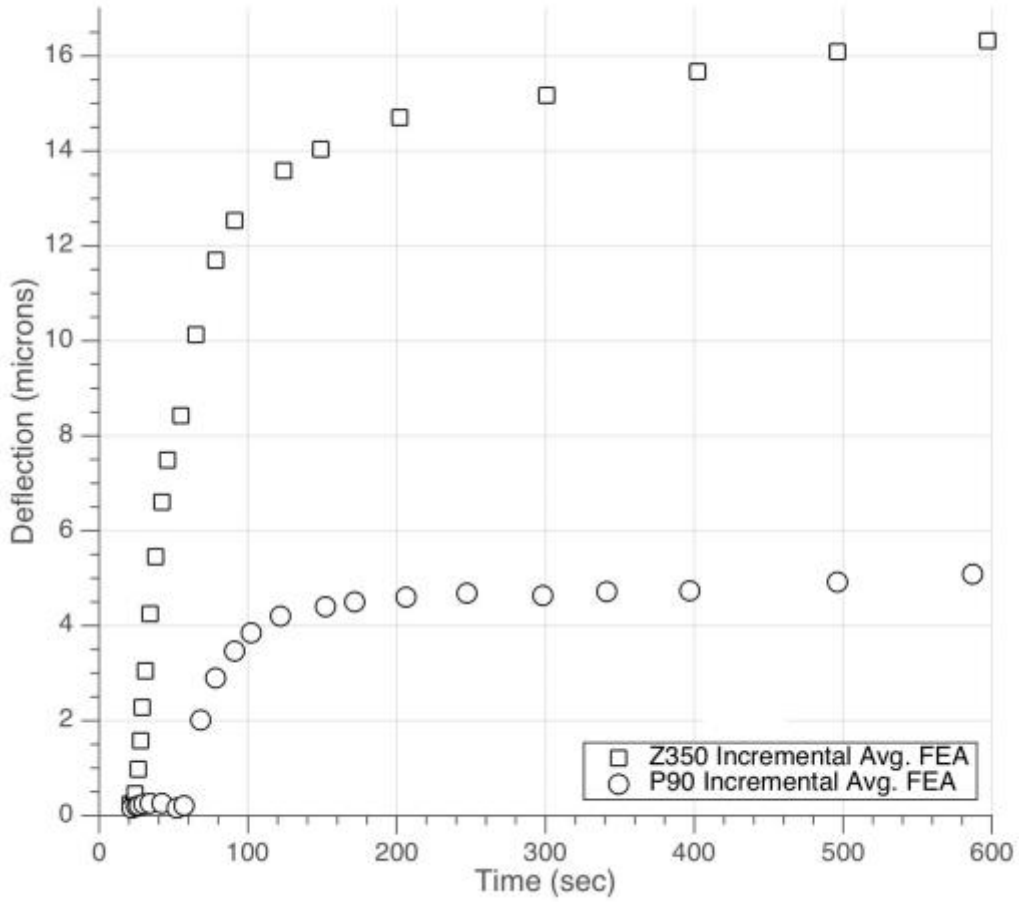

Figure 4.7 Cuspal Deflections of Z350 and P90

4.2.2 Interfacial Stresses

The interfacial normal stresses were calculated at the composite-adhesive interface for Z250, Z350, and P90 in the aluminum block cavity model (Figure 4.8, Figure 4.9, and Figure 4.10, respectively). The following trends are consistent for each resin:

1. FEA results showed that the normal stress was consistently tensile in the cusps and floor.
2. Stress increased from the top to the bottom along the side of the restoration.
3. The highest stress was reported at the bottom corner of the restoration.
4. Stress decreased from the top surface of the composite to the bottom corner of the composite restoration.

These results are consistent with the literature.

For Z250 (Figure 4.8), the greatest tensile stress was 34 MPa. For Z350 (Figure 4.9), the greatest tensile stress was 36 MPa. Z350 was expected to have higher stresses than Z250 because the total volumetric shrinkage is larger [7]. For P90 (Figure 4.10), the greatest tensile stress was 12 MPa. P90 has the lowest volumetric shrinkage [7], which correlates with lowest normal stresses at the interface.

A stress concentration lead to stress outliers at the bottom corner of the model. If the bottom corner of the model were smoother or contained more elements, the stresses

would be expected to be reduced to around 25 MPa, 36 MPa, and 9 MPa for Z250, Z350, and P90, respectively.

An example of the von Mises stress for Z250 at the final time step is shown below in Figure 4.11. The model indicates that there is tensile stress along the interface between the composite and tooth. The highest stress occurs at the bottom corner where a stress concentration occurs. The stress is also lower at the center of the composite, where there are fewer constraints.

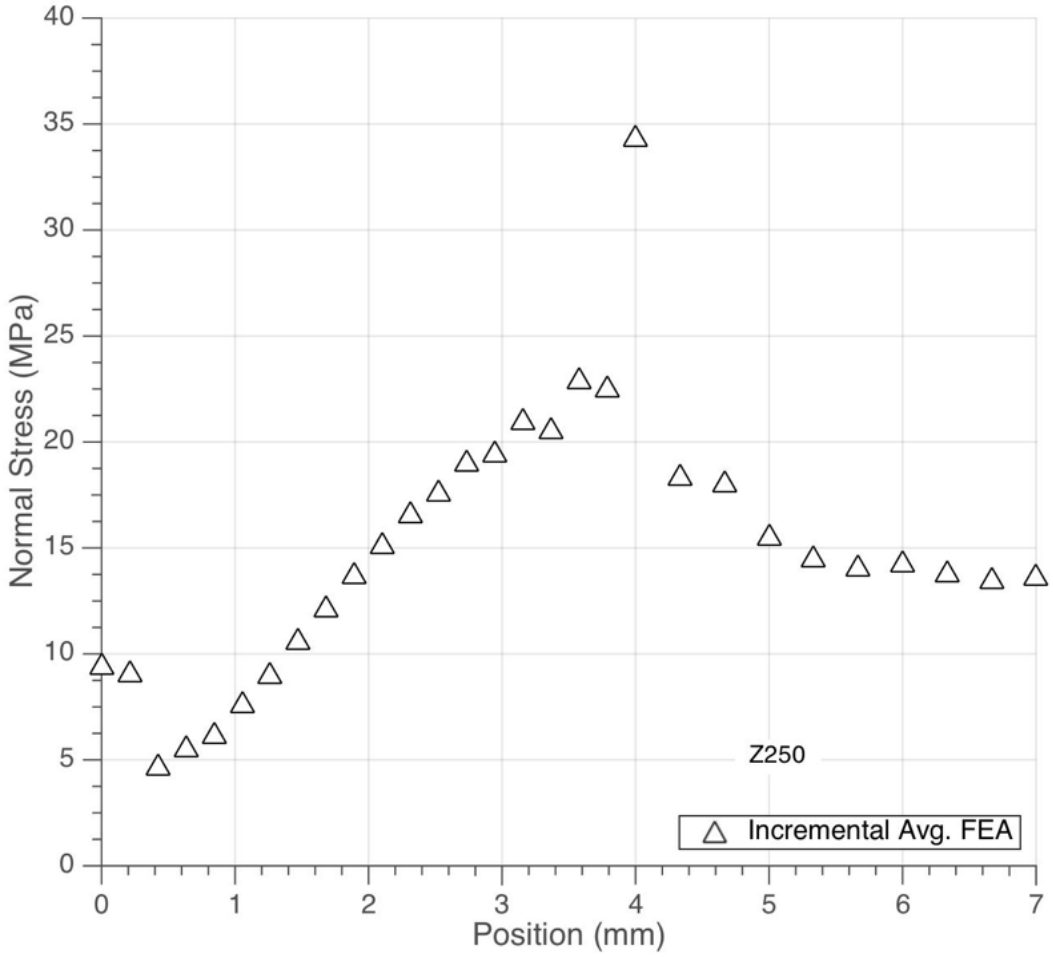

Figure 4.8 Interfacial Normal Stresses for Z250 where the left surface is from 0 mm (top) to 4 mm (bottom). The bottom interface is from 4 mm (left) to 7 mm (center). For the quarter model, the stresses are symmetric about the center.

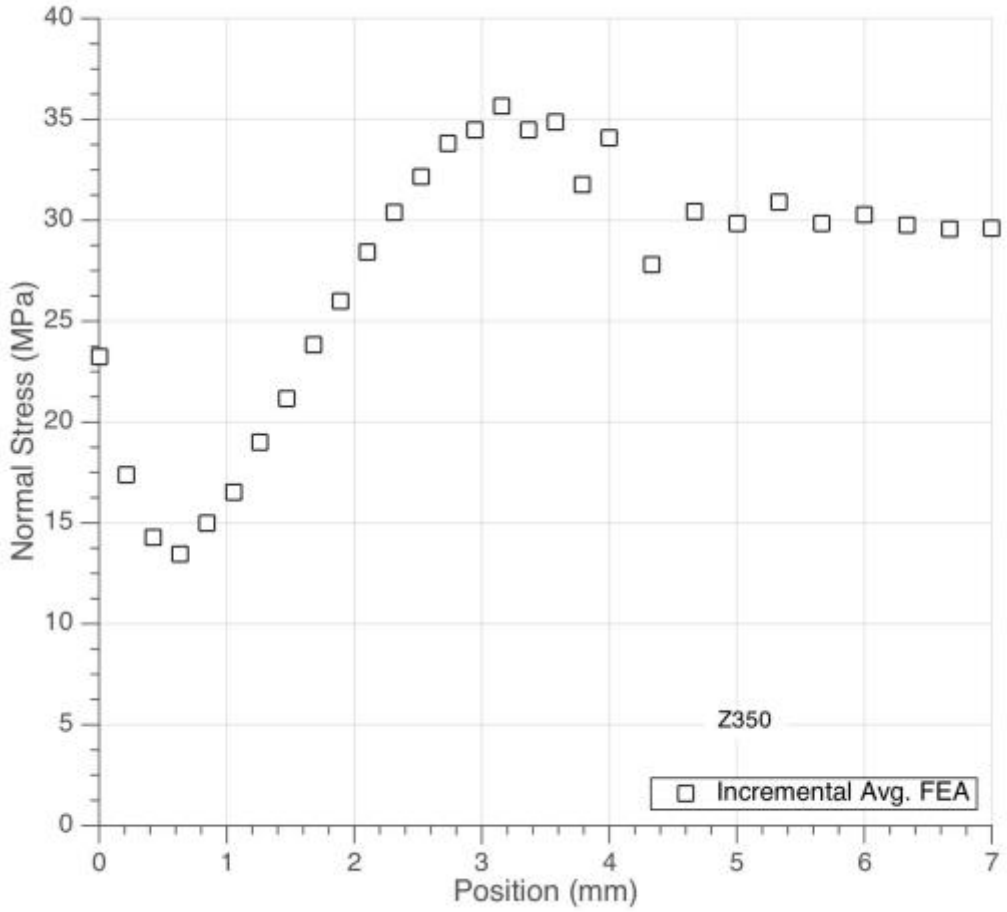

Figure 4.9 Interfacial Normal Stresses for Z350 where the left surface is from 0 mm (top) to 4 mm (bottom). The bottom interface is from 4 mm (left) to 7 mm (center). For the quarter model, the stresses are symmetric about the center.

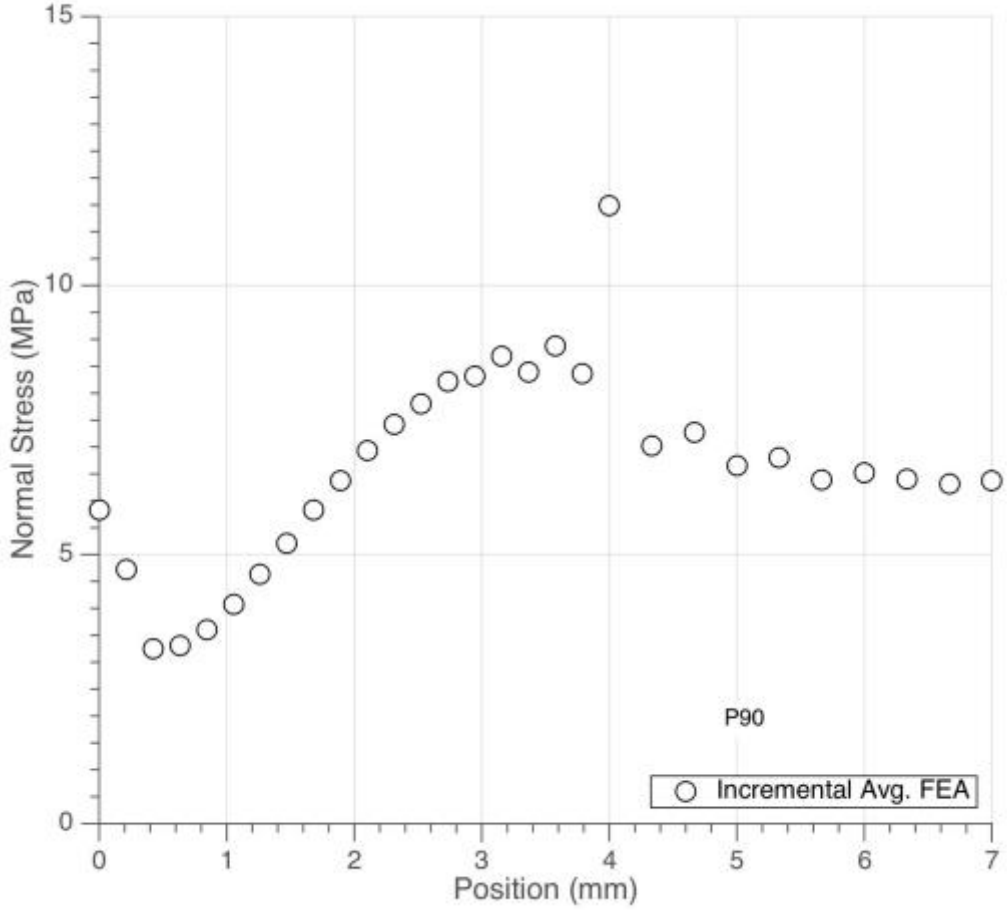

Figure 4.10 Interfacial Normal Stresses for P90 where the left surface is from 0 mm (top) to 4 mm (bottom). The bottom interface is from 4 mm (left) to 7 mm (center). For the quarter model, the stresses are symmetric about the center.

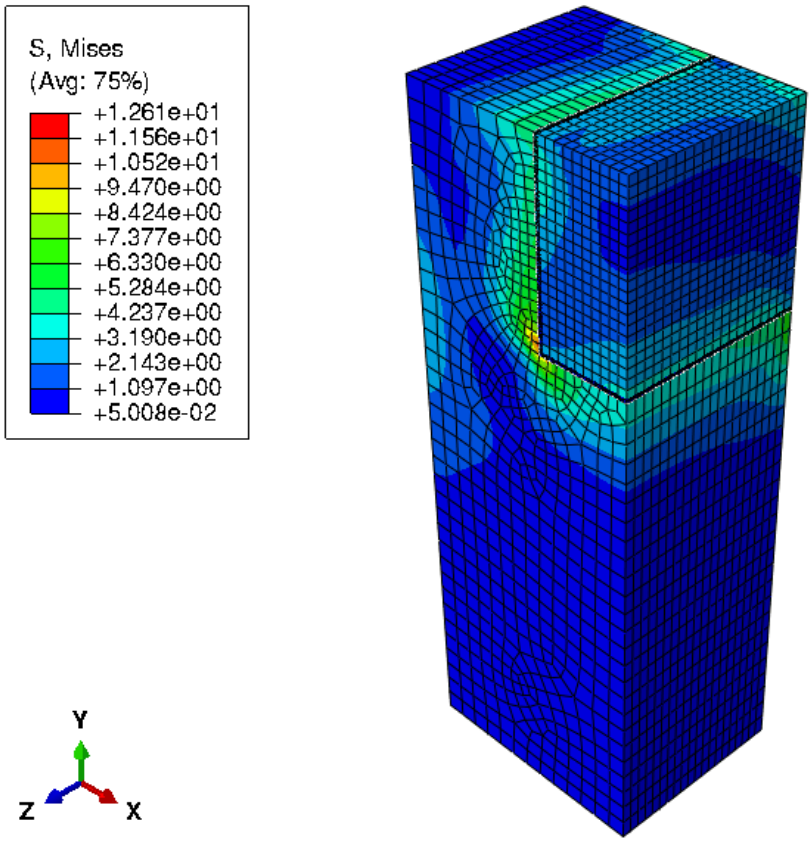

Figure 4.11 Z250 von Mises stress in cuspal deflection model at final time step

4.3 Case Study of a Tooth

In the axisymmetric model of a tooth, two measurements of radial shrinkage stress were calculated. Radial stress versus position and average radial stress versus time were calculated for four dental composites, P10, Z250, Z350, and P90. Two plots are presented for each composite. The first plot for each composite shows the radial stress plotted against the normalized position along the interface between the composite and the enamel/dentine surface. The second plot shows average radial stress computed for all nodes in section 1, close to the top surface where more deflection is seen, and section 2, (where section 1 and section 2 are as defined in Figure 3.5).

P10

Representative stress distributions for the uniform-alpha and layered-alpha tooth models using a P10 restoration can be found in Figure 4.12 and Figure 4.13. Here, the layered-alpha model simulates the change in light intensity as a function of the depth of the composite. The stress contours and the results from Figure 4.14 show that stress is high at the corner of the tooth, which is consistent with the Li's results [3]. At the corner, the composite is constrained in three dimensions, leading to a higher stress. At the top surface, the composite is constrained in only one dimension, resulting in a lower stress and more deflection. Stress increases along the interface as the composite becomes more constrained.

FEA results for P10 are shown in Figure 4.14 and Figure 4.15. In each figure published FEA results from Li [3] are compared with FEA results using the incremental averaged modulus for the uniform-alpha and layered-alpha methods.

For the radial stress versus position (Figure 4.14) and radial stress versus time (Figure 4.15), the stresses predicted by the incremental averaged method are less than those predicted by the step method. This result is consistent with the self-consistency test. Similarly, FEA stress prediction using a layered alpha are consistently less than those for a uniform alpha. The layered alpha results in a composite that is cured layer by layer and subsequently leads to reduced stresses.

The previous result from Li [3] did not report where radial stresses were removed. For the radial stress versus position, the radial stress was removed at element centroids. There is a stress concentration at the top and bottom corners, leading to outliers in the stress results. Li pulled these radial stresses at a slightly different location, leading to a discrepancy.

Figure 4.15 shows that the stress in the restoration increases during cure. It continues to increase more slowly after cure is complete. Stress increases in restorations after they are cured, and can continue building up to 7 days after curing [3]. Stress results for P10 are compared to results for Z250, Z350, and P90 in

Table 4.1 and Table 4.2. Shrinkage stress in section 2 is consistently higher than shrinkage stress in section 1. These results are consistent with results in [3].

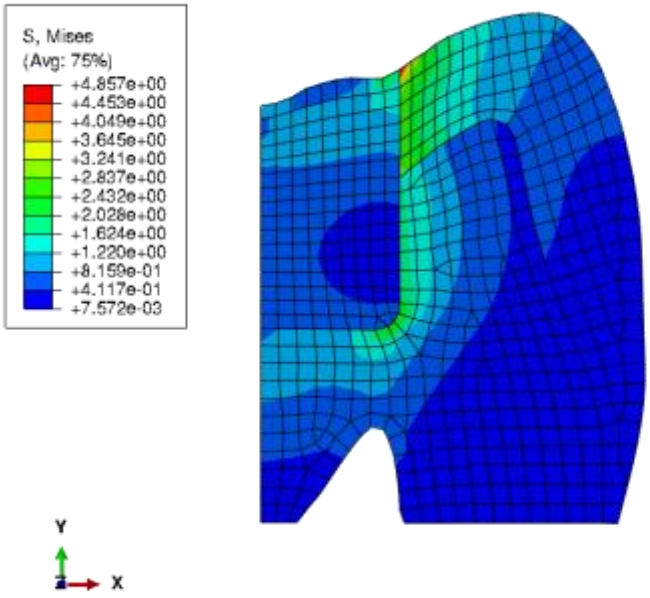

Figure 4.12 P10 von Mises stress at step 1 of uniform alpha axisymmetric tooth model

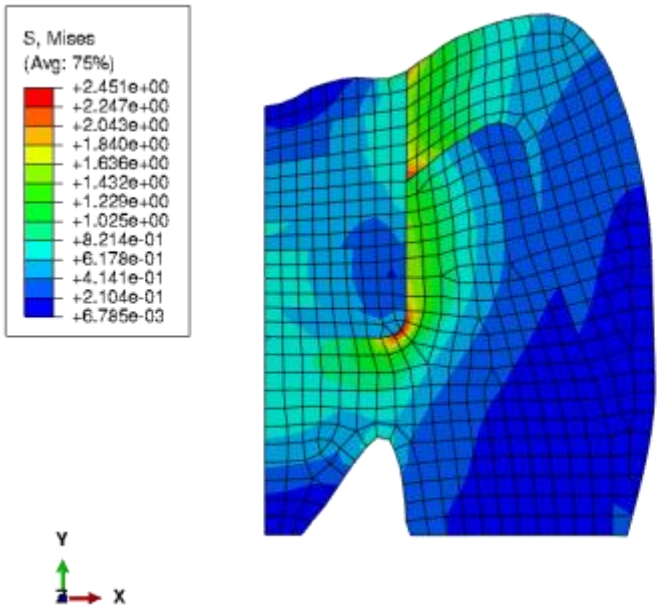

Figure 4.13 P10 von Mises stress at step 1 of layered alpha axisymmetric tooth model

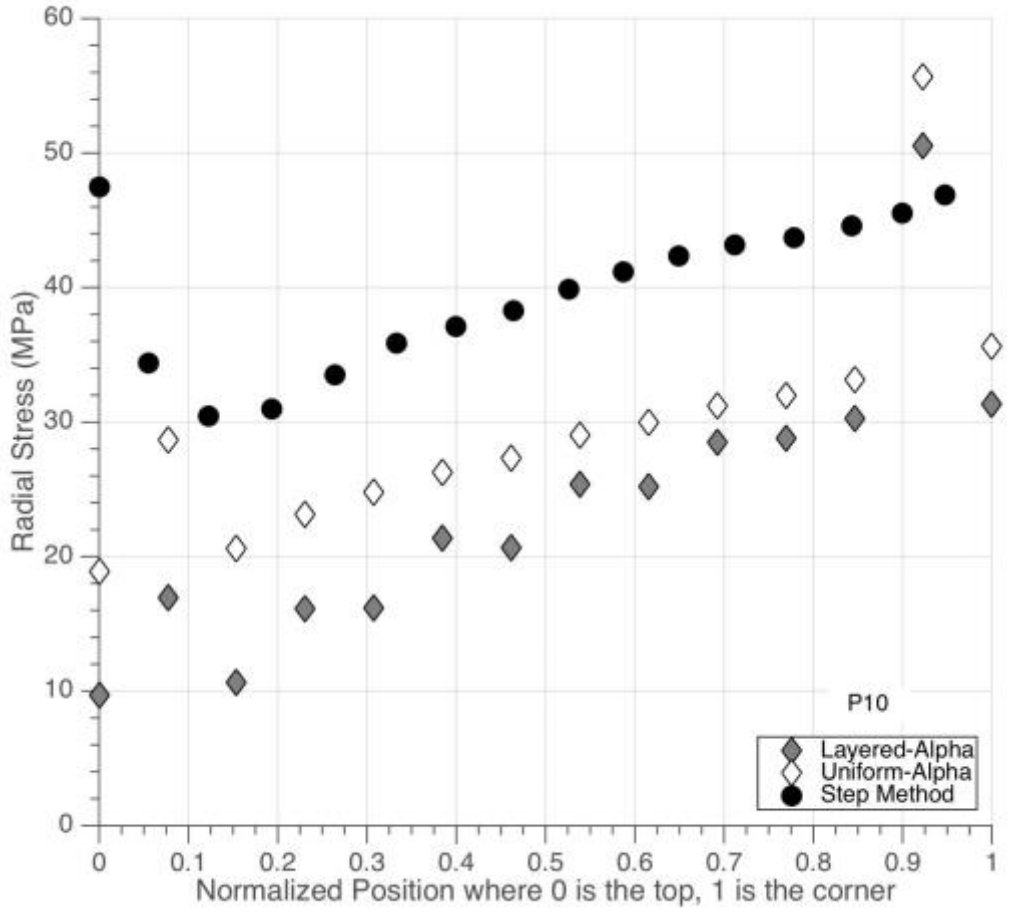

Figure 4.14 P10 radial stress vs. position along the interface compared to experimental results from Li et al. [3]

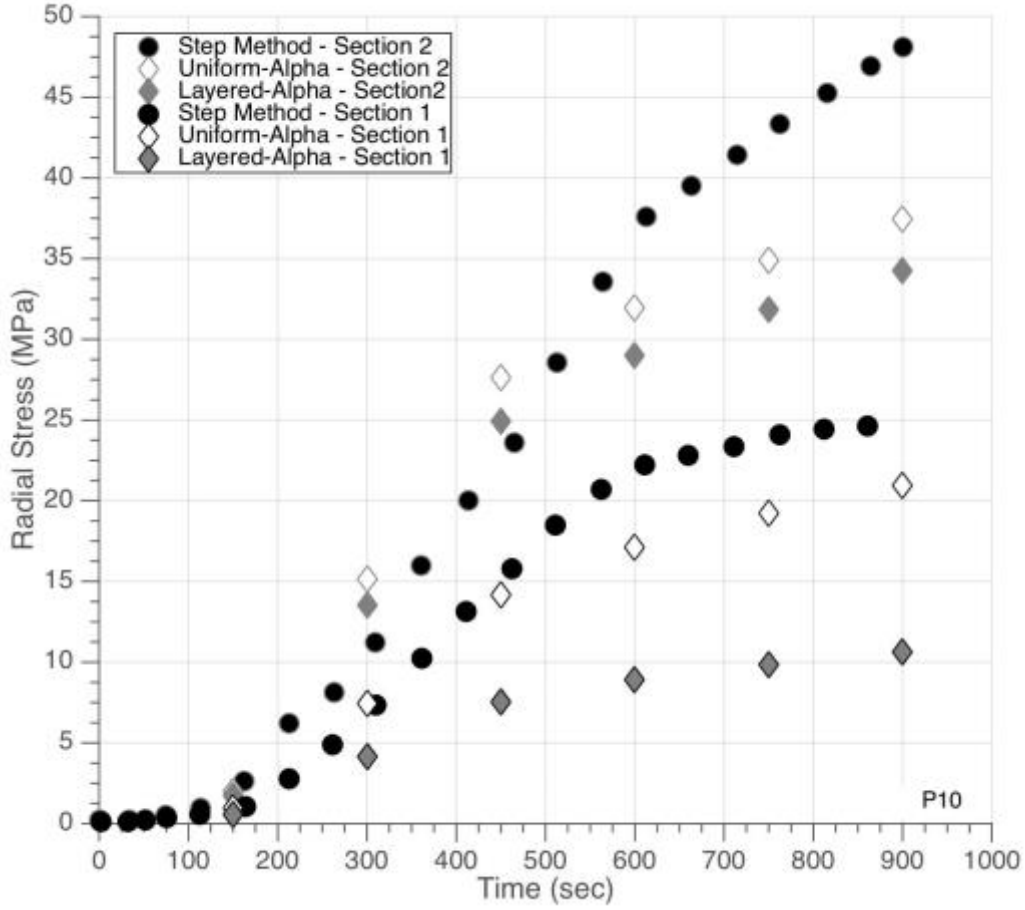

Figure 4.15 Average radial stress over time for P10 in sections 1 and 2 compared to experimental results from Li et al. [3]

Z250, Z350, and P90

FEA predictions of radial stress data for Z250, Z350 and P90 are shown in Figures 4.16 through 4.21. FEA predictions of radial stress versus position are shown in Figure 4.16, Figure 4.18, and Figure 4.20 for Z250, Z350, and P90, respectively. FEA predictions of average radial stress versus time are shown in Figure 4.17, Figure 4.19, and Figure 4.21

for Z250, Z350, and P90, respectively. The FEA results for Z250, Z350, and P90 are consistent with the results for P10. The layered-alpha model consistently predicts lower stresses than the uniform-alpha model. The highest stresses occur at the corner, where the restoration is most constrained, and the lowest stress is at the top corner, where the restoration has fewer constraints.

Comparisons of stresses for each composite are listed in

Table 4.1 and Table 4.2. Z350 shows highest stresses, followed by Z250, P10, and P90. These results agree with the average predicted stress, when the final modulus of each composite was multiplied by the shrinkage strain and divided by two. Predicted stress values for each composite also lie between the maximum stress (stress at the corner of the composite) and minimum stress at the top edge. These results are also consistent with acoustic emission results from [9]. Z250 was shown to have higher stress and more extensive debonding than P90. Debonding was also shown to be most prominent at the corner and bottom surfaces, which agrees with the results of the tooth FEA.

Table 4.1 Comparison of radial stresses at the corner and top sections for FEA methods

	P10		Z250		Z350		P90	
FEA Method	Stress at Corner (MPa)	Stress at Top (MPa)	Stress at Corner (MPa)	Stress at Top (MPa)	Stress at Corner (MPa)	Stress at Top (MPa)	Stress at Corner (MPa)	Stress at Top (MPa)
Step Method	48	45	-	-	-	-	-	-
Incremental Avg. Uniform-Alpha	36	19	65	41	75	42	27	19
Incremental Avg. Layered-Alpha	32	10	56	20	67	21	24	10
Predicted Stress	21.6		44		64.4		14.4	

Table 4.2 Comparison of average radial stresses for FEA methods for section 1 and section 2

FEA Method	P10	Z250	Z350	P90
Step Method - Section 2	48	-	-	-
Uniform-Alpha - Section 2	37	68	79	28
Layered-Alpha - Section 2	34	67	77	27
Step Method - Section 1	24	-	-	-
Uniform-Alpha - Section 1	21	52	56	18
Layered-Alpha - Section 1	11	19	22	7
Predicted Stress	21.6	44	64.4	14.4

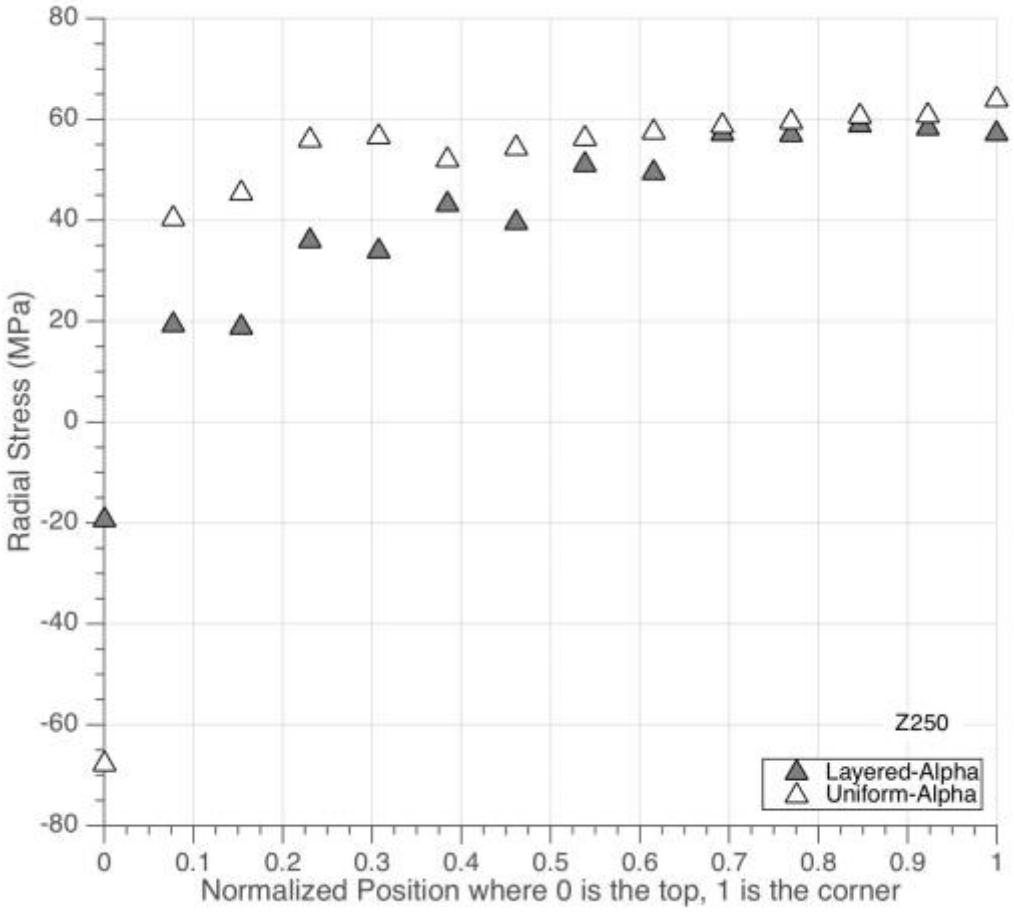

Figure 4.16 Z250 radial stress vs. position along the interface

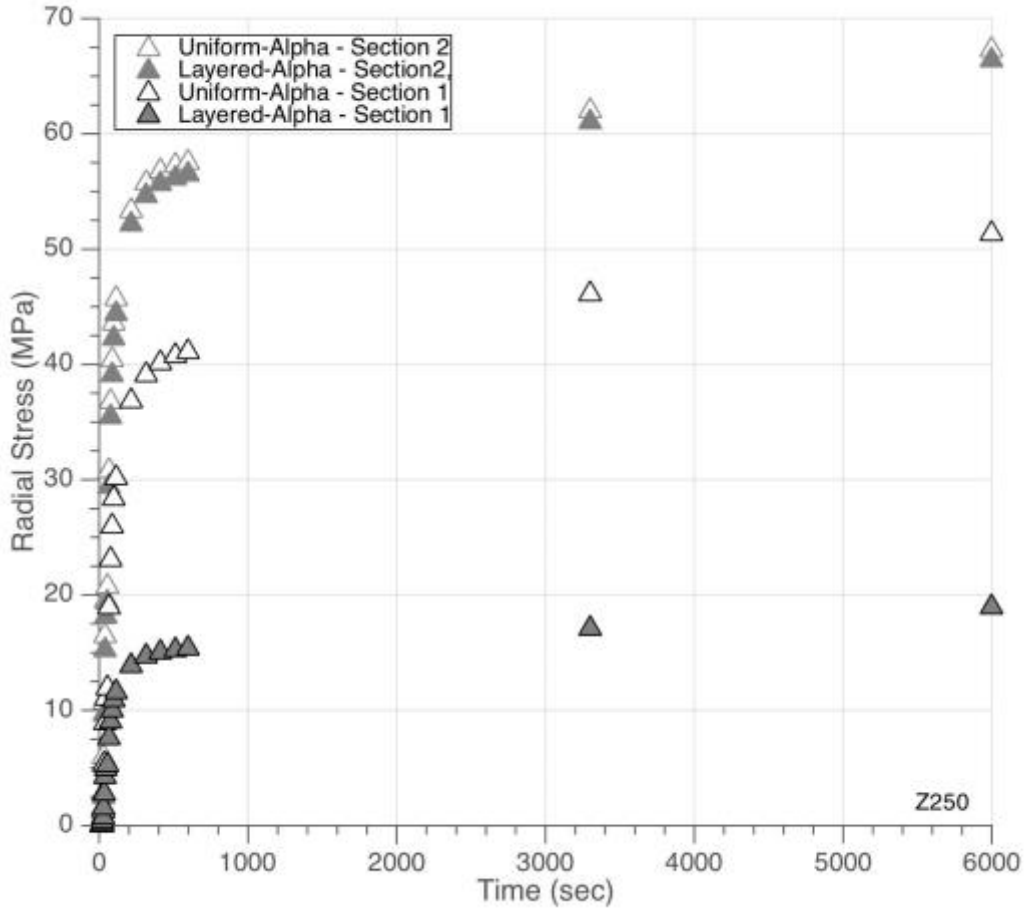

Figure 4.17 Average radial stress over time for Z250 in sections 1 and 2

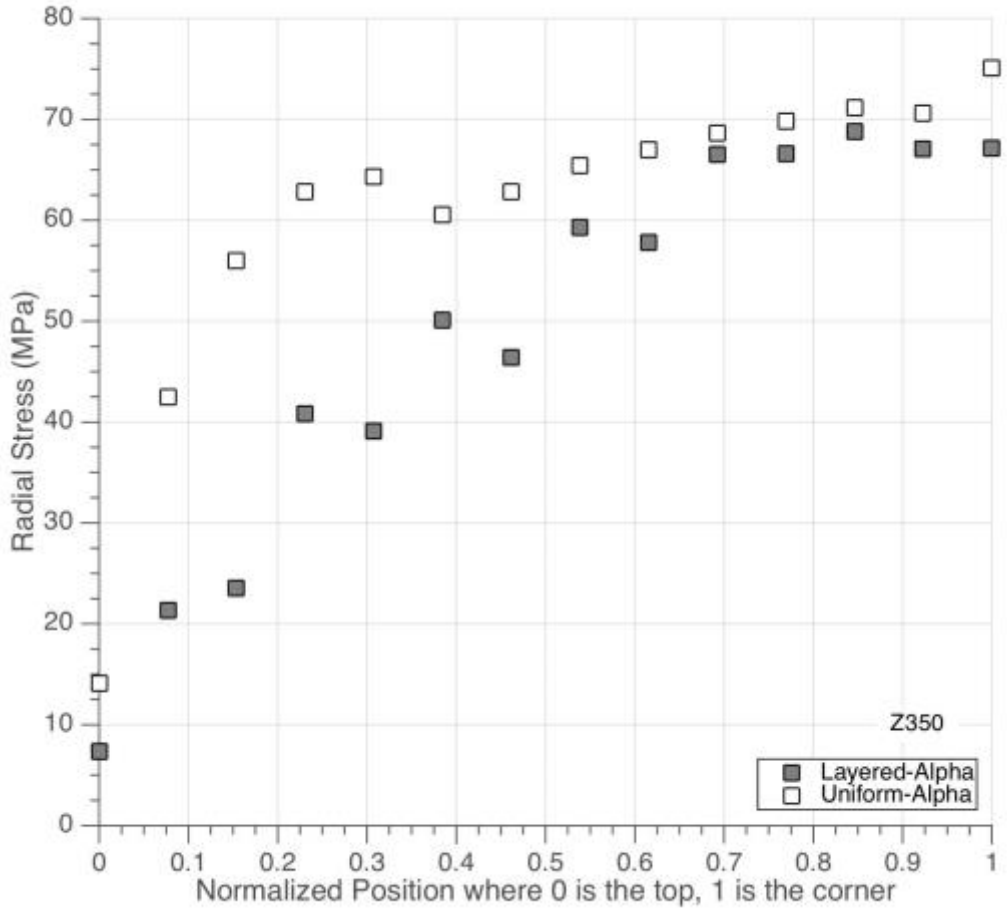

Figure 4.18 Z350 radial stress vs. position along the interface

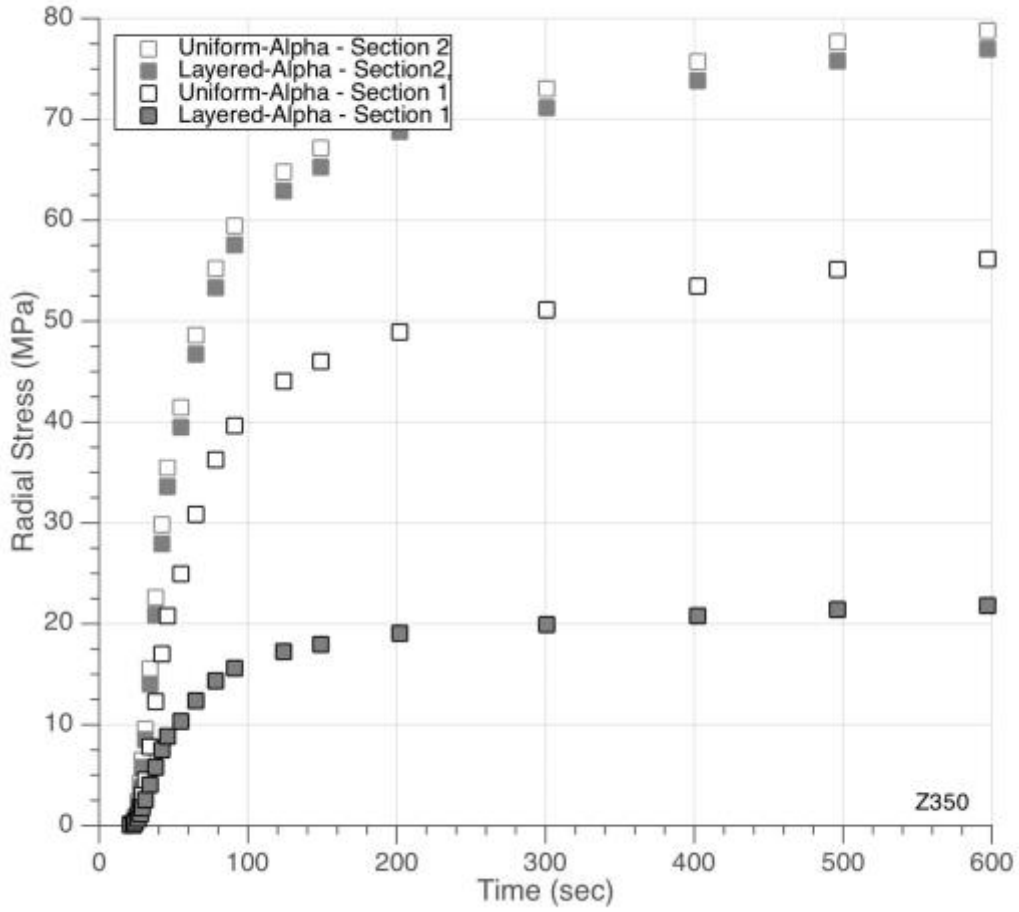

Figure 4.19 Average radial stress over time for Z350 in sections 1 and 2

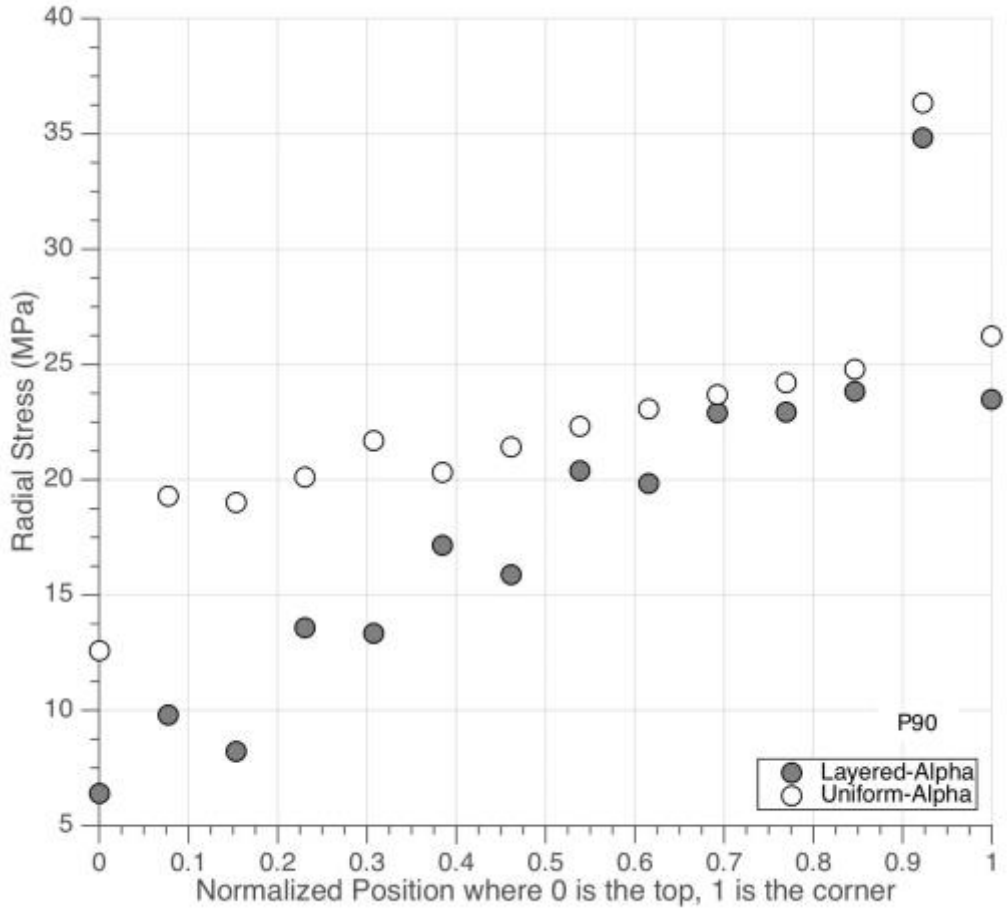

Figure 4.20 P90 radial stress vs. position along the interface

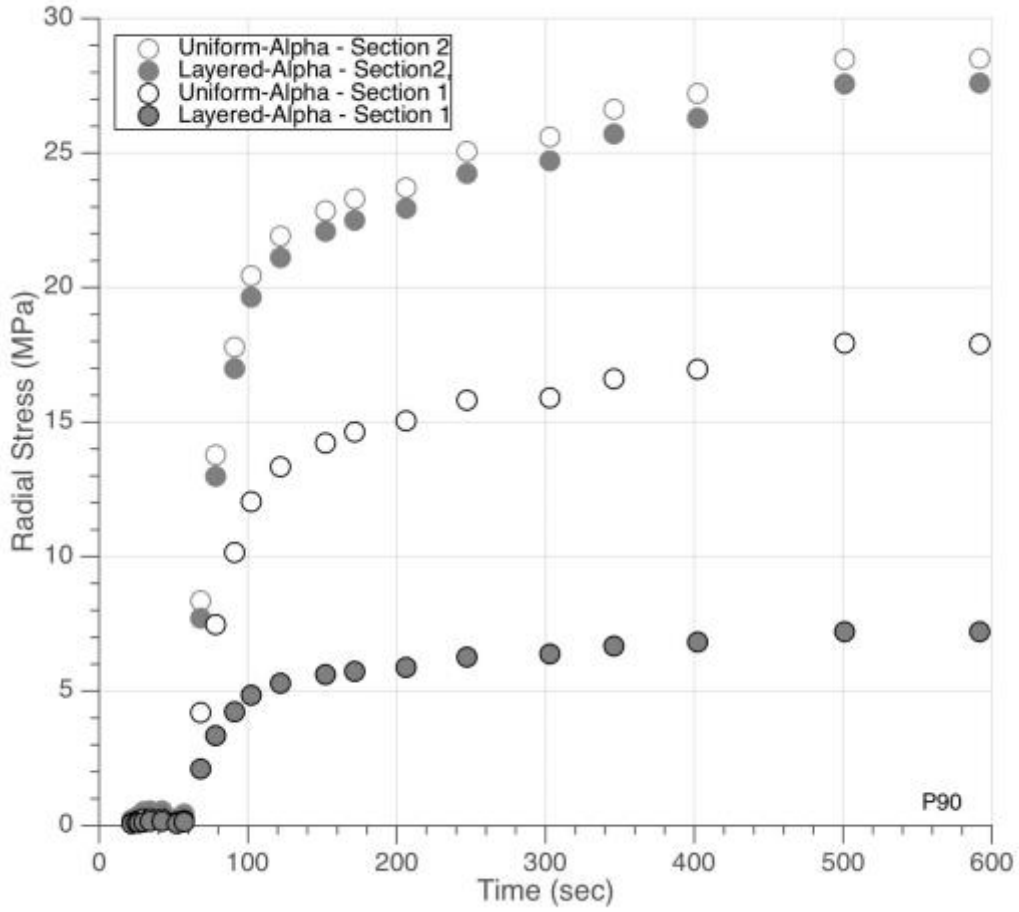

Figure 4.21 Average radial stress over time for P90 in sections 1 and 2

5 Conclusion

5.1 Summary

A new constitutive law for curing dental composites was introduced in this paper. The constitutive law was developed from a Maxwell model, and allows users to find material properties from experimental shrinkage stress and strain data. Specifically, Young's modulus as a function of time was found for three dental composites: Z250, Z350, and P90. The constitutive law results were validated with a spring-disk model and verified with a cuspal deflection model. Predictions of interfacial stresses were produced from an axisymmetric tooth model.

The constitutive law developed for dental composites uses shrinkage stress and shrinkage strain to find the Young's modulus at any point during the cure of the composite. Composites cure quickly, within 100 seconds. Because of the rapid cure rate the viscosity term was omitted from the constitutive law. Shrinkage stress and shrinkage strain are easily measured in a laboratory environment with the cantilever tensometer and free-shrinkage methods, respectively. It is important to note when stress and strain are recorded using different instruments, the experiments should begin at precisely the same time. The conditions (light intensity, direction, etc.) should also remain the same when finding shrinkage stress and shrinkage strain. The constitutive law was developed assuming one-dimensional stress and strain data, so any lateral constraints that occur experimentally must be taken into account when determining the material properties.

Finite element analysis was used to model the dental composite, and certain aspects were found to be necessary. A thermal approach was used to simulate shrinkage of the composite as a function of time. The models were split into multiple steps, and each step was given a coefficient of thermal expansion to simulate shrinkage over that amount of time. All steps were added together to find the cumulative sum of stress or displacement. The incremental averaged method, which has been discussed in detail, uses an average value for Young's modulus and the coefficient of thermal expansion for each step. The average is especially important at the beginning of cure when the composite is curing most rapidly. The final value of Young's modulus was used for each step in the step method, and stress results were shown to be too high when compared to experimental data. It is also important to use a sufficient number of data points when finding material properties for the dental composite. Many data points (in at least 1 second increments) are required when the composite is rapidly curing to achieve accurate results. The opacity of the composite was also found to be necessary for modeling. The change in light intensity with depth was simulated by using different coefficients of thermal expansion to shrink the composite. The composite was split into multiple parts, and each section was given a different coefficient of thermal expansion correlating to the amount of shrinkage in that layer. Finite element results were summed with MATLAB to give the total stress in the model. Matching nodes between adjoining materials in FEA models was also proven to be important in acquiring an exact solution.

The interfacial shrinkage stress was monitored as a function of time in the composite. The adhesive was assumed to be bonded to the tooth surface before the composite was placed. Composites debonded when they reached an interfacial stress of 35 MPa.

The derived material properties were proved to be self-consistent when applied to a spring-disk FEA model that simulated shrinkage stress measurement. Next, the material properties showed good agreement between experimental data and finite element results in an aluminum block cuspal deflection model. The cuspal deflection model showed the validity of the constitutive law. Finally, a case study of a tooth was completed and compared to previous FEA data. Stresses were shown to be much lower than previous results when different coefficients of thermal expansion were used in layers of the dental composite to account for decreasing degree of cure due to light attenuation.

5.2 Future Work

A constitutive law was developed for dental composites during cure. The law was proved by comparing finite element analysis results to experimental data. Future research must be completed to tweak the finite element models to match Z350 and P90 composite experimental data. More thorough investigations of the constitutive law should also be completed with other composite materials.

The model that was developed was proven to be valid for Z250 during cure. Solutions shown here used only 22 steps in models. This result is partially due to the difficulty in adding up steps to achieve final results. If model restart can be used in ABAQUS, it saves many calculations, and more steps should be used to increase the resolution of the solution. Resolution of 1 second or less is suggested, especially at the beginning of cure. Model restart was not used in these solutions, but the input files referenced can be modified using NLGEOM and MODEL RESTART commands to incrementally sum results in ABAQUS.

The cuspal deflection model and axisymmetric tooth model should be investigated with a denser mesh to remove FEA anomalies, which caused interfacial stress outliers.

In results shown here, Poisson's ratio was defined to have a step change at 90% of cure. The reduction of Poisson's ratio is likely more gradual in nature. More research should be completed to define the time dependence of Poisson's ratio during cure for more accurate results.

The adhesive was assumed to cure before the composite was placed. This is not always the case. The temporal bond strength should be investigated as a function of time to and compared to the temporal interfacial shrinkage stress. The debonding results may be

different if the bond strength increases more than the interfacial shrinkage stress at any point.

Because it has been shown experimentally that composites cure at different rates according to the depth from the light-curing source, additional studies should investigate modeling approaches that capture this effect. The current study considered a modeling the coefficient of thermal expansion as a function of depth, however alternate approaches should be considered.

References

[1] Hickman J, Jacobsen PH, Wilson A, Middleton J. Finite element analysis of dental polymeric restorations. Clin Mater 1991;7:39–43. doi:10.1016/0267-6605(91)90055-K.

[2] Hübsch P., Middleton J, Knox J. A finite element analysis of the stress at the restoration–tooth interface, comparing inlays and bulk fillings. Biomaterials 2000;21:1015–9. doi:10.1016/S0142-9612(99)00266-5.

[3] Li J, Li H, Fok SL. A mathematical analysis of shrinkage stress development in dental composite restorations during resin polymerization. Dent Mater 2008;24:923–31. doi:10.1016/j.dental.2007.11.012.

[4] 3M ESPE. Filtek Z250 Universal Restorative System Technical Product Profile 1998. http://multimedia.3m.com/mws/media/78343O/filtektm-z250-universal-restorative.pdf.

[5] 3M ESPE. Filtek Z350 Universal Restorative System Technical Product Profile 2010.

[6] 3M ESPE. Filtek P90 Low Shrink Posterior Restorative Technical Product Profile 2007.

[7] Min S-H, Ferracane J, Lee I-B. Effect of shrinkage strain, modulus, and instrument compliance on polymerization shrinkage stress of light-cured composites during the initial curing stage. Dent Mater 2010;26:1024–33. doi:10.1016/j.dental.2010.07.002.

[8] Niu Y, Ma X, Fan M, Zhu S. Effects of layering techniques on the micro-tensile bond strength to dentin in resin composite restorations 2008;5:129–34. doi:10.1016/j.dental.2008.04.017.

[9] Yang B, Guo J, Huang Q, Heo Y, Fok A, Wang Y. Acoustic properties of interfacial debonding and their relationship with shrinkage stress in Class-I restorations. Dent Mater 2016;32:742–8. doi:10.1016/j.dental.2016.03.007.

[10] Dauvillier BS, Feilzer a J, De Gee a J, Davidson CL. Visco-elastic parameters of dental restorative materials during setting. J Dent Res 2000;79:818–23. doi:10.1177/00220345000790030601.

[11] Versluis A, Tantbirojn D, Pintado MR, DeLong R, Douglas WH. Residual shrinkage stress distributions in molars after composite restoration. Dent Mater 2004;20:554–64. doi:10.1016/j.dental.2003.05.007.

[12] Li J, Li H, Fok ASL, Watts DC. Multiple correlations of material parameters of light-cured dental composites. Dent Mater 2009;25:829–36. doi:10.1016/j.dental.2009.03.011.

[13] Attar N, Tam LE, McComb D. Flow, strength, stiffness and radiopacity of flowable resin composites. J Can Dent Assoc 2003;69:516–21.

[14] Chung SM, Yap a UJ, Tsai KT, Yap FL. Elastic modulus of resin-based dental restorative materials: a microindentation approach. J Biomed Mater Res B Appl Biomater 2005. doi:10.1002/jbm.b.30145.

[15] Sabbagh J. Dynamic and static moduli of elasticity of resin-based materials. Dent Mater 2002;18:64–71. doi:10.1016/S0109-5641(01)00021-5.
[16] Park J, Chang J, Ferracane J, Lee IB. How should composite be layered to reduce shrinkage stress: incremental or bulk filling? Dent Mater 2008;24:1501–5. doi:10.1016/j.dental.2008.03.013.
[17] Li J, Fok ASL, Satterthwaite J, Watts DC. Measurement of the full-field polymerization shrinkage and depth of cure of dental composites using digital image correlation. Dent Mater 2009;25:582–8. doi:10.1016/j.dental.2008.11.001.
[18] Fok ASL. Shrinkage stress development in dental composites--an analytical treatment. Dent Mater 2013;29:1108–15. doi:10.1016/j.dental.2013.08.198.
[19] Rohatgi A. WebPlotDigitizer 2015.
[20] The MathWorks Inc. MATLAB R2014b 2014.
[21] Dassault Systemes Simulia Corp. Abaqus Analysis User's Manual 6.11 n.d.

Appendices

The axisymmetric spring-disc model was run for P90 with an original set of data for 22 steps, as shown below in Table 5.1. There were a couple of large jumps in Young's modulus between steps 8 and 11 from 58 MPa to 1885 MPa, 1885 MPa to 6465 MPa, and 6465 MPa to 9398 MPa. The jumps in Young's modulus caused large increases in the stress between 60 and 90 seconds, as shown in Figure 5.1.

When the number of steps in the model was increased from 22 to 50 and the time in each step was decreased to 2 seconds, the jumps in stress decreased. The final stress went from 0.74 MPa to 0.56 MPa. Experimental data showed a final stress value of 0.49 MPa.

The resolution of the data from [7] is about 2 seconds, which was used to gather data for Table 5.1. If the number of steps was further increased and the step size was decreased, the finite element results are expected to match experimental values.

Table 5.1 P90 original dataset

P90				
Step #	Time (sec)	Young's Modulus (MPa)	Alpha	Poisson's Ratio
1	22	23	-3.68E-05	0.49
2	25	52	-4.71E-05	0.49
3	27	63	-4.26E-05	0.49
4	30	82	-4.72E-05	0.49
5	34	99	-7.08E-06	0.49
6	42	303	0.00E+00	0.49
7	52	75	3.97E-05	0.49
8	57	58	-4.63E-05	0.49
9	68	1885	-6.77E-05	0.49
10	78	6465	-2.89E-05	0.49
11	91	9398	-1.47E-05	0.49
12	102	9581	-1.14E-05	0.49
13	122	9596	-5.72E-06	0.49
14	152	9599	-2.50E-06	0.35
15	172	9600	-1.61E-06	0.35
16	206	9600	-9.30E-07	0.35
17	247	9600	-7.71E-07	0.35
18	303	9600	5.65E-07	0.35
19	346	9600	-7.36E-07	0.35
20	402	9600	0.00E+00	0.35
21	501	9600	-6.39E-07	0.35
22	592	9600	-6.48E-07	0.35

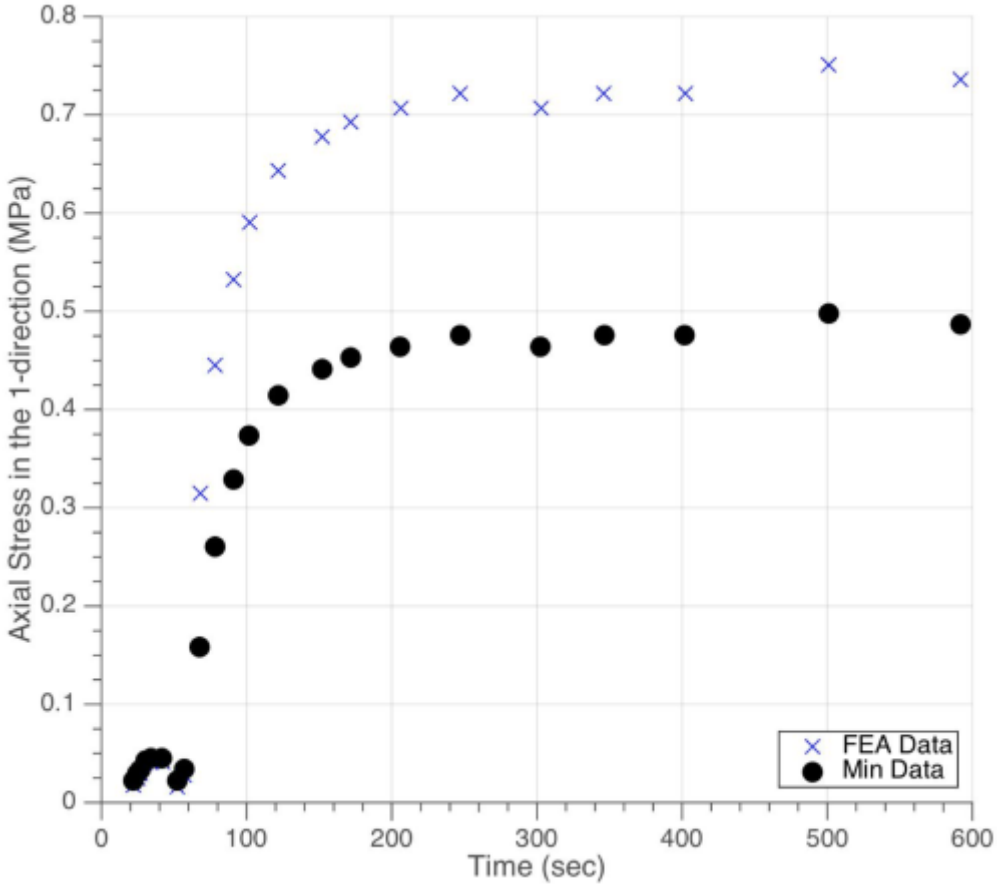

Figure 5.1 Original dataset for P90, axial stress in spring-disc model

Material data for Z250 were calculated for 600 seconds. The "cuspal" deflection experimental data from [16] contained data up to 3500 seconds. To look at the full extent of experimental data, the stress and strain data [7] were extrapolated to two final points and compared.

Two points were chosen on the shrinkage strain-stress plot, Figure 2.4. A time was chosen for each data point. The points were plotted on the shrinkage stress vs time and

shrinkage strain vs time plots. The slope at the end of the plots was checked to see if the value seemed reasonable.

The extrapolated data points were compared to the total displacement vs. time data for Z250. The plot did not show agreement with the final displacement from [16].

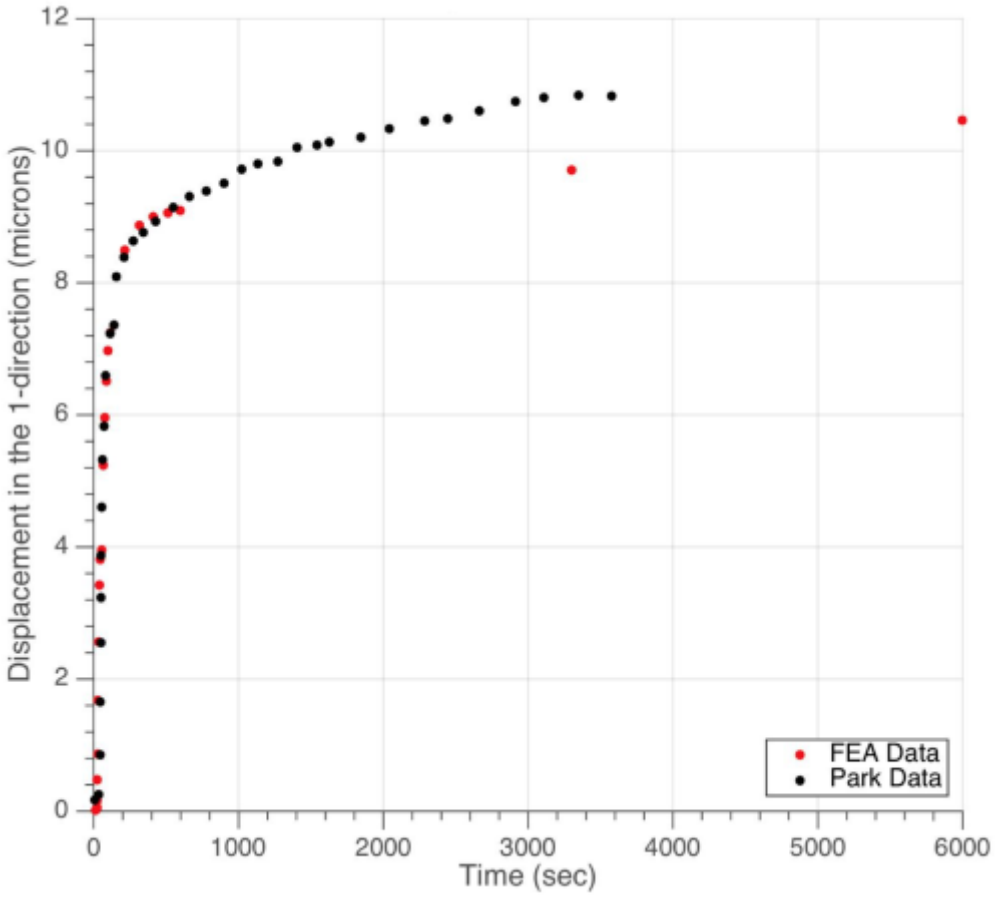

Figure 5.2 Z250 "cuspal" deflection in microns

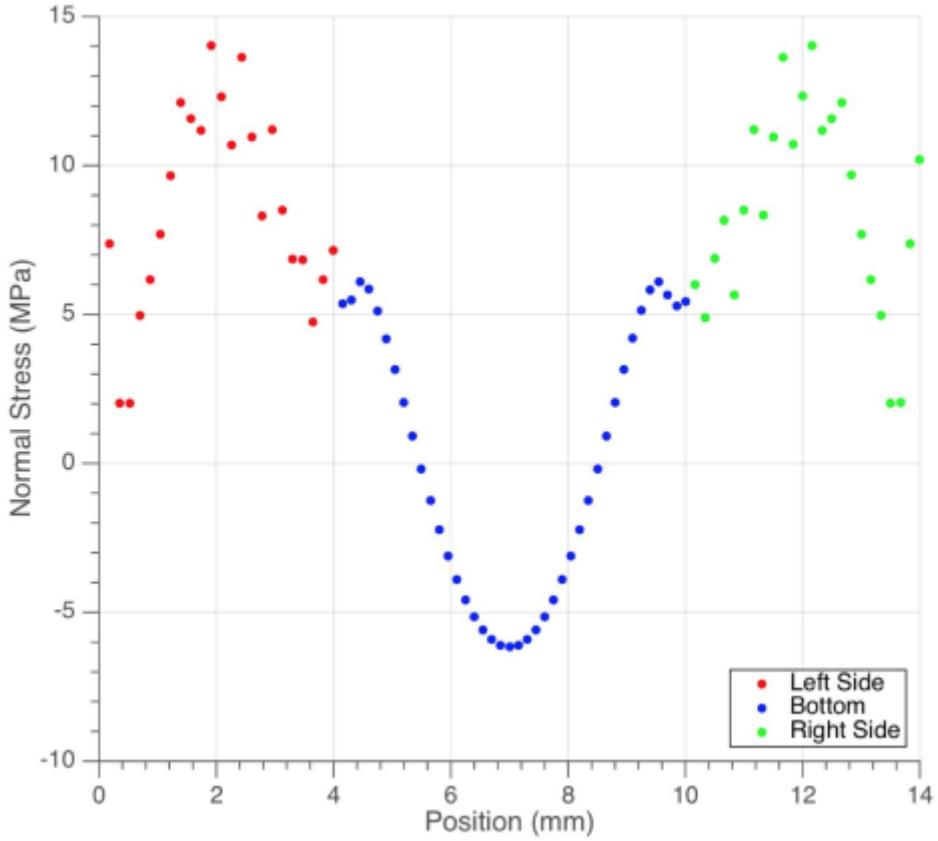

Figure 5.3 Z250 composite-aluminum interface normal stress plotted against position

5.3 Annotated Input File for P90 Cusapl Deflection

```
*Heading
** Job name: Quarter_Model_Z250 Model name: Model-1
** Generated by: Abaqus/CAE 6.11-1
*Preprint, echo=NO, model=NO, history=NO, contact=NO
**
** DEFINE THE PARTS OF THE MODEL
** ----------------------------------------------------------
** Parts
**
*Part, name=Adhesive
*End Part
**
*Part, name=Aluminium
*End Part
```

```
**
*Part, name=Composite
*End Part
**
** DEFINE ASSEMBLIES, INSTANCES, NODES, ETC.
** ----------------------------------------------------------
** Assembly
**
*Assembly, name=Assembly
**
** ADHESIVE SECTION DEFINITION
** ----------------------------------------------------------
*Instance, name=Adhesive-1, part=Adhesive
       10.3,         -6.2,           0.
*Node
      1,  -5.36000013,   3.95000005,           0.
      2,  -5.42000008,   3.95000005,           0.
      3,  -5.48000002,   3.95000005,           0.
      4,  -5.53999996,   3.95000005,           0.
      5,   -5.5999999,   3.95000005,           0.
      6,  -5.65999985,   3.95000005,           0.
      7,  -5.71999979,   3.95000005,           0.
      8,  -5.78000021,   3.95000005,           0.
      9,  -5.82000017,   3.95000005,           0.
** ... PLEASE SEE FULL INPUT FILE FOR FULL SET OF NODES
**
*Element, type=C3D8R
    1,   650,   687,   896,  1123,  1843,  1880,  2089,  2316
    2,   691,  1043,   896,  1191,  1884,  2236,  2089,  2384
    3,   651,   541,   542,   602,  1844,  1734,  1735,  1795
    4,   692,   972,  1044,   604,  1885,  2165,  2237,  1797
    5,   668,  1126,  1045,   605,  1861,  2319,  2238,  1798
    6,   604,   544,   174,   692,  1797,  1737,  1367,  1885
    7,   667,   173,   543,   652,  1860,  1366,  1736,  1845
    8,   173,   667,   602,   542,  1366,  1860,  1795,  1735
    9,   172,   641,   691,   540,  1365,  1834,  1884,  1733
** ... PLEASE SEE FULL INPUT FILE FOR FULL SET OF ELEMENTS
**
*Nset, nset=_PickedSet2, internal, generate
     1,  48913,      1
*Elset, elset=_PickedSet2, internal, generate
     1,  35680,      1
*Elset, elset=_Adhe_Comp_S4, internal
     3,     6,     7,    13,    17,    26,    27,    33,    46,    48,    62,    64,    70,    71,    79,   277
   287,   300,   341,   501,   502,   504,   508,   513,   514,   515,   517,   520,   527,   529,   532,   550
   571,   895,   898,   899,   905,   909,   918,   919,   925,   938,
** ... PLEASE SEE FULL INPUT FILE FOR FULL ELEMENT SET
**
*Elset, elset=_Adhe_Comp_S6, internal
     8,     9,    12,    14,    16,    18,    19,    21,    24,    25,    28,    34,    42,    44,    47,    50
    57,    59,    60,    63,    65,    68,    80,   102,   235,   278,   280,   281,   282,   284,   285,   286
   289,   291,   292,   293,   294,   295,   296,   298,   303,   305,
** ... PLEASE SEE FULL INPUT FILE FOR FULL ELEMENT SET
**
*Elset, elset=_Adhe_Comp_S3, internal
```

```
   85,   87,   88,   91,   92,   96,   98,   99,  104,  106,  111,  113,  119,  120,  121,  122
  125,  127,  131,  132,  133,  136,  140,  146,  147,  151,  153,  157,  159,  160,  162,  164
  169,  171,  172,  174,  176,  177,  179,  188,  195,  198,
** ... PLEASE SEE FULL INPUT FILE FOR FULL ELEMENT SET
**
*Elset, elset=_Adhe_Comp_S5, internal
   90,  117,  128,  130,  139,  141,  143,  166,  168,  181,  185,  187,  190,  192,  194,  213
  215,  217,  221,  230,  234,  238,  239,  241,  245,  248,  252,  254,  263,  265,  267,  270
  274,  312,  325,  380,  383,  397,  407,  483,  551,  552,
** ... PLEASE SEE FULL INPUT FILE FOR FULL ELEMENT SET
**
*Surface, type=ELEMENT, name=Adhe_Comp
_Adhe_Comp_S4, S4
_Adhe_Comp_S6, S6
_Adhe_Comp_S3, S3
_Adhe_Comp_S5, S5
*Elset, elset=_Adhes_Alum_S3, internal
   82,   83,   84,  100,  103,  105,  107,  275,  361,  365,  366,  371,  372,  374,  458,  547
  549,  559,  562,  570,  573,  576,  617,  620,  625,  627,  629,  631,  634,  636,  637,  639
  641,  643,  645,  647,  649,  650,  652,  654,  657,  659,
** ... PLEASE SEE FULL INPUT FILE FOR FULL ELEMENT SET
**
*Elset, elset=_Adhes_Alum_S4, internal
  362,  364,  632,  814, 1254, 1256, 1524, 1706, 2146, 2148, 2416, 2598, 3038, 3040, 3308, 3490
 3930, 3932, 4200, 4382, 4822, 4824, 5092, 5274, 5714, 5716, 5984, 6166, 6606, 6608, 6876, 7058
 7498, 7500, 7768, 7950, 8390, 8392, 8660, 8842, 9282, 9284,
** ... PLEASE SEE FULL INPUT FILE FOR FULL ELEMENT SET
**
*Elset, elset=_Adhes_Alum_S6, internal
  453,  500, 1345, 1392, 2237, 2284, 3129, 3176, 4021, 4068, 4913, 4960, 5805, 5852, 6697, 6744
 7589, 7636, 8481, 8528, 9373, 9420, 10265, 10312, 11157, 11204, 12049, 12096, 12941, 12988, 13833,
13880
 14725, 14772, 15617, 15664, 16509, 16556, 17401, 17448, 18293, 18340, 19185, 19232, 20077, 20124, 20969,
21016
 21861, 21908, 22753, 22800, 23645, 23692, 24537, 24584, 25429, 25476, 26321, 26368, 27213, 27260, 28105,
28152
 28997, 29044, 29889, 29936, 30781, 30828, 31673, 31720, 32565, 32612, 33457, 33504, 34349, 34396, 35241,
35288
**
*Elset, elset=_Adhes_Alum_S5, internal
  304,  362,  519,  524,  525,  536,  540,  542,  543,  545,  546,  548,  624,  626,  628,  630
  633,  635,  638,  640,  642,  644,  646,  648,  651,  653,  655,  656,  658,  660,  662,  664
  666,  668,  674,  676,  679,  681,  684,  686,  688,  691,
** ... PLEASE SEE FULL INPUT FILE FOR FULL ELEMENT SET
**
*Surface, type=ELEMENT, name=Adhes_Alum
_Adhes_Alum_S3, S3
_Adhes_Alum_S4, S4
_Adhes_Alum_S6, S6
_Adhes_Alum_S5, S5
**
** ADHESIVE SECTION DEFINITION
** ----------------------------------------------------------
** Section: Adhesive
*Solid Section, elset=_PickedSet2, material=Adhesive
```

```
,
*End Instance
**
*Instance, name=Aluminium-1, part=Aluminium
*Node
      1,          5.,      -12.25,          0.
      2,          0.,      -12.25,          0.
      3,          0.,        1.75,          0.
      4,          3.,        1.75,          0.
      5,          3.,       -2.25,          0.
      6,          5.,       -2.25,          0.
      7,   4.61538458,      -12.25,          0.
      8,   4.23076916,      -12.25,          0.
      9,   3.84615374,      -12.25,          0.
** ... PLEASE SEE FULL INPUT FILE FOR ALL NODE DEFINITIONS
**
*Element, type=C3D8R
    1,  261,   97,   96,  270,  911,  747,  746,  920
    2,  255,   98,   97,  261,  905,  748,  747,  911
    3,   13,  237,  238,   14,  663,  887,  888,  664
    4,  613,  111,  112,  133, 1263,  761,  762,  783
    5,  260,  101,  100,  257,  910,  751,  750,  907
    6,  276,  102,  101,  260,  926,  752,  751,  910
    7,   99,  256,  257,  100,  749,  906,  907,  750
    8,  320,   15,   14,  238,  970,  665,  664,  888
    9,   12,  236,  237,   13,  662,  886,  887,  663
** ... PLEASE SEE FULL INPUT FILE FOR ALL ELEMENT DEFINITIONS
**
*Nset, nset=_PickedSet2, internal, generate
    1, 13650,      1
*Elset, elset=_PickedSet2, internal, generate
    1, 11880,      1
*Nset, nset=Bottom
    1,    2,    7,    8,    9,   10,   11,   12,   13,   14,   15,   16,   17,   18,  651,  652
  657,  658,  659,  660,  661,  662,  663,  664,  665,  666,  667,  668, 1301, 1302, 1307, 1308
 1309, 1310, 1311, 1312, 1313, 1314, 1315, 1316, 1317, 1318,
** ... PLEASE SEE FULL INPUT FILE FOR ALL NODE SET INFO
**
*Elset, elset=Bottom
    3,    8,    9,   12,   13,   14,   86,   89,   91,   92,   94,  230,  236,  597,  602,  603
  606,  607,  608,  680,  683,  685,  686,  688,  824,  830, 1191, 1196, 1197, 1200, 1201, 1202
 1274, 1277, 1279, 1280, 1282, 1418, 1424, 1785, 1790, 1791,
** ... PLEASE SEE FULL INPUT FILE FOR ALL ELEMENT SET INFO
**
*Elset, elset=_Alum_S5, internal
   27,   28,   48,   70,  114,  124,  621,  622,  642,  664,  708,  718, 1215, 1216, 1236, 1258
 1302, 1312, 1809, 1810, 1830, 1852, 1896, 1906, 2403, 2404, 2424, 2446, 2490, 2500, 2997, 2998
 3018, 3040, 3084, 3094, 3591, 3592, 3612, 3634, 3678, 3688,
** ... PLEASE SEE FULL INPUT FILE FOR ALL ELEMENT SET INFO
**
*Elset, elset=_Alum_S4, internal
   49,   52,   53,   62,   63,   64,   68,  125,  643,  646,  647,  656,  657,  658,  662,  719
 1237, 1240, 1241, 1250, 1251, 1252, 1256, 1313, 1831, 1834, 1835, 1844, 1845, 1846, 1850, 1907
 2425, 2428, 2429, 2438, 2439, 2440, 2444, 2501, 3019, 3022,
** ... PLEASE SEE FULL INPUT FILE FOR ALL ELEMENT SET INFO
```

```
**
*Elset, elset=_Alum_S6, internal
   50,   51,   54,   55,   56,   57,   58,   59,   60,   61,   65,   66,   67,  111,  644,  645
  648,  649,  650,  651,  652,  653,  654,  655,  659,  660,  661,  705, 1238, 1239, 1242, 1243
 1244, 1245, 1246, 1247, 1248, 1249, 1253, 1254, 1255, 1299,
** ... PLEASE SEE FULL INPUT FILE FOR ALL ELEMENT SET INFO
**
*Elset, elset=_Alum_S3, internal
   26,   71,  620,  665, 1214, 1259, 1808, 1853, 2402, 2447, 2996, 3041, 3590, 3635, 4184, 4229
 4778, 4823, 5372, 5417, 5966, 6011, 6560, 6605, 7154, 7199, 7748, 7793, 8342, 8387, 8936, 8981
 9530, 9575, 10124, 10169, 10718, 10763, 11312, 11357
*Surface, type=ELEMENT, name=Alum
_Alum_S5, S5
_Alum_S4, S4
_Alum_S6, S6
_Alum_S3, S3
**
** ALUMINUM SECTION DEFINITION
** ----------------------------------------------------------
** Section: Aluminium
*Solid Section, elset=_PickedSet2, material=Aluminium
,
*End Instance
**
*Instance, name=Composite-1, part=Composite
        -2.,        -6.45,           0.
*Node
     1,   5.05000019,        4.25,          4.
     2,   5.05000019,   4.44750023,          4.
     3,   5.05000019,   4.64499998,          4.
     4,   5.05000019,   4.84250021,          4.
     5,   5.05000019,   5.03999996,          4.
     6,   5.05000019,   5.23750019,          4.
     7,   5.05000019,   5.43499994,          4.
     8,   5.05000019,   5.63250017,          4.
     9,   5.05000019,   5.82999992,          4.
** ... PLEASE SEE FULL INPUT FILE FOR ALL NODE DEFINITIONS
**
*Element, type=C3D8R
  1,  442,  443,  464,  463,    1,    2,   23,   22
  2,  443,  444,  465,  464,    2,    3,   24,   23
  3,  444,  445,  466,  465,    3,    4,   25,   24
  4,  445,  446,  467,  466,    4,    5,   26,   25
  5,  446,  447,  468,  467,    5,    6,   27,   26
  6,  447,  448,  469,  468,    6,    7,   28,   27
  7,  448,  449,  470,  469,    7,    8,   29,   28
  8,  449,  450,  471,  470,    8,    9,   30,   29
  9,  450,  451,  472,  471,    9,   10,   31,   30
** ... PLEASE SEE FULL INPUT FILE FOR ALL ELEMENT DEFINITIONS
**
*Nset, nset=_PickedSet2, internal, generate
   1,  4851,     1
*Elset, elset=_PickedSet2, internal, generate
   1,  4000,     1
*Nset, nset=Composite, generate
```

```
   1,  4851,     1
*Elset, elset=Composite, generate
   1,  4000,     1
*Elset, elset=_Composite_S6, internal, generate
   1,  3981,    20
*Elset, elset=_Composite_S2, internal, generate
  1,  400,    1
*Surface, type=ELEMENT, name=Composite
_Composite_S6, S6
_Composite_S2, S2
** Section: Composite
*Solid Section, elset=_PickedSet2, material=Composite
,
*End Instance
**
*Nset, nset=_PickedSet8, internal, instance=Adhesive-1, generate
 47721,  48913,      1
*Nset, nset=_PickedSet8, internal, instance=Aluminium-1, generate
 13001,  13650,      1
*Nset, nset=_PickedSet8, internal, instance=Composite-1
    1,    2,    3,    4,    5,    6,    7,    8,    9,   10,   11,   12,   13,   14,   15,   16
   17,   18,   19,   20,   21,  442,  443,  444,  445,  446,  447,  448,  449,  450,  451,  452
  453,  454,  455,  456,  457,  458,  459,  460,  461,  462,  883,  884,  885,  886,  887,  888
  889,  890,  891,  892,  893,  894,  895,  896,  897,  898,  899,  900,  901,  902,  903, 1324
 1325, 1326, 1327, 1328, 1329, 1330, 1331, 1332, 1333, 1334, 1335, 1336, 1337, 1338, 1339, 1340
 1341, 1342, 1343, 1344, 1765, 1766, 1767, 1768, 1769, 1770, 1771, 1772, 1773, 1774, 1775, 1776
 1777, 1778, 1779, 1780, 1781, 1782, 1783, 1784, 1785, 2206, 2207, 2208, 2209, 2210, 2211, 2212
 2213, 2214, 2215, 2216, 2217, 2218, 2219, 2220, 2221, 2222, 2223, 2224, 2225, 2226, 2647, 2648
 2649, 2650, 2651, 2652, 2653, 2654, 2655, 2656, 2657, 2658, 2659, 2660, 2661, 2662, 2663, 2664
 2665, 2666, 2667, 3088, 3089, 3090, 3091, 3092, 3093, 3094, 3095, 3096, 3097, 3098, 3099, 3100
 3101, 3102, 3103, 3104, 3105, 3106, 3107, 3108, 3529, 3530, 3531, 3532, 3533, 3534, 3535, 3536
 3537, 3538, 3539, 3540, 3541, 3542, 3543, 3544, 3545, 3546, 3547, 3548, 3549, 3970, 3971, 3972
 3973, 3974, 3975, 3976, 3977, 3978, 3979, 3980, 3981, 3982, 3983, 3984, 3985, 3986, 3987, 3988
 3989, 3990, 4411, 4412, 4413, 4414, 4415, 4416, 4417, 4418, 4419, 4420, 4421, 4422, 4423, 4424
 4425, 4426, 4427, 4428, 4429, 4430, 4431
*Elset, elset=_PickedSet8, internal, instance=Adhesive-1, generate
 34789,  35680,      1
*Elset, elset=_PickedSet8, internal, instance=Aluminium-1, generate
 11287,  11880,      1
*Elset, elset=_PickedSet8, internal, instance=Composite-1
    1,    2,    3,    4,    5,    6,    7,    8,    9,   10,   11,   12,   13,   14,   15,   16
   17,   18,   19,   20,  401,  402,  403,  404,  405,  406,  407,  408,  409,  410,  411,  412
  413,  414,  415,  416,  417,  418,  419,  420,  801,  802,  803,  804,  805,  806,  807,  808
  809,  810,  811,  812,  813,  814,  815,  816,  817,  818,  819,  820, 1201, 1202, 1203, 1204
 1205, 1206, 1207, 1208, 1209, 1210, 1211, 1212, 1213, 1214, 1215, 1216, 1217, 1218, 1219, 1220
 1601, 1602, 1603, 1604, 1605, 1606, 1607, 1608, 1609, 1610, 1611, 1612, 1613, 1614, 1615, 1616
 1617, 1618, 1619, 1620, 2001, 2002, 2003, 2004, 2005, 2006, 2007, 2008, 2009, 2010, 2011, 2012
 2013, 2014, 2015, 2016, 2017, 2018, 2019, 2020, 2401, 2402, 2403, 2404, 2405, 2406, 2407, 2408
 2409, 2410, 2411, 2412, 2413, 2414, 2415, 2416, 2417, 2418, 2419, 2420, 2801, 2802, 2803, 2804
 2805, 2806, 2807, 2808, 2809, 2810, 2811, 2812, 2813, 2814, 2815, 2816, 2817, 2818, 2819, 2820
 3201, 3202, 3203, 3204, 3205, 3206, 3207, 3208, 3209, 3210, 3211, 3212, 3213, 3214, 3215, 3216
 3217, 3218, 3219, 3220, 3601, 3602, 3603, 3604, 3605, 3606, 3607, 3608, 3609, 3610, 3611, 3612
 3613, 3614, 3615, 3616, 3617, 3618, 3619, 3620
*Nset, nset=_PickedSet9, internal, instance=Adhesive-1
   34,   202,   600,  1227,  1395,  1793,  2420,  2588,  2986,  3613,  3781,  4179,  4806,  4974,  5372,  5999
```

6167, 6565, 7192, 7360, 7758, 8385, 8553, 8951, 9578, 9746, 10144, 10771, 10939, 11337, 11964, 12132
12530, 13157, 13325, 13723, 14350, 14518, 14916, 15543, 15711, 16109, 16736, 16904, 17302, 17929, 18097, 18495
19122, 19290, 19688, 20315, 20483, 20881, 21508, 21676, 22074, 22701, 22869, 23267, 23894, 24062, 24460, 25087
25255, 25653, 26280, 26448, 26846, 27473, 27641, 28039, 28666, 28834, 29232, 29859, 30027, 30425, 31052, 31220
31618, 32245, 32413, 32811, 33438, 33606, 34004, 34631, 34799, 35197, 35824, 35992, 36390, 37017, 37185, 37583
38210, 38378, 38776, 39403, 39571, 39969, 40596, 40764, 41162, 41789, 41957, 42355, 42982, 43150, 43548, 44175
44343, 44741, 45368, 45536, 45934, 46561, 46729, 47127, 47754, 47922, 48320
*Nset, nset=_PickedSet9, internal, instance=Aluminium-1
1, 6, 87, 88, 89, 90, 91, 92, 93, 94, 95, 96, 97, 98, 99, 100
101, 102, 103, 104, 105, 106, 107, 108, 109, 110, 651, 656, 737, 738, 739, 740
741, 742, 743, 744, 745, 746, 747, 748, 749, 750, 751, 752, 753, 754, 755, 756
757, 758, 759, 760, 1301, 1306, 1387, 1388, 1389, 1390, 1391, 1392, 1393, 1394, 1395, 1396
1397, 1398, 1399, 1400, 1401, 1402, 1403, 1404, 1405, 1406, 1407, 1408, 1409, 1410, 1951, 1956
2037, 2038, 2039, 2040, 2041, 2042, 2043, 2044, 2045, 2046, 2047, 2048, 2049, 2050, 2051, 2052
2053, 2054, 2055, 2056, 2057, 2058, 2059, 2060, 2601, 2606, 2687, 2688, 2689, 2690, 2691, 2692
2693, 2694, 2695, 2696, 2697, 2698, 2699, 2700, 2701, 2702, 2703, 2704, 2705, 2706, 2707, 2708
2709, 2710, 3251, 3256, 3337, 3338, 3339, 3340, 3341, 3342, 3343, 3344, 3345, 3346, 3347, 3348
3349, 3350, 3351, 3352, 3353, 3354, 3355, 3356, 3357, 3358, 3359, 3360, 3901, 3906, 3987, 3988
3989, 3990, 3991, 3992, 3993, 3994, 3995, 3996, 3997, 3998, 3999, 4000, 4001, 4002, 4003, 4004
4005, 4006, 4007, 4008, 4009, 4010, 4551, 4556, 4637, 4638, 4639, 4640, 4641, 4642, 4643, 4644
4645, 4646, 4647, 4648, 4649, 4650, 4651, 4652, 4653, 4654, 4655, 4656, 4657, 4658, 4659, 4660
5201, 5206, 5287, 5288, 5289, 5290, 5291, 5292, 5293, 5294, 5295, 5296, 5297, 5298, 5299, 5300
5301, 5302, 5303, 5304, 5305, 5306, 5307, 5308, 5309, 5310, 5851, 5856, 5937, 5938, 5939, 5940
5941, 5942, 5943, 5944, 5945, 5946, 5947, 5948, 5949, 5950, 5951, 5952, 5953, 5954, 5955, 5956
5957, 5958, 5959, 5960, 6501, 6506, 6587, 6588, 6589, 6590, 6591, 6592, 6593, 6594, 6595, 6596
6597, 6598, 6599, 6600, 6601, 6602, 6603, 6604, 6605, 6606, 6607, 6608, 6609, 6610, 7151, 7156
7237, 7238, 7239, 7240, 7241, 7242, 7243, 7244, 7245, 7246, 7247, 7248, 7249, 7250, 7251, 7252
7253, 7254, 7255, 7256, 7257, 7258, 7259, 7260, 7801, 7806, 7887, 7888, 7889, 7890, 7891, 7892
7893, 7894, 7895, 7896, 7897, 7898, 7899, 7900, 7901, 7902, 7903, 7904, 7905, 7906, 7907, 7908
7909, 7910, 8451, 8456, 8537, 8538, 8539, 8540, 8541, 8542, 8543, 8544, 8545, 8546, 8547, 8548
8549, 8550, 8551, 8552, 8553, 8554, 8555, 8556, 8557, 8558, 8559, 8560, 9101, 9106, 9187, 9188
9189, 9190, 9191, 9192, 9193, 9194, 9195, 9196, 9197, 9198, 9199, 9200, 9201, 9202, 9203, 9204
9205, 9206, 9207, 9208, 9209, 9210, 9751, 9756, 9837, 9838, 9839, 9840, 9841, 9842, 9843, 9844
9845, 9846, 9847, 9848, 9849, 9850, 9851, 9852, 9853, 9854, 9855, 9856, 9857, 9858, 9859, 9860
10401, 10406, 10487, 10488, 10489, 10490, 10491, 10492, 10493, 10494, 10495, 10496, 10497, 10498, 10499, 10500
10501, 10502, 10503, 10504, 10505, 10506, 10507, 10508, 10509, 10510, 11051, 11056, 11137, 11138, 11139, 11140
11141, 11142, 11143, 11144, 11145, 11146, 11147, 11148, 11149, 11150, 11151, 11152, 11153, 11154, 11155, 11156
11157, 11158, 11159, 11160, 11701, 11706, 11787, 11788, 11789, 11790, 11791, 11792, 11793, 11794, 11795, 11796
11797, 11798, 11799, 11800, 11801, 11802, 11803, 11804, 11805, 11806, 11807, 11808, 11809, 11810, 12351, 12356
12437, 12438, 12439, 12440, 12441, 12442, 12443, 12444, 12445, 12446, 12447, 12448, 12449, 12450, 12451, 12452
12453, 12454, 12455, 12456, 12457, 12458, 12459, 12460, 13001, 13006, 13087, 13088, 13089, 13090, 13091, 13092
13093, 13094, 13095, 13096, 13097, 13098, 13099, 13100, 13101, 13102, 13103, 13104, 13105, 13106, 13107, 13108

13109, 13110
*Nset, nset=_PickedSet9, internal, instance=Composite-1, generate
4411, 4851, 1
*Elset, elset=_PickedSet9, internal, instance=Adhesive-1
483, 500, 1375, 1392, 2267, 2284, 3159, 3176, 4051, 4068, 4943, 4960, 5835, 5852, 6727, 6744
7619, 7636, 8511, 8528, 9403, 9420, 10295, 10312, 11187, 11204, 12079, 12096, 12971, 12988, 13863, 13880
14755, 14772, 15647, 15664, 16539, 16556, 17431, 17448, 18323, 18340, 19215, 19232, 20107, 20124, 20999, 21016
21891, 21908, 22783, 22800, 23675, 23692, 24567, 24584, 25459, 25476, 26351, 26368, 27243, 27260, 28135, 28152
29027, 29044, 29919, 29936, 30811, 30828, 31703, 31720, 32595, 32612, 33487, 33504, 34379, 34396, 35271, 35288
*Elset, elset=_PickedSet9, internal, instance=Aluminium-1
1, 2, 5, 6, 7, 18, 67, 83, 84, 85, 93, 94, 140, 148, 175, 182
194, 198, 218, 234, 235, 238, 247, 248, 271, 595, 596, 599, 600, 601, 612, 661
677, 678, 679, 687, 688, 734, 742, 769, 776, 788, 792, 812, 828, 829, 832, 841
842, 865, 1189, 1190, 1193, 1194, 1195, 1206, 1255, 1271, 1272, 1273, 1281, 1282, 1328, 1336
1363, 1370, 1382, 1386, 1406, 1422, 1423, 1426, 1435, 1436, 1459, 1783, 1784, 1787, 1788, 1789
1800, 1849, 1865, 1866, 1867, 1875, 1876, 1922, 1930, 1957, 1964, 1976, 1980, 2000, 2016, 2017
2020, 2029, 2030, 2053, 2377, 2378, 2381, 2382, 2383, 2394, 2443, 2459, 2460, 2461, 2469, 2470
2516, 2524, 2551, 2558, 2570, 2574, 2594, 2610, 2611, 2614, 2623, 2624, 2647, 2971, 2972, 2975
2976, 2977, 2988, 3037, 3053, 3054, 3055, 3063, 3064, 3110, 3118, 3145, 3152, 3164, 3168, 3188
3204, 3205, 3208, 3217, 3218, 3241, 3565, 3566, 3569, 3570, 3571, 3582, 3631, 3647, 3648, 3649
3657, 3658, 3704, 3712, 3739, 3746, 3758, 3762, 3782, 3798, 3799, 3802, 3811, 3812, 3835, 4159
4160, 4163, 4164, 4165, 4176, 4225, 4241, 4242, 4243, 4251, 4252, 4298, 4306, 4333, 4340, 4352
4356, 4376, 4392, 4393, 4396, 4405, 4406, 4429, 4753, 4754, 4757, 4758, 4759, 4770, 4819, 4835
4836, 4837, 4845, 4846, 4892, 4900, 4927, 4934, 4946, 4950, 4970, 4986, 4987, 4990, 4999, 5000
5023, 5347, 5348, 5351, 5352, 5353, 5364, 5413, 5429, 5430, 5431, 5439, 5440, 5486, 5494, 5521
5528, 5540, 5544, 5564, 5580, 5581, 5584, 5593, 5594, 5617, 5941, 5942, 5945, 5946, 5947, 5958
6007, 6023, 6024, 6025, 6033, 6034, 6080, 6088, 6115, 6122, 6134, 6138, 6158, 6174, 6175, 6178
6187, 6188, 6211, 6535, 6536, 6539, 6540, 6541, 6552, 6601, 6617, 6618, 6619, 6627, 6628, 6674
6682, 6709, 6716, 6728, 6732, 6752, 6768, 6769, 6772, 6781, 6782, 6805, 7129, 7130, 7133, 7134
7135, 7146, 7195, 7211, 7212, 7213, 7221, 7222, 7268, 7276, 7303, 7310, 7322, 7326, 7346, 7362
7363, 7366, 7375, 7376, 7399, 7723, 7724, 7727, 7728, 7729, 7740, 7789, 7805, 7806, 7807, 7815
7816, 7862, 7870, 7897, 7904, 7916, 7920, 7940, 7956, 7957, 7960, 7969, 7970, 7993, 8317, 8318
8321, 8322, 8323, 8334, 8383, 8399, 8400, 8401, 8409, 8410, 8456, 8464, 8491, 8498, 8510, 8514
8534, 8550, 8551, 8554, 8563, 8564, 8587, 8911, 8912, 8915, 8916, 8917, 8928, 8977, 8993, 8994
8995, 9003, 9004, 9050, 9058, 9085, 9092, 9104, 9108, 9128, 9144, 9145, 9148, 9157, 9158, 9181
9505, 9506, 9509, 9510, 9511, 9522, 9571, 9587, 9588, 9589, 9597, 9598, 9644, 9652, 9679, 9686
9698, 9702, 9722, 9738, 9739, 9742, 9751, 9752, 9775, 10099, 10100, 10103, 10104, 10105, 10116, 10165
10181, 10182, 10183, 10191, 10192, 10238, 10246, 10273, 10280, 10292, 10296, 10316, 10332, 10333, 10336, 10345
10346, 10369, 10693, 10694, 10697, 10698, 10699, 10710, 10759, 10775, 10776, 10777, 10785, 10786, 10832, 10840
10867, 10874, 10886, 10890, 10910, 10926, 10927, 10930, 10939, 10940, 10963, 11287, 11288, 11291, 11292, 11293
11304, 11353, 11369, 11370, 11371, 11379, 11380, 11426, 11434, 11461, 11468, 11480, 11484, 11504, 11520, 11521
11524, 11533, 11534, 11557
*Elset, elset=_PickedSet9, internal, instance=Composite-1, generate
3601, 4000, 1
*Nset, nset=_PickedSet10, internal, instance=Adhesive-1, generate
47721, 48913, 1
*Nset, nset=_PickedSet10, internal, instance=Aluminium-1, generate

13001, 13650, 1
*Nset, nset=_PickedSet10, internal, instance=Composite-1
1, 2, 3, 4, 5, 6, 7, 8, 9, 10, 11, 12, 13, 14, 15, 16
17, 18, 19, 20, 21, 442, 443, 444, 445, 446, 447, 448, 449, 450, 451, 452
453, 454, 455, 456, 457, 458, 459, 460, 461, 462, 883, 884, 885, 886, 887, 888
889, 890, 891, 892, 893, 894, 895, 896, 897, 898, 899, 900, 901, 902, 903, 1324
1325, 1326, 1327, 1328, 1329, 1330, 1331, 1332, 1333, 1334, 1335, 1336, 1337, 1338, 1339, 1340
1341, 1342, 1343, 1344, 1765, 1766, 1767, 1768, 1769, 1770, 1771, 1772, 1773, 1774, 1775, 1776
1777, 1778, 1779, 1780, 1781, 1782, 1783, 1784, 1785, 2206, 2207, 2208, 2209, 2210, 2211, 2212
2213, 2214, 2215, 2216, 2217, 2218, 2219, 2220, 2221, 2222, 2223, 2224, 2225, 2226, 2647, 2648
2649, 2650, 2651, 2652, 2653, 2654, 2655, 2656, 2657, 2658, 2659, 2660, 2661, 2662, 2663, 2664
2665, 2666, 2667, 3088, 3089, 3090, 3091, 3092, 3093, 3094, 3095, 3096, 3097, 3098, 3099, 3100
3101, 3102, 3103, 3104, 3105, 3106, 3107, 3108, 3529, 3530, 3531, 3532, 3533, 3534, 3535, 3536
3537, 3538, 3539, 3540, 3541, 3542, 3543, 3544, 3545, 3546, 3547, 3548, 3549, 3970, 3971, 3972
3973, 3974, 3975, 3976, 3977, 3978, 3979, 3980, 3981, 3982, 3983, 3984, 3985, 3986, 3987, 3988
3989, 3990, 4411, 4412, 4413, 4414, 4415, 4416, 4417, 4418, 4419, 4420, 4421, 4422, 4423, 4424
4425, 4426, 4427, 4428, 4429, 4430, 4431
*Elset, elset=_PickedSet10, internal, instance=Adhesive-1, generate
34789, 35680, 1
*Elset, elset=_PickedSet10, internal, instance=Aluminium-1, generate
11287, 11880, 1
*Elset, elset=_PickedSet10, internal, instance=Composite-1
1, 2, 3, 4, 5, 6, 7, 8, 9, 10, 11, 12, 13, 14, 15, 16
17, 18, 19, 20, 401, 402, 403, 404, 405, 406, 407, 408, 409, 410, 411, 412
413, 414, 415, 416, 417, 418, 419, 420, 801, 802, 803, 804, 805, 806, 807, 808
809, 810, 811, 812, 813, 814, 815, 816, 817, 818, 819, 820, 1201, 1202, 1203, 1204
1205, 1206, 1207, 1208, 1209, 1210, 1211, 1212, 1213, 1214, 1215, 1216, 1217, 1218, 1219, 1220
1601, 1602, 1603, 1604, 1605, 1606, 1607, 1608, 1609, 1610, 1611, 1612, 1613, 1614, 1615, 1616
1617, 1618, 1619, 1620, 2001, 2002, 2003, 2004, 2005, 2006, 2007, 2008, 2009, 2010, 2011, 2012
2013, 2014, 2015, 2016, 2017, 2018, 2019, 2020, 2401, 2402, 2403, 2404, 2405, 2406, 2407, 2408
2409, 2410, 2411, 2412, 2413, 2414, 2415, 2416, 2417, 2418, 2419, 2420, 2801, 2802, 2803, 2804
2805, 2806, 2807, 2808, 2809, 2810, 2811, 2812, 2813, 2814, 2815, 2816, 2817, 2818, 2819, 2820
3201, 3202, 3203, 3204, 3205, 3206, 3207, 3208, 3209, 3210, 3211, 3212, 3213, 3214, 3215, 3216
3217, 3218, 3219, 3220, 3601, 3602, 3603, 3604, 3605, 3606, 3607, 3608, 3609, 3610, 3611, 3612
3613, 3614, 3615, 3616, 3617, 3618, 3619, 3620
*Nset, nset=_PickedSet11, internal, instance=Adhesive-1
34, 202, 600, 1227, 1395, 1793, 2420, 2588, 2986, 3613, 3781, 4179, 4806, 4974, 5372, 5999
6167, 6565, 7192, 7360, 7758, 8385, 8553, 8951, 9578, 9746, 10144, 10771, 10939, 11337, 11964, 12132
12530, 13157, 13325, 13723, 14350, 14518, 14916, 15543, 15711, 16109, 16736, 16904, 17302, 17929, 18097,
18495
19122, 19290, 19688, 20315, 20483, 20881, 21508, 21676, 22074, 22701, 22869, 23267, 23894, 24062, 24460,
25087
25255, 25653, 26280, 26448, 26846, 27473, 27641, 28039, 28666, 28834, 29232, 29859, 30027, 30425, 31052,
31220
31618, 32245, 32413, 32811, 33438, 33606, 34004, 34631, 34799, 35197, 35824, 35992, 36390, 37017, 37185,
37583
38210, 38378, 38776, 39403, 39571, 39969, 40596, 40764, 41162, 41789, 41957, 42355, 42982, 43150, 43548,
44175
44343, 44741, 45368, 45536, 45934, 46561, 46729, 47127, 47754, 47922, 48320
*Nset, nset=_PickedSet11, internal, instance=Aluminium-1
1, 6, 87, 88, 89, 90, 91, 92, 93, 94, 95, 96, 97, 98, 99, 100
101, 102, 103, 104, 105, 106, 107, 108, 109, 110, 651, 656, 737, 738, 739, 740
741, 742, 743, 744, 745, 746, 747, 748, 749, 750, 751, 752, 753, 754, 755, 756
757, 758, 759, 760, 1301, 1306, 1387, 1388, 1389, 1390, 1391, 1392, 1393, 1394, 1395, 1396
1397, 1398, 1399, 1400, 1401, 1402, 1403, 1404, 1405, 1406, 1407, 1408, 1409, 1410, 1951, 1956

2037, 2038, 2039, 2040, 2041, 2042, 2043, 2044, 2045, 2046, 2047, 2048, 2049, 2050, 2051, 2052
2053, 2054, 2055, 2056, 2057, 2058, 2059, 2060, 2601, 2606, 2687, 2688, 2689, 2690, 2691, 2692
2693, 2694, 2695, 2696, 2697, 2698, 2699, 2700, 2701, 2702, 2703, 2704, 2705, 2706, 2707, 2708
2709, 2710, 3251, 3256, 3337, 3338, 3339, 3340, 3341, 3342, 3343, 3344, 3345, 3346, 3347, 3348
3349, 3350, 3351, 3352, 3353, 3354, 3355, 3356, 3357, 3358, 3359, 3360, 3901, 3906, 3987, 3988
3989, 3990, 3991, 3992, 3993, 3994, 3995, 3996, 3997, 3998, 3999, 4000, 4001, 4002, 4003, 4004
4005, 4006, 4007, 4008, 4009, 4010, 4551, 4556, 4637, 4638, 4639, 4640, 4641, 4642, 4643, 4644
4645, 4646, 4647, 4648, 4649, 4650, 4651, 4652, 4653, 4654, 4655, 4656, 4657, 4658, 4659, 4660
5201, 5206, 5287, 5288, 5289, 5290, 5291, 5292, 5293, 5294, 5295, 5296, 5297, 5298, 5299, 5300
5301, 5302, 5303, 5304, 5305, 5306, 5307, 5308, 5309, 5310, 5851, 5856, 5937, 5938, 5939, 5940
5941, 5942, 5943, 5944, 5945, 5946, 5947, 5948, 5949, 5950, 5951, 5952, 5953, 5954, 5955, 5956
5957, 5958, 5959, 5960, 6501, 6506, 6587, 6588, 6589, 6590, 6591, 6592, 6593, 6594, 6595, 6596
6597, 6598, 6599, 6600, 6601, 6602, 6603, 6604, 6605, 6606, 6607, 6608, 6609, 6610, 7151, 7156
7237, 7238, 7239, 7240, 7241, 7242, 7243, 7244, 7245, 7246, 7247, 7248, 7249, 7250, 7251, 7252
7253, 7254, 7255, 7256, 7257, 7258, 7259, 7260, 7801, 7806, 7887, 7888, 7889, 7890, 7891, 7892
7893, 7894, 7895, 7896, 7897, 7898, 7899, 7900, 7901, 7902, 7903, 7904, 7905, 7906, 7907, 7908
7909, 7910, 8451, 8456, 8537, 8538, 8539, 8540, 8541, 8542, 8543, 8544, 8545, 8546, 8547, 8548
8549, 8550, 8551, 8552, 8553, 8554, 8555, 8556, 8557, 8558, 8559, 8560, 9101, 9106, 9187, 9188
9189, 9190, 9191, 9192, 9193, 9194, 9195, 9196, 9197, 9198, 9199, 9200, 9201, 9202, 9203, 9204
9205, 9206, 9207, 9208, 9209, 9210, 9751, 9756, 9837, 9838, 9839, 9840, 9841, 9842, 9843, 9844
9845, 9846, 9847, 9848, 9849, 9850, 9851, 9852, 9853, 9854, 9855, 9856, 9857, 9858, 9859, 9860
10401, 10406, 10487, 10488, 10489, 10490, 10491, 10492, 10493, 10494, 10495, 10496, 10497, 10498, 10499,
10500
10501, 10502, 10503, 10504, 10505, 10506, 10507, 10508, 10509, 10510, 11051, 11056, 11137, 11138, 11139,
11140
11141, 11142, 11143, 11144, 11145, 11146, 11147, 11148, 11149, 11150, 11151, 11152, 11153, 11154, 11155,
11156
11157, 11158, 11159, 11160, 11701, 11706, 11787, 11788, 11789, 11790, 11791, 11792, 11793, 11794, 11795,
11796
11797, 11798, 11799, 11800, 11801, 11802, 11803, 11804, 11805, 11806, 11807, 11808, 11809, 11810, 12351,
12356
12437, 12438, 12439, 12440, 12441, 12442, 12443, 12444, 12445, 12446, 12447, 12448, 12449, 12450, 12451,
12452
12453, 12454, 12455, 12456, 12457, 12458, 12459, 12460, 13001, 13006, 13087, 13088, 13089, 13090, 13091,
13092
13093, 13094, 13095, 13096, 13097, 13098, 13099, 13100, 13101, 13102, 13103, 13104, 13105, 13106, 13107,
13108
13109, 13110
*Nset, nset=_PickedSet11, internal, instance=Composite-1, generate
4411, 4851, 1
*Elset, elset=_PickedSet11, internal, instance=Adhesive-1
483, 500, 1375, 1392, 2267, 2284, 3159, 3176, 4051, 4068, 4943, 4960, 5835, 5852, 6727, 6744
7619, 7636, 8511, 8528, 9403, 9420, 10295, 10312, 11187, 11204, 12079, 12096, 12971, 12988, 13863,
13880
14755, 14772, 15647, 15664, 16539, 16556, 17431, 17448, 18323, 18340, 19215, 19232, 20107, 20124, 20999,
21016
21891, 21908, 22783, 22800, 23675, 23692, 24567, 24584, 25459, 25476, 26351, 26368, 27243, 27260, 28135,
28152
29027, 29044, 29919, 29936, 30811, 30828, 31703, 31720, 32595, 32612, 33487, 33504, 34379, 34396, 35271,
35288
*Elset, elset=_PickedSet11, internal, instance=Aluminium-1
1, 2, 5, 6, 7, 18, 67, 83, 84, 85, 93, 94, 140, 148, 175, 182
194, 198, 218, 234, 235, 238, 247, 248, 271, 595, 596, 599, 600, 601, 612, 661
677, 678, 679, 687, 688, 734, 742, 769, 776, 788, 792, 812, 828, 829, 832, 841
842, 865, 1189, 1190, 1193, 1194, 1195, 1206, 1255, 1271, 1272, 1273, 1281, 1282, 1328, 1336

1363, 1370, 1382, 1386, 1406, 1422, 1423, 1426, 1435, 1436, 1459, 1783, 1784, 1787, 1788, 1789
1800, 1849, 1865, 1866, 1867, 1875, 1876, 1922, 1930, 1957, 1964, 1976, 1980, 2000, 2016, 2017
2020, 2029, 2030, 2053, 2377, 2378, 2381, 2382, 2383, 2394, 2443, 2459, 2460, 2461, 2469, 2470
2516, 2524, 2551, 2558, 2570, 2574, 2594, 2610, 2611, 2614, 2623, 2624, 2647, 2971, 2972, 2975
2976, 2977, 2988, 3037, 3053, 3054, 3055, 3063, 3064, 3110, 3118, 3145, 3152, 3164, 3168, 3188
3204, 3205, 3208, 3217, 3218, 3241, 3565, 3566, 3569, 3570, 3571, 3582, 3631, 3647, 3648, 3649
3657, 3658, 3704, 3712, 3739, 3746, 3758, 3762, 3782, 3798, 3799, 3802, 3811, 3812, 3835, 4159
4160, 4163, 4164, 4165, 4176, 4225, 4241, 4242, 4243, 4251, 4252, 4298, 4306, 4333, 4340, 4352
4356, 4376, 4392, 4393, 4396, 4405, 4406, 4429, 4753, 4754, 4757, 4758, 4759, 4770, 4819, 4835
4836, 4837, 4845, 4846, 4892, 4900, 4927, 4934, 4946, 4950, 4970, 4986, 4987, 4990, 4999, 5000
5023, 5347, 5348, 5351, 5352, 5353, 5364, 5413, 5429, 5430, 5431, 5439, 5440, 5486, 5494, 5521
5528, 5540, 5544, 5564, 5580, 5581, 5584, 5593, 5594, 5617, 5941, 5942, 5945, 5946, 5947, 5958
6007, 6023, 6024, 6025, 6033, 6034, 6080, 6088, 6115, 6122, 6134, 6138, 6158, 6174, 6175, 6178
6187, 6188, 6211, 6535, 6536, 6539, 6540, 6541, 6552, 6601, 6617, 6618, 6619, 6627, 6628, 6674
6682, 6709, 6716, 6728, 6732, 6752, 6768, 6769, 6772, 6781, 6782, 6805, 7129, 7130, 7133, 7134
7135, 7146, 7195, 7211, 7212, 7213, 7221, 7222, 7268, 7276, 7303, 7310, 7322, 7326, 7346, 7362
7363, 7366, 7375, 7376, 7399, 7723, 7724, 7727, 7728, 7729, 7740, 7789, 7805, 7806, 7807, 7815
7816, 7862, 7870, 7897, 7904, 7916, 7920, 7940, 7956, 7957, 7960, 7969, 7970, 7993, 8317, 8318
8321, 8322, 8323, 8334, 8383, 8399, 8400, 8401, 8409, 8410, 8456, 8464, 8491, 8498, 8510, 8514
8534, 8550, 8551, 8554, 8563, 8564, 8587, 8911, 8912, 8915, 8916, 8917, 8928, 8977, 8993, 8994
8995, 9003, 9004, 9050, 9058, 9085, 9092, 9104, 9108, 9128, 9144, 9145, 9148, 9157, 9158, 9181
9505, 9506, 9509, 9510, 9511, 9522, 9571, 9587, 9588, 9589, 9597, 9598, 9644, 9652, 9679, 9686
9698, 9702, 9722, 9738, 9739, 9742, 9751, 9752, 9775, 10099, 10100, 10103, 10104, 10105, 10116, 10165
10181, 10182, 10183, 10191, 10192, 10238, 10246, 10273, 10280, 10292, 10296, 10316, 10332, 10333, 10336, 10345
10346, 10369, 10693, 10694, 10697, 10698, 10699, 10710, 10759, 10775, 10776, 10777, 10785, 10786, 10832, 10840
10867, 10874, 10886, 10890, 10910, 10926, 10927, 10930, 10939, 10940, 10963, 11287, 11288, 11291, 11292, 11293
11304, 11353, 11369, 11370, 11371, 11379, 11380, 11426, 11434, 11461, 11468, 11480, 11484, 11504, 11520, 11521
11524, 11533, 11534, 11557
*Elset, elset=_PickedSet11, internal, instance=Composite-1, generate
3601, 4000, 1
** Constraint: Adhesive_Composite
*Tie, name=Adhesive_Composite, adjust=yes
Adhesive-1.Adhe_Comp, Composite-1.Composite
** Constraint: Aluminium_Adhesive
*Tie, name=Aluminium_Adhesive, adjust=yes
Adhesive-1.Adhes_Alum, Aluminium-1.Alum
*Elset, elset=LeftSide, internal, instance=Composite-1
20, 19, 18, 17, 16, 15, 14, 13, 12, 11, 10, 9, 8, 7, 6, 5, 4, 3, 2, 1
*Elset, elset=BottomEdge, internal, instance=Composite-1
401, 801, 1201, 1601, 2001, 2401, 2801, 3201, 3601
**Nset, nset=RightNode, internal, instance=Aluminum-1
**13052
*End Assembly
**
** DEFINE AMPLITUDES
** --
** Amplitudes
**
** THIS SECTION WILL BE USED TO DEFINE THE TEMPERATURE RANGE FOR EACH STEP. I ASSUME THAT TEMPERATURE WILL BE CONSTANT OVER EACH STEP. I.E. FOR STEP 1, AT 0 (THE BEGINNING OF THE STEP) AND 1 (THE END OF THE STEP), THE TEMPERATURE IS 22 DEGREES. BECAUSE OF OUR

```
INITIAL CONDITION OF 0 DEGREES, THIS MEANS THE DELTA USED IN THE CTE EQUATION IS 22-0 = 22
DEGREES.
**
** THE AMPLITUDES WILL BE DEFINED BY THEIR NAMES (Constant_1 AND SO ON).
**
*AMPLITUDE, NAME=Constant_1, DEFINITION=TABULAR
    0.0, 22.0, 1.0, 22.0
*AMPLITUDE, NAME=Constant_2, DEFINITION=TABULAR
    1.0, 3.0, 2.0, 3.0
*AMPLITUDE, NAME=Constant_3, DEFINITION=TABULAR
    2.0, 2.0, 3.0, 2.0
*AMPLITUDE, NAME=Constant_4, DEFINITION=TABULAR
    3.0, 3.0, 4.0, 3.0
*AMPLITUDE, NAME=Constant_5, DEFINITION=TABULAR
    4.0, 4.0, 5.0, 4.0
*AMPLITUDE, NAME=Constant_6, DEFINITION=TABULAR
    5.0, 8.0, 6.0, 8.0
*AMPLITUDE, NAME=Constant_7, DEFINITION=TABULAR
    6.0, 10.0, 7.0, 10.0
*AMPLITUDE, NAME=constant_8, DEFINITION=TABULAR
    7.0, 5.0, 8.0, 5.0
*AMPLITUDE, NAME=Constant_9, DEFINITION=TABULAR
    8.0, 11.0, 9.0, 11.0
*AMPLITUDE, NAME=Constant_10, DEFINITION=TABULAR
    9.0, 10.0, 10.0, 10.0
*AMPLITUDE, NAME=Constant_11, DEFINITION=TABULAR
    10.0, 13.0, 11.0, 13.0
*AMPLITUDE, NAME=Constant_12, DEFINITION=TABULAR
    11.0, 11.0, 12.0, 11.0
*AMPLITUDE, NAME=Constant_13, DEFINITION=TABULAR
    12.0, 20.0, 13.0, 20.0
*AMPLITUDE, NAME=Constant_14, DEFINITION=TABULAR
    13.0, 30.0, 14.0, 30.0
*AMPLITUDE, NAME=Constant_15, DEFINITION=TABULAR
    14.0, 20.0, 15.0, 20.0
*AMPLITUDE, NAME=Constant_16, DEFINITION=TABULAR
    15.0, 34.0, 16.0, 34.0
*AMPLITUDE, NAME=Constant_17, DEFINITION=TABULAR
    16.0, 41.0, 17.0, 41.0
*AMPLITUDE, NAME=Constant_18, DEFINITION=TABULAR
    17.0, 51.0, 18.0, 51.0
*AMPLITUDE, NAME=Constant_19, DEFINITION=TABULAR
    18.0, 43.0, 19.0, 43.0
*AMPLITUDE, NAME=Constant_20, DEFINITION=TABULAR
    19.0, 56.0, 20.0, 56.0
*AMPLITUDE, NAME=Constant_21, DEFINITION=TABULAR
    20.0, 99.0, 21.0, 99.0
*AMPLITUDE, NAME=Constant_22, DEFINITION=TABULAR
    21.0, 91.0, 22.0, 91.0
**
** MATERIAL DEFINITIONS
** ------------------------------------------------------
** Materials
**
** ADHESIVE MATERIAL DEFINED AS ELASTIC
```

```
*Material, name=Adhesive
*Elastic
** Modulus, Poissons Ratio
    1000., 0.49
** ALUMINUM MATERIAL DEFINED AS ELASTIC
*Material, name=Aluminium
*Elastic
** Modulus, Poissons Ratio
   69000., 0.3
**
** COMPOSITE MATERIAL DEFINED AS ELASTIC. FIRST SECTION RELATES THE MODULUS TO FIELD
VARIABLES AS SHOWN IN THE FIRST SECTION BELOW. THE COMPOSITE ALSO HAS EXPANSION
PROPERTIES (CTE IS RELATED TO FIELD VARIABLES AS SHOWN IN SECTION SECTION BELOW).
**
*Material, name=Composite
*Elastic, dependencies=1
**    Modulus, Poissons Ratio,     , Field Variable
      23.2130,          0.49,     ,     0
      23.2130,          0.49,     ,     1
      52.3620,          0.49,     ,     2
      63.4370,          0.49,     ,     3
      82.0410,          0.49,     ,     4
      99.3930,          0.49,     ,     5
     303.2800,          0.49,     ,     6
      74.8530,          0.49,     ,     7
      57.8470,          0.49,     ,     8
    1885.3000,          0.49,     ,     9
    6465.2000,          0.49,     ,     10
    9398.4000,          0.49,     ,     11
    9580.8000,          0.49,     ,     12
    9596.1000,          0.49,     ,     13
    9599.0000,          0.35,     ,     14
    9599.6000,          0.35,     ,     15
    9599.7000,          0.35,     ,     16
    9599.8000,          0.35,     ,     17
    9599.8000,          0.35,     ,     18
    9599.8000,          0.35,     ,     19
    9599.8000,          0.35,     ,     20
    9599.8000,          0.35,     ,     21
    9599.8000,          0.35,     ,     22
*EXPANSION, DEPENDENCIES = 1, TYPE = ISO
**          CTE,     , Field Variable
    -3.6750e-05,     ,     0
    -3.6750e-05,     ,     1
    -4.7134e-05,     ,     2
    -4.2566e-05,     ,     3
    -4.7244e-05,     ,     4
    -7.0812e-06,     ,     5
    -0.0000e-00,     ,     6
     3.9659e-05,     ,     7
    -4.6282e-05,     ,     8
    -6.7725e-05,     ,     9
    -2.8915e-05,     ,     10
    -1.4704e-05,     ,     11
    -1.1386e-05,     ,     12
```

```
    -5.7168e-06,     ,     13
    -2.4981e-06,     ,     14
    -1.6064e-06,     ,     15
    -9.3028e-07,     ,     16
    -7.7145e-07,     ,     17
     5.6481e-07,     ,     18
    -7.3557e-07,     ,     19
     0.0000e-00,     ,     20
    -6.3898e-07,     ,     21
    -6.4758e-07,     ,     22
**
** BOUNDARY CONDITIONS DEFINED
** ----------------------------------------------------------
** Boundary Conditions
**
** APPLY FIXED CONDITION TO BOTTOM ALUMINUM BLOCK SURFACE
** Name: Bottom Type: Symmetry/Antisymmetry/Encastre
*Boundary
Aluminium-1.Bottom, ENCASTRE
**
** APPLY SYMMETRY OF MODEL ABOUT X-AXIS
** Name: YX_Sym Type: Symmetry/Antisymmetry/Encastre
*Boundary
_PickedSet9, XSYMM
**
** APPLY SYMMETRY OF MODEL ABOUT Z-AXIS
** Name: YZ_Sym Type: Symmetry/Antisymmetry/Encastre
*Boundary
_PickedSet8, ZSYMM
**
** PREDEFINED FIELDS DEFINED
** ----------------------------------------------------------
** Predefined Fields
**
** ASSIGNS A TEMPERATURE OF 0 DEGREES AS AN INITIAL CONDITION TO THE MODEL. THIS MEANS
THAT SUBSEQUENT STEPS ONLY USE A DELTA TEMPERATURE, NOT ABSOLUTE.
**
** Name: Predefined Field-1   Type: Temperature
*Initial Conditions, type=TEMPERATURE
Composite-1.Composite, 0.
**
** STEP DEFINITIONS
** ----------------------------------------------------------
**
** THE FIRST STEP WILL BE WELL-DEFINED. ALL OTHER STEPS FOLLOW THE SAME PROCESS, SEE
BELOW.
** ********************************************************
**
** STEP: Step-1
** ..........................................................
** DEFINE THE STEP NAME (Step-1). IF YOU WOULD LIKE TO USE MODEL RESTART, USE NLGEOM = YES.
WE WILL INCREMENT BY 1 SECOND FOR WITH 22 SECONDS TOTAL IN THIS STEP.
*Step, name=Step-1, nlgeom=YES, inc=1
*Static, direct
22., 22.,
```

```
**
** DEFINE THE STEP'S BOUNDARY CONDITIONS.
** .....................................................
** SAME BOUNDARY CONDITIONS AS BEFORE. IN ORDER, FIXED ALUMINUM BOTTOM, X-SYMMETRY OF MODEL, AND Z-SYMMETRY OF MODEL.
**
** Name: Bottom1 Type: Symmetry/Antisymmetry/Encastre
*Boundary
Aluminium-1.Bottom, ENCASTRE
** Name: XY_Sym1 Type: Symmetry/Antisymmetry/Encastre
*Boundary
_PickedSet11, XSYMM
** Name: YZ_sym1 Type: Symmetry/Antisymmetry/Encastre
*Boundary
_PickedSet10, ZSYMM
**
** PREDEFINED FIELDS
** .....................................................
** DEFINE THE FIELD VARIABLE THAT SHOULD BE USED IN THIS STEP. IN THIS CASE, COMPOSITE-1 SHOULD USE FIELD VARIABLE #1 AT STEP 1.
*FIELD , variable=1
Composite-1.Composite, 1
**
** DEFINE THE TEMPERATURE DELTA. IN THIS CASE, THE TEMPERATURE WILL BE FROM AMPLITUDE #1, AS SHOWN ABOVE. THE TEMPERATURE DELTA FROM AMPLITUDE 1 IS USED. DEFINE THE DELTA IN THE AMPLITUDE SECTION.
*Temperature, amplitude=Constant_1
Composite-1.Composite, 1.
**
** OUTPUT REQUESTS
** .....................................................
** RESTART THE MODEL AND WRITE RESULTS AT EVERY SECOND.
*Restart, write, frequency=1
**
** PRINT ELEMENTS IN THE FIRST SECTION FO THE COMPOSITE. THIS WILL PRINT CENTROIDAL STRESSES IN THE ELEMENT SET "LeftSide," SHOWN ABOVE. YOU COULD ALSO USE THE N PRINT COMMAND TO PRINT NODE RESULTS LIKE DEFLECTIONS.
*EL PRINT, elset=LeftSide, POSITION=CENTROIDAL
S
**
** PRINT ELEMENTS IN THE SECOND SECTION OF THE COMPOSITE. THIS WILL PRINT CENTROIDAL STRESSES OF THE ELEMENT SET "BottomEdge."
** Print the elements in the second section of the composite
*EL PRINT, elset=BottomEdge, POSITION=CENTROIDAL
S
**
** FIELD OUTPUT: F-Output-1
** .....................................................
** PRESELECTED FIELD VARIABLES WILL BE PRINTED. IF YOU HAVE ANY SPECIAL VARIABLES THAT YOU WOULD LIKE TO PRINT, CHANGE THIS OPTION.
*Output, field, variable=PRESELECT
**
** HISTORY OUTPUT: H-Output-1
** .....................................................
```

```
** PRESELECTED HISTORY VARIABLES WILL BE OUTPUTTED. IF YOU HAVE ANY SPECIAL VARIABLES
THAT YOU WOULD LIKE TO PRINT, CHANGE THIS OPTION.
*Output, history, variable=PRESELECT
**
*End Step
**
** ----------------------------------------------------------
**
** STEP: Step-2
**
*Step, name=Step-2, nlgeom=YES, inc=1
*Static, direct
3., 3.,
**
** BOUNDARY CONDITIONS
**
** Name: Bottom1 Type: Symmetry/Antisymmetry/Encastre
*Boundary
Aluminium-1.Bottom, ENCASTRE
** Name: XY_Sym1 Type: Symmetry/Antisymmetry/Encastre
*Boundary
_PickedSet11, XSYMM
** Name: YZ_sym1 Type: Symmetry/Antisymmetry/Encastre
*Boundary
_PickedSet10, ZSYMM
**
** PREDEFINED FIELDS
**
*FIELD , variable=1
Composite-1.Composite, 2
*Temperature, amplitude=Constant_2
Composite-1.Composite, 1.
**
** OUTPUT REQUESTS
**
*Restart, write, frequency=1
**
** Print the elements in the first section of the composite
*EL PRINT, elset=LeftSide, POSITION=CENTROIDAL
S
** Print the elements in the second section of the composite
*EL PRINT, elset=BottomEdge, POSITION=CENTROIDAL
**
** FIELD OUTPUT: F-Output-1
**
*Output, field, variable=PRESELECT
**
** HISTORY OUTPUT: H-Output-1
**
*Output, history, variable=PRESELECT
*End Step
** ----------------------------------------------------------
**
** STEP: Step-3
**
```

```
*Step, name=Step-3, nlgeom=YES, inc=1
*Static, direct
2., 2.,
**
** BOUNDARY CONDITIONS
**
** Name: Bottom1 Type: Symmetry/Antisymmetry/Encastre
*Boundary
Aluminium-1.Bottom, ENCASTRE
** Name: XY_Sym1 Type: Symmetry/Antisymmetry/Encastre
*Boundary
_PickedSet11, XSYMM
** Name: YZ_sym1 Type: Symmetry/Antisymmetry/Encastre
*Boundary
_PickedSet10, ZSYMM
**
** PREDEFINED FIELDS
**
*FIELD , variable=1
Composite-1.Composite, 3
*Temperature, amplitude=Constant_3
Composite-1.Composite, 1.
**
** OUTPUT REQUESTS
**
*Restart, write, frequency=1
**
** Print the elements in the first section of the composite
*EL PRINT, elset=LeftSide, POSITION=CENTROIDAL
S
** Print the elements in the second section of the composite
*EL PRINT, elset=BottomEdge, POSITION=CENTROIDAL
**
** FIELD OUTPUT: F-Output-1
**
*Output, field, variable=PRESELECT
**
** HISTORY OUTPUT: H-Output-1
**
*Output, history, variable=PRESELECT
*End Step
** ----------------------------------------------------------
**
** STEP: Step-4
**
*Step, name=Step-4, nlgeom=YES, inc=1
*Static, direct
3., 3.,
**
** BOUNDARY CONDITIONS
**
** Name: Bottom1 Type: Symmetry/Antisymmetry/Encastre
*Boundary
Aluminium-1.Bottom, ENCASTRE
** Name: XY_Sym1 Type: Symmetry/Antisymmetry/Encastre
```

```
*Boundary
_PickedSet11, XSYMM
** Name: YZ_sym1 Type: Symmetry/Antisymmetry/Encastre
*Boundary
_PickedSet10, ZSYMM
**
** PREDEFINED FIELDS
**
*FIELD , variable=1
Composite-1.Composite, 4
*Temperature, amplitude=Constant_4
Composite-1.Composite, 1.
**
** OUTPUT REQUESTS
**
*Restart, write, frequency=1
**
** Print the elements in the first section of the composite
*EL PRINT, elset=LeftSide, POSITION=CENTROIDAL
S
** Print the elements in the second section of the composite
*EL PRINT, elset=BottomEdge, POSITION=CENTROIDAL
**
** FIELD OUTPUT: F-Output-1
**
*Output, field, variable=PRESELECT
**
** HISTORY OUTPUT: H-Output-1
**
*Output, history, variable=PRESELECT
*End Step
** ----------------------------------------------------------
** STEP: Step-5
**
*Step, name=Step-5, nlgeom=YES, inc=1
*Static, direct
4., 4.,
**
** BOUNDARY CONDITIONS
**
** Name: Bottom1 Type: Symmetry/Antisymmetry/Encastre
*Boundary
Aluminium-1.Bottom, ENCASTRE
** Name: XY_Sym1 Type: Symmetry/Antisymmetry/Encastre
*Boundary
_PickedSet11, XSYMM
** Name: YZ_sym1 Type: Symmetry/Antisymmetry/Encastre
*Boundary
_PickedSet10, ZSYMM
**
** PREDEFINED FIELDS
**
*FIELD , variable=1
Composite-1.Composite, 5
*Temperature, amplitude=Constant_5
```

```
Composite-1.Composite, 1.
**
** OUTPUT REQUESTS
**
*Restart, write, frequency=1
**
** Print the elements in the first section of the composite
*EL PRINT, elset=LeftSide, POSITION=CENTROIDAL
S
** Print the elements in the second section of the composite
*EL PRINT, elset=BottomEdge, POSITION=CENTROIDAL
**
** FIELD OUTPUT: F-Output-1
**
*Output, field, variable=PRESELECT
**
** HISTORY OUTPUT: H-Output-1
**
*Output, history, variable=PRESELECT
*End Step
** ************************************************************
** STEP: Step-6
**
*Step, name=Step-6, nlgeom=YES, inc=1
*Static, direct
8., 8.,
**
** BOUNDARY CONDITIONS
**
** Name: Bottom1 Type: Symmetry/Antisymmetry/Encastre
*Boundary
Aluminium-1.Bottom, ENCASTRE
** Name: XY_Sym1 Type: Symmetry/Antisymmetry/Encastre
*Boundary
_PickedSet11, XSYMM
** Name: YZ_sym1 Type: Symmetry/Antisymmetry/Encastre
*Boundary
_PickedSet10, ZSYMM
**
** PREDEFINED FIELDS
**
*FIELD , variable=1
Composite-1.Composite, 6
*Temperature, amplitude=Constant_6
Composite-1.Composite, 1.
**
** OUTPUT REQUESTS
**
*Restart, write, frequency=1
**
** Print the elements in the first section of the composite
*EL PRINT, elset=LeftSide, POSITION=CENTROIDAL
S
** Print the elements in the second section of the composite
*EL PRINT, elset=BottomEdge, POSITION=CENTROIDAL
```

```
**
** FIELD OUTPUT: F-Output-1
**
*Output, field, variable=PRESELECT
**
** HISTORY OUTPUT: H-Output-1
**
*Output, history, variable=PRESELECT
*End Step
** ----------------------------------------------------------
**
** STEP: Step-7
**
*Step, name=Step-7, nlgeom=YES, inc=1
*Static, direct
10., 10.,
**
** BOUNDARY CONDITIONS
**
** Name: Bottom1 Type: Symmetry/Antisymmetry/Encastre
*Boundary
Aluminium-1.Bottom, ENCASTRE
** Name: XY_Sym1 Type: Symmetry/Antisymmetry/Encastre
*Boundary
_PickedSet11, XSYMM
** Name: YZ_sym1 Type: Symmetry/Antisymmetry/Encastre
*Boundary
_PickedSet10, ZSYMM
**
** PREDEFINED FIELDS
**
*FIELD , variable=1
Composite-1.Composite, 7
*Temperature, amplitude=Constant_7
Composite-1.Composite, 1.
**
** OUTPUT REQUESTS
**
*Restart, write, frequency=1
**
** Print the elements in the first section of the composite
*EL PRINT, elset=LeftSide, POSITION=CENTROIDAL
S
** Print the elements in the second section of the composite
*EL PRINT, elset=BottomEdge, POSITION=CENTROIDAL
**
** FIELD OUTPUT: F-Output-1
**
*Output, field, variable=PRESELECT
**
** HISTORY OUTPUT: H-Output-1
**
*Output, history, variable=PRESELECT
*End Step
** ----------------------------------------------------------
```

```
** STEP: Step-8
**
*Step, name=Step-8, nlgeom=YES, inc=1
*Static, direct
5., 5.,
**
** BOUNDARY CONDITIONS
**
** Name: Bottom1 Type: Symmetry/Antisymmetry/Encastre
*Boundary
Aluminium-1.Bottom, ENCASTRE
** Name: XY_Sym1 Type: Symmetry/Antisymmetry/Encastre
*Boundary
_PickedSet11, XSYMM
** Name: YZ_sym1 Type: Symmetry/Antisymmetry/Encastre
*Boundary
_PickedSet10, ZSYMM
**
** PREDEFINED FIELDS
**
*FIELD , variable=1
Composite-1.Composite, 8
*Temperature, amplitude=Constant_8
Composite-1.Composite, 1.
**
** OUTPUT REQUESTS
**
*Restart, write, frequency=1
**
** Print the elements in the first section of the composite
*EL PRINT, elset=LeftSide, POSITION=CENTROIDAL
S
** Print the elements in the second section of the composite
*EL PRINT, elset=BottomEdge, POSITION=CENTROIDAL
**
** FIELD OUTPUT: F-Output-1
**
*Output, field, variable=PRESELECT
**
** HISTORY OUTPUT: H-Output-1
**
*Output, history, variable=PRESELECT
*End Step
** ----------------------------------------------------------
** STEP: Step-9
**
*Step, name=Step-9, nlgeom=YES, inc=1
*Static, direct
11., 11.,
**
** BOUNDARY CONDITIONS
**
** Name: Bottom1 Type: Symmetry/Antisymmetry/Encastre
*Boundary
Aluminium-1.Bottom, ENCASTRE
```

```
** Name: XY_Sym1 Type: Symmetry/Antisymmetry/Encastre
*Boundary
_PickedSet11, XSYMM
** Name: YZ_sym1 Type: Symmetry/Antisymmetry/Encastre
*Boundary
_PickedSet10, ZSYMM
**
** PREDEFINED FIELDS
**
*FIELD , variable=1
Composite-1.Composite, 9
*Temperature, amplitude=Constant_9
Composite-1.Composite, 1.
**
** OUTPUT REQUESTS
**
*Restart, write, frequency=1
**
** Print the elements in the first section of the composite
*EL PRINT, elset=LeftSide, POSITION=CENTROIDAL
S
** Print the elements in the second section of the composite
*EL PRINT, elset=BottomEdge, POSITION=CENTROIDAL
**
** FIELD OUTPUT: F-Output-1
**
*Output, field, variable=PRESELECT
**
** HISTORY OUTPUT: H-Output-1
**
*Output, history, variable=PRESELECT
*End Step
** ----------------------------------------------------------
** STEP: Step-10
**
*Step, name=Step-10, nlgeom=YES, inc=1
*Static, direct
10., 10.,
**
** BOUNDARY CONDITIONS
**
** Name: Bottom1 Type: Symmetry/Antisymmetry/Encastre
*Boundary
Aluminium-1.Bottom, ENCASTRE
** Name: XY_Sym1 Type: Symmetry/Antisymmetry/Encastre
*Boundary
_PickedSet11, XSYMM
** Name: YZ_sym1 Type: Symmetry/Antisymmetry/Encastre
*Boundary
_PickedSet10, ZSYMM
**
** PREDEFINED FIELDS
**
*FIELD , variable=1
Composite-1.Composite, 10
```

```
*Temperature, amplitude=Constant_10
Composite-1.Composite, 1.
**
** OUTPUT REQUESTS
**
*Restart, write, frequency=1
**
** Print the elements in the first section of the composite
*EL PRINT, elset=LeftSide, POSITION=CENTROIDAL
S
** Print the elements in the second section of the composite
*EL PRINT, elset=BottomEdge, POSITION=CENTROIDAL
**
** FIELD OUTPUT: F-Output-1
**
*Output, field, variable=PRESELECT
**
** HISTORY OUTPUT: H-Output-1
**
*Output, history, variable=PRESELECT
*End Step
** ----------------------------------------------------------
** STEP: Step-11
**
*Step, name=Step-11, nlgeom=YES, inc=1
*Static, direct
13., 13.,
**
** BOUNDARY CONDITIONS
**
** Name: Bottom1 Type: Symmetry/Antisymmetry/Encastre
*Boundary
Aluminium-1.Bottom, ENCASTRE
** Name: XY_Sym1 Type: Symmetry/Antisymmetry/Encastre
*Boundary
_PickedSet11, XSYMM
** Name: YZ_sym1 Type: Symmetry/Antisymmetry/Encastre
*Boundary
_PickedSet10, ZSYMM
**
** PREDEFINED FIELDS
**
*FIELD , variable=1
Composite-1.Composite, 11
*Temperature, amplitude=Constant_11
Composite-1.Composite, 1.
**
** OUTPUT REQUESTS
**
*Restart, write, frequency=1
**
** Print the elements in the first section of the composite
*EL PRINT, elset=LeftSide, POSITION=CENTROIDAL
S
** Print the elements in the second section of the composite
```

```
*EL PRINT, elset=BottomEdge, POSITION=CENTROIDAL
**
** FIELD OUTPUT: F-Output-1
**
*Output, field, variable=PRESELECT
**
** HISTORY OUTPUT: H-Output-1
**
*Output, history, variable=PRESELECT
*End Step
** ----------------------------------------------------------
** STEP: Step-12
**
*Step, name=Step-12, nlgeom=YES, inc=1
*Static, direct
11., 11.,
**
** BOUNDARY CONDITIONS
**
** Name: Bottom1 Type: Symmetry/Antisymmetry/Encastre
*Boundary
Aluminium-1.Bottom, ENCASTRE
** Name: XY_Sym1 Type: Symmetry/Antisymmetry/Encastre
*Boundary
_PickedSet11, XSYMM
** Name: YZ_sym1 Type: Symmetry/Antisymmetry/Encastre
*Boundary
_PickedSet10, ZSYMM
**
** PREDEFINED FIELDS
**
*FIELD , variable=1
Composite-1.Composite, 12
*Temperature, amplitude=Constant_12
Composite-1.Composite, 1.
**
** OUTPUT REQUESTS
**
*Restart, write, frequency=1
**
** Print the elements in the first section of the composite
*EL PRINT, elset=LeftSide, POSITION=CENTROIDAL
S
** Print the elements in the second section of the composite
*EL PRINT, elset=BottomEdge, POSITION=CENTROIDAL
**
** FIELD OUTPUT: F-Output-1
**
*Output, field, variable=PRESELECT
**
** HISTORY OUTPUT: H-Output-1
**
*Output, history, variable=PRESELECT
*End Step
** ----------------------------------------------------------
```

```
**
** STEP: Step-13
**
*Step, name=Step-13, nlgeom=YES, inc=1
*Static, direct
20., 20.,
**
** BOUNDARY CONDITIONS
**
** Name: Bottom1 Type: Symmetry/Antisymmetry/Encastre
*Boundary
Aluminium-1.Bottom, ENCASTRE
** Name: XY_Sym1 Type: Symmetry/Antisymmetry/Encastre
*Boundary
_PickedSet11, XSYMM
** Name: YZ_sym1 Type: Symmetry/Antisymmetry/Encastre
*Boundary
_PickedSet10, ZSYMM
**
** PREDEFINED FIELDS
**
*FIELD , variable=1
Composite-1.Composite, 13
*Temperature, amplitude=Constant_13
Composite-1.Composite, 1.
**
** OUTPUT REQUESTS
**
*Restart, write, frequency=1
**
** Print the elements in the first section of the composite
*EL PRINT, elset=LeftSide, POSITION=CENTROIDAL
S
** Print the elements in the second section of the composite
*EL PRINT, elset=BottomEdge, POSITION=CENTROIDAL
**
** FIELD OUTPUT: F-Output-1
**
*Output, field, variable=PRESELECT
**
** HISTORY OUTPUT: H-Output-1
**
*Output, history, variable=PRESELECT
*End Step
** ----------------------------------------------------------
**
** STEP: Step-14
**
*Step, name=Step-14, nlgeom=YES, inc=1
*Static, direct
30., 30.,
**
** BOUNDARY CONDITIONS
**
** Name: Bottom1 Type: Symmetry/Antisymmetry/Encastre
```

```
*Boundary
Aluminium-1.Bottom, ENCASTRE
** Name: XY_Sym1 Type: Symmetry/Antisymmetry/Encastre
*Boundary
_PickedSet11, XSYMM
** Name: YZ_sym1 Type: Symmetry/Antisymmetry/Encastre
*Boundary
_PickedSet10, ZSYMM
**
** PREDEFINED FIELDS
**
*FIELD , variable=1
Composite-1.Composite, 14
*Temperature, amplitude=Constant_14
Composite-1.Composite, 1.
**
** OUTPUT REQUESTS
**
*Restart, write, frequency=1
**
** Print the elements in the first section of the composite
*EL PRINT, elset=LeftSide, POSITION=CENTROIDAL
S
** Print the elements in the second section of the composite
*EL PRINT, elset=BottomEdge, POSITION=CENTROIDAL
**
** FIELD OUTPUT: F-Output-1
**
*Output, field, variable=PRESELECT
**
** HISTORY OUTPUT: H-Output-1
**
*Output, history, variable=PRESELECT
*End Step
** ----------------------------------------------------
**
** STEP: Step-15
**
*Step, name=Step-15, nlgeom=YES, inc=1
*Static, direct
20., 20.,
**
** BOUNDARY CONDITIONS
**
** Name: Bottom1 Type: Symmetry/Antisymmetry/Encastre
*Boundary
Aluminium-1.Bottom, ENCASTRE
** Name: XY_Sym1 Type: Symmetry/Antisymmetry/Encastre
*Boundary
_PickedSet11, XSYMM
** Name: YZ_sym1 Type: Symmetry/Antisymmetry/Encastre
*Boundary
_PickedSet10, ZSYMM
**
** PREDEFINED FIELDS
```

```
**
*FIELD , variable=1
Composite-1.Composite, 15
*Temperature, amplitude=Constant_15
Composite-1.Composite, 1.
**
** OUTPUT REQUESTS
**
*Restart, write, frequency=1
**
** Print the elements in the first section of the composite
*EL PRINT, elset=LeftSide, POSITION=CENTROIDAL
S
** Print the elements in the second section of the composite
*EL PRINT, elset=BottomEdge, POSITION=CENTROIDAL
**
** FIELD OUTPUT: F-Output-1
**
*Output, field, variable=PRESELECT
**
** HISTORY OUTPUT: H-Output-1
**
*Output, history, variable=PRESELECT
*End Step
** ----------------------------------------------------------
** STEP: Step-16
**
*Step, name=Step-16, nlgeom=YES, inc=1
*Static, direct
34., 34.,
**
** BOUNDARY CONDITIONS
**
** Name: Bottom1 Type: Symmetry/Antisymmetry/Encastre
*Boundary
Aluminium-1.Bottom, ENCASTRE
** Name: XY_Sym1 Type: Symmetry/Antisymmetry/Encastre
*Boundary
_PickedSet11, XSYMM
** Name: YZ_sym1 Type: Symmetry/Antisymmetry/Encastre
*Boundary
_PickedSet10, ZSYMM
**
** PREDEFINED FIELDS
**
*FIELD , variable=1
Composite-1.Composite, 16
*Temperature, amplitude=Constant_16
Composite-1.Composite, 1.
**
** OUTPUT REQUESTS
**
*Restart, write, frequency=1
**
** Print the elements in the first section of the composite
```

```
*EL PRINT, elset=LeftSide, POSITION=CENTROIDAL
S
** Print the elements in the second section of the composite
*EL PRINT, elset=BottomEdge, POSITION=CENTROIDAL
**
** FIELD OUTPUT: F-Output-1
**
*Output, field, variable=PRESELECT
**
** HISTORY OUTPUT: H-Output-1
**
*Output, history, variable=PRESELECT
*End Step
** ----------------------------------------------------------
**
** STEP: Step-17
**
*Step, name=Step-17, nlgeom=YES, inc=1
*Static, direct
41., 41.,
**
** BOUNDARY CONDITIONS
**
** Name: Bottom1 Type: Symmetry/Antisymmetry/Encastre
*Boundary
Aluminium-1.Bottom, ENCASTRE
** Name: XY_Sym1 Type: Symmetry/Antisymmetry/Encastre
*Boundary
_PickedSet11, XSYMM
** Name: YZ_sym1 Type: Symmetry/Antisymmetry/Encastre
*Boundary
_PickedSet10, ZSYMM
**
** PREDEFINED FIELDS
**
*FIELD , variable=1
Composite-1.Composite, 17
*Temperature, amplitude=Constant_17
Composite-1.Composite, 1.
**
** OUTPUT REQUESTS
**
*Restart, write, frequency=1
**
** Print the elements in the first section of the composite
*EL PRINT, elset=LeftSide, POSITION=CENTROIDAL
S
** Print the elements in the second section of the composite
*EL PRINT, elset=BottomEdge, POSITION=CENTROIDAL
**
** FIELD OUTPUT: F-Output-1
**
*Output, field, variable=PRESELECT
**
** HISTORY OUTPUT: H-Output-1
```

```
**
*Output, history, variable=PRESELECT
*End Step
** ----------------------------------------------------------
**
** STEP: Step-18
**
*Step, name=Step-18, nlgeom=YES, inc=1
*Static, direct
56., 56.,
**
** BOUNDARY CONDITIONS
**
** Name: Bottom1 Type: Symmetry/Antisymmetry/Encastre
*Boundary
Aluminium-1.Bottom, ENCASTRE
** Name: XY_Sym1 Type: Symmetry/Antisymmetry/Encastre
*Boundary
_PickedSet11, XSYMM
** Name: YZ_sym1 Type: Symmetry/Antisymmetry/Encastre
*Boundary
_PickedSet10, ZSYMM
**
** PREDEFINED FIELDS
**
*FIELD , variable=1
Composite-1.Composite, 18
*Temperature, amplitude=Constant_18
Composite-1.Composite, 1.
**
** OUTPUT REQUESTS
**
*Restart, write, frequency=1
**
** Print the elements in the first section of the composite
*EL PRINT, elset=LeftSide, POSITION=CENTROIDAL
S
** Print the elements in the second section of the composite
*EL PRINT, elset=BottomEdge, POSITION=CENTROIDAL
**
** FIELD OUTPUT: F-Output-1
**
*Output, field, variable=PRESELECT
**
** HISTORY OUTPUT: H-Output-1
**
*Output, history, variable=PRESELECT
*End Step
** ----------------------------------------------------------
** STEP: Step-19
**
*Step, name=Step-19, nlgeom=YES, inc=1
*Static, direct
43., 43.,
**
```

```
** BOUNDARY CONDITIONS
**
** Name: Bottom1 Type: Symmetry/Antisymmetry/Encastre
*Boundary
Aluminium-1.Bottom, ENCASTRE
** Name: XY_Sym1 Type: Symmetry/Antisymmetry/Encastre
*Boundary
_PickedSet11, XSYMM
** Name: YZ_sym1 Type: Symmetry/Antisymmetry/Encastre
*Boundary
_PickedSet10, ZSYMM
**
** PREDEFINED FIELDS
**
*FIELD , variable=1
Composite-1.Composite, 19
*Temperature, amplitude=Constant_19
Composite-1.Composite, 1.
**
** OUTPUT REQUESTS
**
*Restart, write, frequency=1
**
** Print the elements in the first section of the composite
*EL PRINT, elset=LeftSide, POSITION=CENTROIDAL
S
** Print the elements in the second section of the composite
*EL PRINT, elset=BottomEdge, POSITION=CENTROIDAL
**
** FIELD OUTPUT: F-Output-1
**
*Output, field, variable=PRESELECT
**
** HISTORY OUTPUT: H-Output-1
**
*Output, history, variable=PRESELECT
*End Step
** ----------------------------------------------------------
**
** STEP: Step-20
**
*Step, name=Step-20, nlgeom=YES, inc=1
*Static, direct
56., 56.,
**
** BOUNDARY CONDITIONS
**
** Name: Bottom1 Type: Symmetry/Antisymmetry/Encastre
*Boundary
Aluminium-1.Bottom, ENCASTRE
** Name: XY_Sym1 Type: Symmetry/Antisymmetry/Encastre
*Boundary
_PickedSet11, XSYMM
** Name: YZ_sym1 Type: Symmetry/Antisymmetry/Encastre
*Boundary
```

```
_PickedSet10, ZSYMM
**
** PREDEFINED FIELDS
**
*FIELD , variable=1
Composite-1.Composite, 20
*Temperature, amplitude=Constant_20
Composite-1.Composite, 1.
**
** OUTPUT REQUESTS
**
*Restart, write, frequency=1
**
** Print the elements in the first section of the composite
*EL PRINT, elset=LeftSide, POSITION=CENTROIDAL
S
** Print the elements in the second section of the composite
*EL PRINT, elset=BottomEdge, POSITION=CENTROIDAL
**
** FIELD OUTPUT: F-Output-1
**
*Output, field, variable=PRESELECT
**
** HISTORY OUTPUT: H-Output-1
**
*Output, history, variable=PRESELECT
*End Step
** ----------------------------------------------------------
** STEP: Step-21
**
*Step, name=Step-21, nlgeom=YES, inc=1
*Static, direct
99., 99.,
**
** BOUNDARY CONDITIONS
**
** Name: Bottom1 Type: Symmetry/Antisymmetry/Encastre
*Boundary
Aluminium-1.Bottom, ENCASTRE
** Name: XY_Sym1 Type: Symmetry/Antisymmetry/Encastre
*Boundary
_PickedSet11, XSYMM
** Name: YZ_sym1 Type: Symmetry/Antisymmetry/Encastre
*Boundary
_PickedSet10, ZSYMM
**
** PREDEFINED FIELDS
**
*FIELD , variable=1
Composite-1.Composite, 21
*Temperature, amplitude=Constant_21
Composite-1.Composite, 1.
**
** OUTPUT REQUESTS
**
```

```
*Restart, write, frequency=1
**
** Print the elements in the first section of the composite
*EL PRINT, elset=LeftSide, POSITION=CENTROIDAL
S
** Print the elements in the second section of the composite
*EL PRINT, elset=BottomEdge, POSITION=CENTROIDAL
**
** FIELD OUTPUT: F-Output-1
**
*Output, field, variable=PRESELECT
**
** HISTORY OUTPUT: H-Output-1
**
*Output, history, variable=PRESELECT
*End Step
** ----------------------------------------------------------
** STEP: Step-22
**
*Step, name=Step-22, nlgeom=YES, inc=1
*Static, direct
91., 91.,
**
** BOUNDARY CONDITIONS
**
** Name: Bottom1 Type: Symmetry/Antisymmetry/Encastre
*Boundary
Aluminium-1.Bottom, ENCASTRE
** Name: XY_Sym1 Type: Symmetry/Antisymmetry/Encastre
*Boundary
_PickedSet11, XSYMM
** Name: YZ_sym1 Type: Symmetry/Antisymmetry/Encastre
*Boundary
_PickedSet10, ZSYMM
**
** PREDEFINED FIELDS
**
*FIELD , variable=1
Composite-1.Composite, 22
*Temperature, amplitude=Constant_22
Composite-1.Composite, 1.
**
** OUTPUT REQUESTS
**
*Restart, write, frequency=1
**
** FIELD OUTPUT: F-Output-1
**
*Output, field, variable=PRESELECT
**
** Print the elements in the first section of the composite
*EL PRINT, elset=LeftSide, POSITION=CENTROIDAL
S
** Print the elements in the second section of the composite
*EL PRINT, elset=BottomEdge, POSITION=CENTROIDAL
```

```
**
** HISTORY OUTPUT: H-Output-1
**
*Output, history, variable=PRESELECT
*End Step
** ----------------------------------------------------------------
```